

PLANNING DISTRIBUTION SYSTEM RESOURCE ISLANDS CONSIDERING  
RELIABILITY, COST AND THE IMPACT OF PENETRATION OF  
PLUG-IN HYBRID ELECTRIC VEHICLES

ARTHUR LAKES LIBRARY  
COLORADO SCHOOL OF MINES  
GOLDEN, CO 80401

by

Julieta Giráldez Miner

ProQuest Number: 10795335

All rights reserved

INFORMATION TO ALL USERS

The quality of this reproduction is dependent upon the quality of the copy submitted.

In the unlikely event that the author did not send a complete manuscript and there are missing pages, these will be noted. Also, if material had to be removed, a note will indicate the deletion.



ProQuest 10795335

Published by ProQuest LLC (2018). Copyright of the Dissertation is held by the Author.

All rights reserved.

This work is protected against unauthorized copying under Title 17, United States Code  
Microform Edition © ProQuest LLC.

ProQuest LLC.  
789 East Eisenhower Parkway  
P.O. Box 1346  
Ann Arbor, MI 48106 – 1346

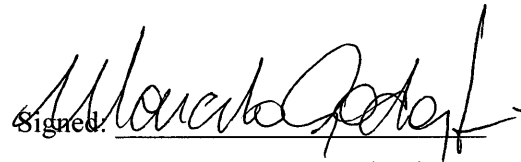
A thesis submitted to the Faculty and the Board of Trustees of the Colorado School of Mines in partial fulfillment of the requirements for the degree of Master of Science (Engineering).

Golden, Colorado

Date 4/18/11

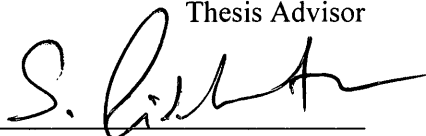
Signed: 

Julieta Giráldez Miner

Signed: 

Dr. Marcelo Simoes

Thesis Advisor

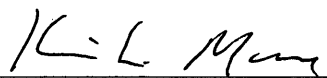
Signed: 

Dr. Siddharth Suryanarayanan

Thesis Co-advisor

Golden, Colorado

Date 4/18/11

Signed: 

Dr. K. Moore

Professor and Head

Department of Engineering

## ABSTRACT

In response to the discussion on how electric power distribution systems should evolve under the Smart Grid, this thesis explores methodologies for the redesign of electric distribution systems by incorporating elements of emerging distribution systems. Firstly, an optimization problem is defined to simultaneously determine locations for Distributed Generation (DG) and feeder intertie connections in a legacy radial distribution system to improve reliability in the islanded mode of operation – i.e., microgrid. For that, an extended methodology of an existing Multi Objective Genetic Algorithm (MOGA) is proposed. The MOGA is applied to a test system in which two types of modeling the load are explored and satisfactory design solutions are obtained.

Secondly, a methodology is proposed to determine the impact of penetration of a plug-in hybrid vehicle (PHEV) fleet with vehicle-to-grid (V2G) features on distribution systems. The methodology is based on a probabilistic simulation of daily behavior of a PHEV fleet to determine the charging patterns of the vehicles for utility peak-shaving purposes and for the benefit of the owner through a Linear Programming (LP) optimization method. The charging patterns of the PHEV simulated fleet are used to determine the impact of PHEVs in a distribution test system under islanded mode of operation. Finally, the impact of PHEVs in the redesign of such distribution system islands is also considered.

## TABLE OF CONTENTS

ABSTRACT.....	iii
TABLE OF CONTENTS.....	iv
LIST OF FIGURES .....	vii
LIST OF TABLES.....	ix
ACKNOWLEDGEMENTS.....	xi
NOMENCLATURE .....	xii
CHAPTER 1 INTRODUCTION .....	1
1.1 Objective.....	1
1.2 Motivation.....	1
1.3 Scope.....	3
1.4 Literature Search.....	4
1.4.1 Evolution of distribution systems with smart grids.....	4
1.4.2 Distribution planning methods.....	7
1.4.3 State-of-the-art in PHEV studies .....	11
1.4.4 Tools and methods .....	13
1.5 Organization of Thesis.....	15
CHAPTER 2 OPTIMIZATION OF ISLANDED ELECTRIC DISTRIBUTION SYSTEMS.....	17
2.1 Modeling a radial electric distribution system.....	17
2.1.1 Modeling of the annual load .....	18
2.1.2 Modeling of DG.....	20
2.1.3 Basic reliability concepts .....	22
2.1.4 Power systems simulation tool.....	24
2.2 Definition of the distribution system redesign problem.....	25
2.3 Genetic algorithm structure.....	27
2.3.1 Multi-objective Genetic Algorithm (MOGA).....	27
2.3.2 Objective function and constraints.....	29
2.3.3 Initial population and its importance for convergence.....	31
2.3.4 Evaluation by the fitness function.....	33

CHAPTER 3 CASE STUDIES OF DISTRIBUTED RESOURCE ISLAND RECONFIGURATION USING THE MULTI-OBJECTIVE GENETIC ALGORITHM .....	37
3.3. Roy Billinton Test System (RBTS) .....	46
3.3.1. RBTS data.....	46
3.3.2. Results of the MOGA applied to RBTS Case I .....	52
3.3.3. Results of the MOGA applied to RBTS Case II .....	55
3.3.5. Computational time of the expanded MOGA applied to the RBTS .....	59
 CHAPTER 4 IMPACT OF PLUG-IN HYBRID ELECTRIC VEHICLES ON AN ELECTRIC DISTRIBUTION SYSTEM ISLAND .....	 63
4.1 PHEVs in electric distribution systems.....	63
4.1.1 PHEVs with V2G technology .....	64
4.1.2 Key assumptions to determine the impact of PHEVs .....	65
4.2 Probabilistic simulation of a PHEV fleet.....	67
4.2.1 PHEV class population size .....	69
4.2.2 PHEV design parameters and battery size .....	70
4.2.3 PHEV daily data .....	71
4.3 LP algorithm for the PHEV fleet charging problem .....	73
4.3.1 Mathematical formulation.....	74
4.3.1.1 LP algorithm for peak shaving purposes.....	74
4.3.1.2 LP algorithm for minimizing the vehicle owners consumption.....	78
4.3.2 LP algorithm implementation .....	79
4.4 Application of the PHEV fleet probabilistic simulation and LP algorithms to the RBTS test system.....	80
4.4.1 PHEV fleet simulation applied to the RBTS test system.....	80
4.4.2 LP algorithm applied to the RBTS test system.....	81
4.4.3 Impact of uncontrolled and delayed charging strategies without V2G in the RBTS test system.....	90
4.5 Reliability impact of PHEVs in the RBTS system .....	91
4.5.1 Reliability impact of PHEVs in the RBTS radial system .....	92
4.5.2 Reliability impact of PHEVs in the RBTS redesigned test system.....	96
4.5.3 Redesign of the RBTS test system with PHEVs.....	97

CHAPTER 5 CONCLUSIONS AND FUTURE WORK .....	101
5.1 Conclusions.....	101
5.1.1 Conclusions to the extended MOGA .....	101
5.1.2 Conclusions to the study of the impact of PHEVs.....	102
5.2 Future work.....	103
REFERENCES .....	105
APPENDIX.....	119
A.1 Components of the 3FDR and RBTS system.....	119
A.2 Electronic appendix.....	120

## LIST OF FIGURES

Figure 2.1: Elements of traditional radial feeders in electric distribution systems. ....	18
Figure 2.2: Evolution of electric distribution systems towards meshed systems with DG. ....	18
Figure 2.3: Step-load duration curve representing the annual peak load over a year. ....	20
Figure 2.4: Power systems operation under balanced three-phase conditions. ....	25
Figure 2.5: Chromosome encoding for $N_c$ possible connections to be added and $N_g$ possible locations of DG. ....	32
Figure 2.6: Initial population: (i) $N_c$ = all possible connections between distinct feeders combined with one random possible location of DG unit; (ii) $N_c$ = all possible connections between distinct feeders combined with possible locations of a DG unit within the buses in the feeder from which the connection is made; (iii) same as (ii) but $N_c$ = possible connections no longer than 3km between distinct feeders. ....	34
Figure 2.7: Flowchart of the fitness function proposed to evaluate the objective functions of the candidate solutions while satisfying the system and design constraints. ....	36
Figure3.1: Solution 4 for the MOGA applied to the 3FDR system with wind based DGs. ....	42
Figure3.2: Solution 5 for the MOGA applied to the 3FDR system with wind based DGs. ....	42
Figure3.3: Pareto front of the MOGA applied to the 3FDR test system. Triangles are solutions with wind based DG and stars are solutions with solar based DG. ....	44
Figure3.4: Solution 4 for the MOGA applied to the 3FDR system with solar based DGs. ....	45
Figure3.5: Solution 5 for the MOGA applied to the 3FDR system with solar based DGs. ....	45
Figure 3.6: RBTS bus 3 test system with annual average loads. ....	47
Figure 3.7: Line-to-neutral equivalent circuit of a three-phase line segment serving a balanced three-phase load, taken directly from [136]. ....	49
Figure 3.8: Six step-load duration curve reproduced from [132]. ....	51
Figure 3.9: Solution 2 of the MOGA applied to RBTS Case I. ....	56
Figure 3.10: Solution 4 of the MOGA applied to RBTS Case I. ....	57
Figure 3.11 Solution 6 of the MOGA applied to the RBTS Case I system corresponding to one of the maximum improvements of the reliability with ENS of 21.33 MWh at a cost of \$18.91 millions of US \$ ....	57
Figure 3.12: Computational time of RBTS Case I (cylinder) and II (box) for 50 generations and three types of configuration of the initial population. ....	60
Figure 3.13: Computational time of RBTS Case I (cylinder) and II (box) for 25 generations and three types of configuration of the initial population. ....	60



Figure 3.14: Pareto front of the MOGA applied to RBTS Case I with initial population type (ii) (rhombus) and initial population type (iii) (dots).....	61
Figure 4.1: Methodology proposed to determine the impact of a PHEV fleet on the annual reliability of distribution systems under islanded mode of operation. ....	66
Figure 4.2: Ontario Electricity TOU price periods for the summer and winter weekdays, and for the weekends and holidays. ....	79
Figure 4.3: Synthetic data of TOU price periods for the summer and winter weekdays. ....	79
Figure 4.4: Seasonal hourly load in percent of the daily peak load for weekdays ( <i>wd</i> ) and weekends ( <i>we</i> ) reproduced from [134]. ....	83
Figure 4.5: Winter hourly load profile for non-residential type of load (synthetic data).....	84
Figure 4.6: Load duration curve of the RBTS system base load, base load and PHEVs optimized for peak shaving purposes, base load and PHEV loads optimized for customers profit.....	85
Figure 4.7: Individual optimized PHEV battery charging patterns of four vehicles and total load for a weekday residential demand for peak shaving purposes. ....	86
Figure 4.8: Individual optimized PHEV battery charging patterns of two vehicles and total load for a weekday commercial demand for peak shaving purposes.....	87
Figure 4.9: Individual optimized PHEV battery charging patterns of four vehicles and total load for a weekday in winter with TOU pricing. ....	89
Figure 4.10: Individual optimized PHEV battery charging patterns of two vehicles and total commercial load for a weekday in winter with TOU pricing. ....	90
Figure 4.11: Load duration curve of the RBTS base load (1), base load and PHEV uncontrolled charging fleet (2), base load and PHEV delayed charging fleet (3). ....	91
Figure 4.12: Step-load duration curve of the RBTS test system without PHEVs (base load (1)) and with PHEVs optimized for peak shaving (2) and for customer benefit (3).....	92

## LIST OF TABLES

Table 2.1 Sets, parameters and variables of the MOGA.....	29
Table 3.1 Annual average load in the 3FDR test system [20] .....	38
Table 3.2 Parameters required for implementing the MOGA in the 3FDR test system .....	39
Table 3.3 results of the MOGA applied to the 3FDR test system with wind based DG.....	40
Table 3.4 Results of the MOGA applied to the 3FDR test system with solar based DG.....	43
Table 3.5 Design parameters for DG in the RBTS test system.....	48
Table 3.6 ACSR Flamingo data. Values for resistance, impedance and cost are reproduced from [108]. .....	50
Table 3.7 Annual average load and maximum peak load per load point in the RBTS test system [130]. .....	50
Table 3.8 Load levels in per units form the step-load duration curve and their respective duration in hours, reproduced from [134].....	50
Table 3.9 Solutions of the MOGA applied to RBTS Case I, numbered in increasing order of cost of the redesign .....	55
Table 3.10 Solutions of the MOGA applied to RBTS Case II, numbered in increasing order of cost of the redesign .....	58
Table 4.1 Parameters of the approximated function (4.1), taken directly from [90]. .....	68
Table 4.2 $K_{phev}$ ranges per class assuming $B_C$ SOC ranges, reproduced from [90].....	69
Table 4.3 Random battery size and $k_{phev}$ parameter obtained from <i>PHEVSim ()</i> .....	71
Table 4.4 Time parameters mean and standard deviation for weekday and weekends reproduced from [90] .....	72
Table 4.5 Probabilistic results of population size per vehicle class .....	81
Table 4.6 Size of the sets of indexes of the LP in the RBTS test system .....	82
Table 4.7 Weekly peak load in percent of annual peak load, taken directly from [134] .....	83
Table 4.8 Daily load in percent of weekly load directly taken from [134]. .....	84
Table 4.9 Annual average demand per load point in the RBTS base load system and the RBTS with PHEVs .....	93
Table 4.10 Annual maximum peak load per load point in the RBTS base load system and the RBTS with PHEVs .....	93
Table 4. 11 RBTS load levels in per unit from the step-load duration curves and their respective duration in hours (base load and with PHEVs).....	94
Table 4. 12 ENS of the RBTS radial legacy system with average annual demand .....	95

Table 4. 13 PNS per load level in the RBTS radial legacy system and annual ENS95  
Table 4.14 ENS of the RBTS system for redesign solutions of the RBTS test system ..... 97  
Table 4.15 Redesign solutions of the MOGA applied to the RBTS test system with PHEVs  
and with annual average demand modeled in the system. .... 99

Table A1.1 Line data of the existing connections in the 3FDR test system, reproduced  
from [20] ..... 119  
Table A1.2 Line data of the possible connections to be added in the 3FDR system  
reproduced from [20]. ..... 120

## ACKNOWLEDGEMENTS

I am very thankful to the Electrical Department in the Division of Engineering at the Colorado School of Mines (CSM). First of all, I would like to thank Dr. Suryanarayanan for the unique opportunity he afforded me, to join the graduate program of CSM as his research assistant. On the one hand, his rigorous and pedagogic approach to science and on the other hand, the confidence of success that he places on his students, makes Dr. Suryanarayanan an exceptional advisor. Secondly, I would like to warmly express my gratitude to Dr. Johnson. She gave me the opportunity of arranging my stay at CSM and supervising my independent research project required to finish my undergrad degree. I admire very much her generosity and sincerity, and I am very thankful for the unconditional help and support that she provided me in joining the graduate program at CSM. My life would have been very different without having met Dr. Johnson. In addition, I would like to thank the rest of the members of my committee, and specifically Dr. Simoes for his support and guidance. Finally, I am very grateful to Dr. Sen for his passion for teaching and transmitting his knowledge in power systems, Dr. Newman for her admirable dedication, enthusiasm and time placed on teaching optimization and operations research and to Dr. Moore, for his committed support in administrative affairs.

It is my pleasure my family back in Spain. To my mother and my father, I am very thankful for the only one of its kind inspiring environment that they created for their daughters to grow up, and their believe in our success. To my sister, for being my “other half” and reassuring me that my thoughts are always understood. I must also thank my family in the US. A very sincere thanks to Brian, for his patience and confidence in me and in life, and I am delighted to share my future with him. Also, thanks to the rest of the “Qs” for the love and happiness they spread. Finally, I would also like to state my gratefulness to my fellow students at CSM. In particular, to Steve for sharing his broad knowledge and always being available to help me, to Ricardo for helping me out in stressful moments, and to Cicero, Goele, Denise and Virtu for their fun times.

The work contained in this thesis was supported in part by PSERC Project T-41, “Implications of the Smart Grid Initiative on Distribution System Engineering”. I would like to thank Hillary. E Brown for her patience and kindness in educating me and sharing with me her research.

Gracias...!

## NOMENCLATURE

3FDR	Simplified three-feeder test system
$a_c^E$	Performance parameter per class $c$ for the approximation function of $E_c$
$A_{d,c,v}$	Arrival time for vehicle $v$ - of class- $c$ on day- $d$
ACO	Ant Colony Optimization
AGC	Automatic Generation Control
AMI	Advanced Metering Infrastructure
AMPL	A Mathematical Programming Language
ANL	Argonne National Laboratory
ARRA	American Recovery and Reinvestment Act of 2007
ASAI	Average System Availability Index
$B_c$	Battery capacity per class $c$
$b_c^E$	Performance parameter per class $c$ for the approximation function of $E_c$
$b_{Lk}$	percentage loading on branch $k$
$C_{d,c,v,t}$	Charge in the battery by the end of time period $t$ on day $d$ , vehicle class $c$ and vehicle $v$
$C_{d,c,v,t}^+$	Charge rate into the battery in time period $t$ on day $d$ , vehicle class $c$ and vehicle $v$
$C_{d,c,v,t}^-$	Discharge rate out of the battery in time period $t$ on day $d$ , vehicle class $c$ and vehicle $v$
CD	Charge Depleting
CDG	Conventional Distributed Generation
$C_g^{DG}$	Cost of a DG located at bus $g$
CF	Capacity Factor
$C_i^C$	Cost of the possible connection $i$
$c_j$	Objective function $j$
CPP	Critical Peak Pricing
CS	Charge Sustaining
$D_{d,v}$	Departure time for vehicle $v$ of class $c$ on day $d$
DA	Distribution Automation
$DE_{d,c,v}$	daily recharge energy
DER	Distributed energy resource
DG	Distributed generation
DOE	US Department of Energy
DR	Demand response
DRP	Demand Response program
DS	Distributed Storage
DSM	Demand Side Management
$E_c$	Energy required driven per vehicle class $c$
EISA07	Energy Independence and Security Act of 2007
EMS	Energy Management System
ENS	Energy Not Supplied
ESS	Energy Storage System

GA	Genetic Algorithm
GAOT	Genetic Algorithm Optimization Toolbox
GEP	Generation Expansion Problem
HWFET	Highway Fuel Economy Test
IC	Internal Combustion
IDP	Interruptible Demand Program
IT	Information Technology
$K_{drop}$	K drop factor
$K_{phev}$	Amount of driving energy supplied by electricity
$L$	Lower triangular matrix of the Cholesky factorization of the covariance matrix $\Sigma$
$L_{\beta}$	Load level $\beta$
$L_{\beta max}$	annual maximum load level $\beta$ (peak demand)
$L_{\beta min}$	annual minimum load level $\beta$ (base load)
$L_{d,i,t}$	Load on day $d$ at load point type $i$ and time period $t$
$L_{d,i}^{av}$	Average annual load on day $d$ and load type $i$
$L_{d,i,t}^{peak}$	Peak load on day $d$ , load type $i$ and time period $t$
$L_g$	Sum of the average installed loads at bus $g$
$L_i^C$	Length of the possible connection $i$
$L_{iALoad}$	Average annual load at load point $i$
$L_{i\beta}$	Demand at load point $i$ and load level $\beta$
$L_{iPLmax}$	Highest annual peak demand at load point $i$
$L_{i,t}$	Demand at load point $i$ and hour $t$
LEPS	Local Electric Power System
LP	Linear Program
$M^D$	Charge depleting distance
$M_{d,v}$	Distance driven on day $d$ by vehicle $v$
MOGA	Multi-Objective Genetic Algorithm
$N$	Standard normal value
$N_{\beta}$	Number load levels $\beta$
$N_{branch}$	Number of branch loading violations
$N_{bus}$	Number of bus voltage violations
$N_c$	Number of possible connections
$N^C$	Number of vehicle classes $c$
$N^D$	Number of days in a year
$N^I$	Number of load point types
$N_g$	Number of possible DG locations at bus $g$
$N_t$	Total number of transportation vehicles
$N^T$	Number of hours in a day
$N^V$	Number of vehicles
NREL	National Renewable Energy Laboratory
P	Overall penalty function
Pbranch	Branch penalty function
Pbus	Volatge penalty function
$P_{d,t}$	Daily energy price per time period $t$

$P_g^{DG}$	Power output of a DG located at bus $g$
$P_{out}$	Power output of a DG
$P_s$	Power output of slack bus $s$
PHEV	Plug-in Hybrid Electric Vehicle
PNS	Power Not Supplied
PSAT	Powertrain System Analysis Toolkit
PSERC	Power Systems Engineering Research Center
PSO	Particle Swarm Optimization
$R$	Total rating of a DG source
RE	Renewable Energy
RBTS	Roy Billinton Test System
RTP	Real Time Pricing
RTS	Reliability Test System
$S_{ab}$	Loading in the line from bus $a$ to $b$
SA	Simulated Annealing
SGI	Smart Grid Initiative
SOC	State of charge
$T_{d,v}$	either the arrival time or the departure time on day $d$ for vehicle $v$
TNEP	Transmission Network Expansion Problem
TOU	Time-of-use
$U$	Annual outage time of a system as a fraction of a year
UDDS	Urban Dynamometer Driving Schedule
US06	Updated federal test driving cycle 2006
$U_1, U_2$	Pseudo random numbers
$V_{d,c,v,t}^+$	Positive difference between $C_{d,c,v,t}^+$ and $C_{d,c,v,t}^-$
$V_{drop}$	Voltage drop
$V_k$	Per unit voltage at bus $k$
V2G	Vehicle-to-grid
VOLL	Value of lost of load
$W_{d,c,v,t}^+$	Absolute value of the difference between $V_{d,c,v,t}^+$ and $V_{d,c,v,t+1}^+$
$X$	Vector of variables
$X_g$	Binary variable of DG location at bus $g$
$X_i$	Binary variable, connection $i$ closed
$Z_{d,i,t}$	Absolute value of the difference between $L_{d,i,t}$ and $L_{d,i}^{av}$
$\Delta$	step size of load levels
$\Delta T_\beta$	Hours in a year for which the load level is less than or equal to $L_\beta$
$\mu$	Mean of a probabilistic distribution
$\Omega$	Solution space (feasible region)
$\sigma$	Standard deviation of a probabilistic distribution
$\Sigma$	Covariance matrix

## CHAPTER 1

### INTRODUCTION

#### 1.1 Objective

The objective of this thesis is to extend methodologies for the redesign of electric distribution systems by incorporating elements of emerging distribution systems. First, the purpose is to enhance an existing technique to improve the reliability of radial distribution systems under islanded mode of operation through the optimal integration of Distributed Generation (DG) and addition of networked lines. Secondly, the objective of this thesis is to develop a methodology to analyze the contribution of Plug-in Hybrid Electric Vehicles (PHEVs) to the reliability of such power system islands.

#### 1.2 Motivation

In the U.S., the Smart Grid Initiative (SGI) is outlined in Title XIII of the Energy Independence and Security Act of 2007 (EISA07) [1]. It is the policy of the United States to support the modernization of the Nation's electricity transmission and distribution system to maintain a reliable and secure electricity infrastructure that can meet future demand growth. The US Department of Energy explains the necessity of the SGI, and describes that the grid's development has mirrored the growth in population and global economy and as a result, the reliability of the grid is the biggest risk of the grid as it is nowadays: there have been five massive blackouts over the past 40 years, three of which have occurred in the past nine years, and outages and power quality issues are estimated to cost American businesses more than \$100 billion on average each year [2]. Moreover, the savings from a more efficient grid is seen as an opportunity for improvement. The outages are also viewed as a national security issue, and finally, the desire of being more attuned to environmental aspects and climate change are addressed, as well as increasing the global competitiveness of the U.S. in the modern energy market. In Europe, the modernizations efforts on the grid are beheld in the European Energy Commission's 2006 Green Paper "A European Strategy for Sustainable, Competitive and Secure Energy"[3]; this is presented in three main themes, namely sustainable energy mix, security of power supply, and competitive energy market. The European technical platform for the electricity networks of the future presents Smart Grids as a necessary response to the environmental, social, and political



demands placed on energy supply [4]. Finally Asia and South America are moving towards smart grids [5,6]. However, the challenges are more diverse in Asia and South America than in Europe or the United States, where the challenge depending on the country is more grid renovation than grid extension. The most notable policy from a Smart Grid perspective in China is the 2007 Energy Policy declaration [7] and in India is the National Electricity Policy of 2005 [8], where the need to do important grid related activities is addressed such as strengthen regional power grids and power transmission and distribution networks, develop an emergency response system for power safety and reliability, strengthen power Demand Side Management (DSM) and reinforce the priority policies for renewable energy electricity among others.

This general overview of the motivations from all over the world for modernizing the power grid has common directions of work at the distribution level. It is widely expected that most of the recommendations of the SGI are going to affect the distribution sector of the electricity delivery infrastructure, to make inroads into load relief of the transmission system by increasing the generation in the distribution system and enabling new ways of physical and virtual storage to balance consumption and production in order to improve reliability in supply. One of the implementation topologies that caters to the SGI is the distributed islanded resource or microgrid [9]. This entity is defined as a self-contained autonomous subset of the area electric power system, operating at voltages at or below the primary distribution voltage and with access to micro-sources, distribution system assets, control and protection gears, and at least one end-user facility and capable of operating in one of the following two modes – grid islanded and grid interconnected [10,11]. There are concentrated efforts in research, development, and demonstration (RD&D) currently in progress in Europe, the United States, Japan, and Canada on microgrids which are able to provide power quality and reliability different from general macro-grid standards [12].

In addition, if proper policy is in place, PHEVs can provide a promising solution to increasing generation in the consumer end side of the grid and enabling new ways of physical storage, acting as mobile decentralized storage. The American Recovery and Reinvestment Act of 2009 (ARRA) provides energy incentives for both individuals and businesses for qualifying plug-in electric drive vehicles purchased after 31 December, 2009 [13]. The US Department of Energy (DOE) has already identified a range of policies, incentives and regulations designed to enhance the probability of success in commercializing PHEVs as they enter the automotive marketplace starting in 2010 [14]. The entire concept of using the battery of a vehicle as a Distributed Energy Resource (DER) – load and resource – is known as the vehicle-to-grid or V2G

concept [15]. In this capacity, PHEVs can serve in two modes: V2G where power flows from vehicle to grid and the reverse, grid to vehicle where power flows from the grid to the battery vehicle. The mobility of the energy storage in PHEVs allows for strategic placement of the DG source to optimize power system needs. Widespread deployment of PHEVs will allow for increased energy storage, and improved reliability and stability of the electric grid [16]. Linking the transportation and power systems through PHEVs will allow for electrical energy storage on a scale much larger than is currently feasible [15]. The additional energy capacity will be directly proportional to the penetration of PHEVs into the automobile market, and modeling is needed to determine the increase in capacity across the space and time dimensions [17].

As the SGI progresses toward implementation, it is imperative to study the design of the emerging distribution systems as an evolution of the legacy system – specifically, from the radial topology to a partially meshed network system with DG, seemingly resembling a transmission system so as to maximize the reliability of the distributed islanded resource [18]. Furthermore, it is apparent that customers who own PHEVs would seek to attain optimal operational profits from the V2G capability of their cars while the utilities to which such customers connect may potentially use the PHEV for peak shaving purposes and increase energy storage, as with Distributed Energy Resources (DER) installations [19]. Modeling of a PHEV fleet, with an emphasis on maximizing consumer profit and/or utility peak shaving capability is attractive to determine their possible contribution to the reliability of emerging electric distribution systems under islanded mode of operation.

### 1.3 Scope

The scope of this thesis includes an extension of an existing method described in [20], to selectively modify a legacy radial topology to maximize reliability on an islanded distribution system. The enhancements presented here are: consider simultaneous co-location of DG and feeder interties, as opposed to assumed locations of DGs, use annual load duration curve for expressing the load in the distributed island resource as opposed to average loads alone, and measure of the impact of PHEVs on the reliability of legacy radial and redesigned distribution systems. The extended method presented in this thesis models DG as in [20], where the capacity factor (CF) of the generators is used to represent their power output.

Furthermore, a methodology to determine the contribution of PHEVs with V2G capabilities to the reliability of islanded distribution systems is presented. This technique is based

on optimal charging patterns of a simulated PHEV fleet behavior over a year, to maximize the profit of the customers as well as for utility Demand Response (DR) actions.

However, the scope of this thesis precludes protection and control topics that are key features for the operation of such electric power systems with generation on the customer end of the grid, but also for the operation of DGs themselves (including PHEVs with V2G technology).

## 1.4 Literature Search

This section describes primarily the evolution of electric distribution systems under the smart grid paradigm. Following which, the literature review is split in three themes: first, current research on distribution planning methodologies, secondly, a discussion of the state-of-art of PHEVs studies on distribution networks and at last, a section on tools and methods used in this thesis.

### 1.4.1 Evolution of distribution systems with smart grids

“Smart Grids” have been defined as electricity networks that can intelligently integrate the behavior and actions of all users connected to it - generators, consumers and those that do both - in order to efficiently deliver sustainable, economic and secure electricity supplies, employing innovative products and services together with intelligent monitoring, control, communication, and self-healing technologies. [4]. “Grid 2030” report, a policy that aided the smart grid concept, identified several promising technologies for incorporation in the electricity grid, such as DG, distributed intelligence, advanced energy storage, smart controllers, and power electronics, with the vision of creating a national electricity backbone, providing efficient generation from many sources to take advantage of varying seasonal and regional peak differences, which would be supported by regional interconnections and local distribution systems, which may be mini- and/or micro-grids [21]. In this thesis, a smart grid is understood as a way of operating the power system using a set of enabling technologies (communication, power electronics and storage) to balance new types of production and consumption at all levels, i.e., from the generation side to the customer side.

Title XIII of the EISA07 [1], characterizes a smart grid which includes:

- Deployment and integration of distributed resources and generation including renewable resources
- Development and incorporation of DR, demand-side resources, and energy-efficiency resources
- Deployment of 'smart' technologies (real-time, automated, interactive technologies that optimize the physical operation of appliances and consumer devices) for metering, communications concerning grid operations and status, and distribution automation
- Deployment and integration of advanced electricity storage and peak-shaving technologies, including PHEVs, and thermal-storage air conditioning.
- Provision to consumers of timely information and control options

The power grid is moving from a centralized generation characterized by large power plants in the generation side, towards a small and dispersed generation on the distribution side. Centralized generation has been the traditional way of production of electrical power to the transmission system of the grid, which is finally distributed to the users. DG or DER are characterized by being placed in the distribution side of the grid and by small power generation and/or storage. Definitions of DGs or DERs in the literature prepared by different Institutes, Agencies, Governments, etc, are presented in [22-24]. For low levels of penetration of up to 15% of peak demand, DGs do not have a large effect on distribution systems [25]. However, a smart grid must have the potential to integrate large sources of DER in which case, the distribution systems may begin to resemble to a small transmission system and similar design issues need to be considered such as non-radial topologies. Small generation at the customer interface such as DG but also PHEVs with V2G capabilities complicate the power flow analysis and control of the network. Protection and control schemes will need to account for bidirectional power flow and multiple fault sources [26] as well as interconnection issues different from those of conventional systems [27]. However, as mentioned earlier, the protections and control aspects are out of the scope of this thesis.

Over the years, there have been numerous studies that suggest that consumers would use less electricity if they knew how much it was costing them [28]. DR enables the capability of a more active network at the distribution level where demand-side resources are managed to meet the available generation and the grid's power delivery at any time [29]. For that, Advanced Metering Infrastructure (AMI) needs to be deployed to improve demand-side management,

energy efficiency, and a self-healing electrical grid. Smart meters empower an AMI which is able to react almost in real time, provide fine-grained energy production or consumption info and adapt its behavior proactively. Smart meters provide new opportunities and challenges in networked embedded system design and electronics integration. They are able not only to provide (near) real-time data but also process them and take decisions based on their capabilities and collaboration with external services. That in turn has a significant impact on existing and future energy management models. Households and companies are able to react to market fluctuations by increasing or decreasing consumption or production, thus directly contributing to increased energy efficiency [30].

The result of the electricity market structure is that the wholesale price of electricity, reflecting the supply and demand interaction, varies constantly. Real Time Pricing (RTP) of electricity describes a system that charges different retail electricity prices for different hours of the day and for different days, based on end-use and supply availability. The end-use costumers and devices can have visibility of possible distribution grid conditions and dynamic prices and are able to control their consumption. An existing form of implementation of dynamic pricing is time-of-use (TOU). Under TOU, the retail price varies in a preset way within certain blocks of time. Because TOU rates do not capture the price variation within a price block, TOU pricing is often combined with a separate charge for peak usage. These “demand charges” are a price per kilowatt for the highest usage by the consumer during the billing period (usually a month). Reference [31] describes five types of programs for introducing greater economic incentives into electricity demand: RTP, TOU with or without demand charges, Critical Peak Pricing (CPP), Demand Reduction Programs (DRPs), and Interruptible Programs (IDPs). CPP programs usually start with a TOU rate structure, but then they add one more rate that applies to “critical” peak hours, which the utility can call on short notice. (DRPs) pay a customer to reduce their consumption at certain times and IDPs give the system operator the right to instruct the customer to cease consumption on very short notice. In return, the customer receives some sort of compensation in its electricity rate. All of these programs attempt to give end-use customers economic incentives to reduce their demand at times when the supply/demand balance in the system is tight. The importance of developing such programs from the utility side is a necessary factor to reflect hourly and daily change in pricing due to seasonal changes- thus, providing the end user with information and control capability.

Distribution Automation (DA) refers to monitoring, control, and communication functions located on the feeder [25]. The medium-voltage distribution network has traditionally

been passive, implying that it merely delivers power from bulk supply points to customers. DA enables a more active distribution network through key electrical power technologies and information systems such as adaptive and integrated protection systems required to provide flexible and optimized reaction to network fault conditions and real-time network simulation and analysis methods, key to providing decision support for operation and management systems [32]. Electric power utilities worldwide are increasingly adopting the computer aided monitoring, control and management of electric power distribution system to provide better services to electric consumers. Therefore, research and development activities worldwide are being carried out to automate the electric power distribution system utilizing recent advancement in the area of Information Technology (IT) and data communication system. Reference [33] reports the present and past status of the research and development activities in the area of electric power distribution automation both in developed as well as in developing countries and highlights advanced sensors and distributed communication links as essential to allow the transfer of real-time power system data. One of the features provided by DA is feeder reconfiguration which will be described in more detail in the next section 1.4.2.

Finally, the SGI encourages integration storage and peak-shaving technologies including PHEVs. Stressed and less secure power system operating conditions have encouraged both power utilities and large industrial power consumers to look for bulk energy storage systems. Reference [34] reports on the need of development of techniques to enable the benefits of Energy Storage Systems (ESS). The peak-shaving application is particularly attractive for large industrial plants [35], where battery ESS can be used to reduce peak demand and thus reducing the plant electricity bill by discharging stored energy during peak loads. ESS working in parallel to DG, to the advantage of DG owners is also an emerging area of research. References [36,37] develop techniques to drive the operation of residential DER with ESS toward regions of operational profit. Energy can be stored in PHEV batteries during the night - when the price is expected to be low and is withdrawn during peak-time when the price is high. By acting in such a way, they are suitable for peak-shaving purposes as well as for ancillary services. In a further section 1.4.3, the state-of-the-art in many fields of research regarding the impacts of PHEV deployment on electrical power systems is presented.

#### 1.4.2 Distribution planning methods

Under the smart grid paradigm, new capabilities are expected from electric distribution systems that are moving towards an automated and intelligent distribution network. Distribution

systems are expected to be planned more as an integrated network of distribution lines and distributed resources.

One of the features that DA enables is the reconfiguration of distribution systems at the operation level. The feeder reconfiguration problem consists of changing the topology of a distribution system through resetting the status of the switches located at certain points of the network [38]. Reconfiguration is performed to improve the distribution systems operating conditions while satisfying the network constraints such as voltage tolerance and line loading limits. Because feeder reconfiguration is a combinatorial optimization problem, soft computing methods are commonly used including GA (Genetic Algorithm), ACO (Ant Colony Optimization), SA (Simulated Annealing) or PSO (Particle Swarm Optimization) [39]. The more traditional class of approaches has been based on heuristic search techniques [40].

Reference [41] compares a linear programming method and two heuristic methods order to reduce the losses in distribution systems. Linear programming methods have proven unsuitable for feeder reconfiguration since the objective function and constraints are inherently non linear. The first heuristic technique is based on optimal load flow method and requires efficient and accurate methods for solving such power flow problem repeatedly which can make the approach too inefficient. The second one is a heuristic search method considering all possible switching options and although more time consuming than the optimal load flow method, it is reasonably fast. Heuristics techniques have been widely used for loss reduction such as non-linear methods based on discrete ascent considered in [42] and based on optimal power flow calculations in [43]. Moving towards evolutionary techniques, Genetic Algorithms (GAs) are among the most used methodologies. References [44 -46] approach the loss minimization problem through network reconfiguration using GAs. Other objective improvements of distribution systems through feeder reconfiguration using GAs are considered in the literature such as the cost of the reconfiguration [47], time-delay for network control systems [48], DG penetration in distribution networks [49], and congestion management [50]. In recent years, the reconfiguration problem has been addressed in a multi-objective manner to increase the complexity of the problem by improving multiple objectives which may be in conflict with each other. GAs are used for multi-objective approaches for real power loss and voltage drop due to three-phase fault minimization [51], and losses and reliability improvement [52]. Other evolutionary techniques have been applied such as Artificial Immune Systems (AIS) and ACO considering system loss, transformer load balance and voltage deviation from nominal value [53], and fuzzy-logic [54], applied for the minimization

of the system power loss, the deviation of node voltages, the branch current constraint violation and finally the load balancing among various feeders.

The ability enabled by DA to quickly and flexibly reconfigure and interconnect network feeders is a key component of the Smart Grid which has an impact on the distribution system design. However, the related work to the reconfiguration problem presented above is done from an operational perspective and considers only the network with radial topologies and rarely considers the presence of DG. The problem addressed in this thesis is the reconfiguration of radial legacy distribution systems from a design point view [40].

The problem of expansion planning to a distribution system consists of determining the capacity, sitting, and timing of installation of new distribution equipment, taking capacity restrictions on feeders, voltage performance, and demand forecasts into account [55]. DG offers an alternative that utility planners should explore in their search for the best solution to electric supply problems, in particular for deferring investments in the transmission infrastructure. DER installations can be strategically placed in power systems for operational improvement of distribution systems such as loss reduction, on-peak operating costs, voltage profiles and load factors, reliability, etc. Reference [56] presents analytical approaches for optimal placement of a DG power unit in a radial and in a networked system to reduce the system losses. The proposed approach was non-iterative unlike power flow programs. Therefore, there is no convergence problem involved, and results could be obtained quickly. However, the authors have indicated that other constraints such as voltage and line limits may affect the DG placement. Heuristic methods have gained attention because they can work in a straightforward fashion with nonlinear constraints and objective function; although there is no guarantee that an optimum solution can be found [57]. Additionally in this approach, it is also easy to introduce aspects, such as losses, reliability, and uncertainties. Notable among heuristic methods are the branch-exchange algorithms [58] and algorithms based on evolutionary computation such as GAs [59-63]. Other heuristic methods that have been used for the problem include the ACO [64], SA [65], and tabu search [66]. A method based on GAs, able to support distribution network operator in planning phase is proposed for solving distributed generation planning problem in different utility scenarios as an optimization problem [60]. The objective function is based on supply-demand chain which aims to minimize the investment and operating costs of local candidate DGs, payments toward purchasing the required extra power by a distribution company, payments toward loss compensation services, as well as the investment cost of other chosen new facilities



for different market scenarios. Among the feasible network upgrades, the method selects the new lines to build that minimize the mean square error of the buses voltages. Another GA search technique for DG allocation is presented in [61] where it is used to reduce losses and improve voltage profile. Not only the siting but the sizing has also been considered using GAs in order to reduce power losses and improve voltage profile [62], as well as to minimize the cost of power losses, service interruptions, network upgrading and cost of energy [63].

Distribution systems, having the potential to integrate large sources of DER affect the topology of distribution systems i.e., they begin to resemble small transmission systems. Another design issue is related to the ability of distribution systems to operate as an electrical island. DGs, either utility or private owned, can be used to sustain a distribution system during unavailability of the transmission feeds. The experience of Hydro-Quebec in islanding for the maintenance of a transmission line is given in [67], where studies that should be done prior to planned islanding of distribution systems with DER such as protection, stability, flicker and power factor are presented. In general, such distribution island or microgrid, may comprise part of medium/low voltage distribution systems served by distributed resources. A microgrid may operate with a point of common coupling to the rest of the grid and can shift between a grid-dependent mode or a grid-independent (autonomous mode) depending on power exchange and interaction of such microgrid with the main grid [68]. This ability relies on the flexibility of advanced power electronics that control the interface between distributed sources and the network. Power electronics control and communication capabilities that permit a microgrid to function as a semiautonomous power system is a key feature for islanding [69]. IEEE 1547 2003 Standard for Interconnecting Distributed Resources With Electric Power System is the first in the 1547 series of planned interconnection standards [70]. This standard rests on certain assumptions about the contribution of DER to power quality and reliability. Although IEEE 1547 does not use the term microgrid, it allows for implementation of a group of DER, which it refers as a Local Electric Power System (LEPS) and applies at the point where LEPS or microgrid connects to the grid, i.e. applied to a microgrid containing many small DER devices would be the same as for one large DER [71]. However the applicability of IEEE 1547 is limited to DER rating of 10 MVA, which may be smaller than the ratings expected for microgrids [70]. From a distribution systems planning perspective, the approach is to develop microgrids that may be networked in structure and conform to the US DOE vision of microgrid, and can operate in both grid-connected and islanded modes [9]. Once again, analytical techniques to solve the problem of developing optimal microgrid architectures have been developed [72, 73], as well as heuristic methods such as PSO

[74] and SA [75]. Yet, fewer studies have considered the topological design of distribution networks and DG assessment in microgrids. Reference [76] envisions the development of optimal microgrid architectures based on PSO consisting of two aspects: optimal sizing and siting of DG, and optimal network topology, comprising an optimal set of interconnections and associated capacities.

#### 1.4.3 State-of-the-art in PHEV studies

Under the SGI, PHEV is one of the tools to integrate electricity storage and peak-shaving technologies. A PHEV is defined by the IEEE, as “vehicles that have a battery storage system rating of 4 kWh or more, a means of recharging the battery from an external source, and the ability to drive at least 10 miles in all electric mode” [77]. PHEVs presence on the market has emerged and there are vehicles with PHEV technology currently available [78]. Prototypes are being built by universities and research centers and auto manufacturers are developing next generation PHEV technology [79]. A rapidly growing number of studies report on PHEV performance and impacts. These studies typically fall into one or more of the following categories: (1) vehicle performance studies that look at the cost of ownership and emissions impacts; (2) supply adequacy studies that aim to assess the potential to meet growing demand with existing generation assets; (3) vehicle-to-grid (V2G) studies, that look at the value of vehicles for the provision of bi-directional grid support services; and (4) distribution system studies, which study the impact of increasing PHEVs on the medium/low voltage network infrastructure. In all categories, the need of simulation tools to model the real-world drive cycles characterizing the US vehicles fleet behavior is a requirement, in order to replicate and study vehicles performance and impact and contribution to the power grid. PHEVs can be externally charged to directly displace petroleum during short trips while operating in a Charge-Depleting (CD) mode. After depleting the externally charged energy, PHEVs still achieve high fuel economy through regenerative energy recovery during braking, turning the engine off instead of idling, and enabling higher engine efficiency. This operation is referred to as the Charge-Sustaining (CS) mode.

The dual operating modes that make PHEVs attractive also make it difficult to estimate their in-use fuel economy directly dependent on the miles driven by each vehicle, and necessary information to study the vehicle’s performance. Simulation tools such as ADVISOR [80] have been developed by the National Renewable Energy Laboratory (NREL). Another modeling software for PHEVs is Powerdrive Simulation Analysis Tool (PSAT) [81], a major simulation

tool of DOE developed by the Argonne National Laboratory (ANL) and has been used for numerous studies to assist DOE in identifying future research directions regarding plug-in hybrid electric vehicles. The increased complexity and diversity of the technologies has led to a partnership, initiated by General Motors in 2007, to develop the next generation of automotive simulation tools [82]. In the past three years, ANL has developed a new tool, called Autonomie [83], to accelerate the development and introduction of advanced technologies through plug-and-play architecture. Autonomie enables the evaluation of new powertrain and propulsion technologies for improving fuel economy through virtual design and analysis.

Vehicle performance studies of PHEVs include, battery and power requirements as well cost analyses and emissions are [84-90]. PHEV penetration could significantly reduce CO<sub>2</sub> emissions from the automotive sector and advances in battery technology have already put practical electric vehicles within reach; however, further advancements in manufacturing costs and storage capacity are needed to make such vehicles appealing to the mass market. Concerning category (2), i.e. power supply adequacy, there is a general agreement that as long as PHEVs do not increase peak demand, their use will not require the construction of new power plants. The vast majority of existing studies find that there is sufficient surplus of generation capacity during off-peak hours to fuel a large number of PHEV penetration [89-92]. However, this is only the case if the charging of vehicles is optimized. In addition, changes in demand and new structures for electricity prices and emissions standards created by the introduction of PHEVs, may lead to negative consequences in some regions if the current utility plan is not changed [93].

V2G study is the term used in the literature to describe the use of bi-directional charge/discharge capabilities of PHEVs. PHEV with V2G capabilities can increase grid reliability, lower electricity generation costs, potentially reduce emissions by facilitating the integration of renewable based generation and provide a revenue stream for electric vehicle owners [15]. A detailed description of four electric markets and their suitability to purchase V2G power concluding their participation in ancillary service market and regulation is provided in [15], and reference [94] evaluates the feasibility and practicality of vehicles providing a grid ancillary service called regulation. Regulation, also referred to as Automatic Generation Control (AGC) or frequency control, is used to control the frequency and voltage of the grid by matching generation to load demand at the second and minute time scale [15]. V2G implementation and business models are also being the focus of research. The deployment of PHEVs with V2G capabilities for integration of large scale solar for peak power and large scale wind for base load power is being considered to stabilize the grid [95,96]. Additionally, V2G is also seen as storage

source for future large offshore wind power [97]. Reference [98] presents techno-economic issues of plug-in hybrid vehicles with V2G operation, including the policies needed to integrate in the electricity market. In category (3), researchers are working on long-term infrastructure and information architectures required for a massive market infiltration of PHEVs. The grid operator may send request of power for supply to each individual vehicle, or to the office of a fleet operator, or through a third party aggregator of dispersed individual vehicles. In order to achieve infiltration of the ancillary services market, V2G must satisfy the requirements of the grid system operator of industry standard availability and reliability from the V2G system [99, 100]. On the other hand, the vehicle owner will demand a return on their investment in V2G technology which requires development of the economics of V2G using pricing techniques [99-101].

Finally, moving from the contribution of PHEVs to their impact on the power grid in category (4), the additional load that PHEVs add in distribution systems typically designed for specific load carrying capability based on load consumption patterns of customers is a concern. PHEV market penetration is likely to be higher in some areas than others, and it is important for utilities to be aware of these regions in order to appropriately focus on maintenance and monitoring resources, particularly in transformers just as when traditional electric loads increase in parts of the grid [89, 90], [102, 103]. As mentioned earlier, the charging of PHEVs has an impact on the adequacy assessment of generation but also on distribution systems if undesirable and larger peaks occur in the electrical consumption [104]. The improvements in power quality and efficiency [105], and benefits in cost and emissions of coordinated charging patterns have been explored [88]. However, so far few publications have explored the optimal coordination between of PHEVs. A time coordinated optimal flow model for integrating PHEVs and tap changers in order to minimize power loss and tap changers usage is suggested in [106]. A quadratic and dynamic programming model for assessing the impacts of PHEVs on the distribution grid of Belgium when PHEVs are charged at home is developed in [107, 108], and are applied both to deterministic and stochastic methods to reduce power loss and voltage drop.

#### 1.4.4 Tools and methods

This thesis is organized in two main parts: first, Chapters 2 and 3 address the redesign of legacy distribution systems to increase the reliability by means of feeder interties and DG under islanded mode of operation; and secondly, the impact of PHEVs on such systems is quantified in Chapter 4.

For the first part, the optimization problem of the redesign of distribution systems is approached by using an evolutionary technique. Reference [20] shows that the solution space for the feeder reconfiguration problem from a design perspective is very large. A heuristic and a GA technique are compared and it is proven that as the number of possible topologies increases, the performance of the heuristic approach decreases [20]. However, the GA uses evolutionary operators to perform a multi-directional search by maintaining a population of potential solutions. The “population-to population” approach avoids the local minima within the search [109]. From a generation to another, a population undergoes a simulated evolution by means of selection, crossover and mutation evolutionary operators. Elitism is also employed from a generation to another, to preserve the best individuals in a population to evolve to the next [109]. For that reason and based on the conclusions presented in [20], the GA is the desired technique in the first part of this thesis.

The GA is implemented in Matlab™. This software has a Genetic Algorithms for Optimization Toolbox (GAOT) which provides many inbuilt functions [110]. The basic call of the multi-objective GA function which runs the simulated evolution requires an evaluation function unique to the problem at hand which is the fitness function. The fitness function unique to the redesign problem must evaluate the fitness of an individual in terms of cost and reliability and verify that such solution does not violate any system constraints. To obtain the reliability of a candidate solution and to determine any system constraint violations, a power flow calculation must be performed. Power flow computer programs are used for solving the power flow, i.e., computation of the voltage magnitude and angle at each bus and real and reactive power for the equipment interconnecting the buses in a power system under balanced three-phase steady-state conditions [111]. In this thesis, PowerWorld Simulator™ is the software tool used to perform such calculations [112]. This software has an add-on called Simulator Automation Server™ (SimAuto™), which allows the user to remotely access PowerWorld Simulator™ from an external program such as Matlab™ [113]. SimAuto™ enables to access the data of a test system modeled in PowerWorld™, perform data manipulations, compute a power flow calculation and send results back to the original application. In this thesis the original application is the fitness function and required by the multi-objective GA function used in Matlab™ to solve the redesign problem.

With regard to the study of the impact of PHEVs in the second part of this thesis, the optimization problem addressed is to determine the expected hourly charging patterns over a year of a fleet of PHEVs in a given distribution system. For that, the problem is formulated in as a

Linear Program (LP). LP has been used to optimize the operation Energy Management System (EMS) such as PV-battery storage systems [114], and as verification of a heuristic technique for scheduling a residential DER installation containing PV arrays and local energy storage [19]. AMPL™ is the mathematical computing environment used to program the LP, and IBM ILOG CPLEX™ is the solver employed. The Simplex method is the algorithm used by IBM ILOG CPLEX™ and is based on a search within adjacent extreme points in which the objective function value is computed. If a feasible extreme point provides an objective function value at least as good as that provided by its adjacent feasible extreme points, the extreme point provides an optimal solution [115]. In other words, due to the convex property of a feasible region in LP, a local optimal solution is globally optimal. For more information on the Simplex Method, refer to [116,117]. Finally, in order to provide the behavioral and design parameters of the PHEVs required by the LP in order to constraint the problem and compute the charging patterns, a probabilistic simulation methodology proposed in [90] is used.

The literature review provided above reflects the fundamental changes that are currently taking place or predicted to occur shortly in electric distribution systems. This thesis incorporates islanded mode of operation as a design problem to take into account in distribution systems planning as well as the move towards meshed network delivery systems with DG. Finally, a manner of quantifying the contribution of PHEVs with V2G as load and as generation to distribution systems is explored, based on optimized management of the electric vehicles by the owner or the utility that has not been explored so far, to the best knowledge of the author.

## 1.5 Organization of Thesis

The introduction to this thesis is followed by Chapter 2, where the modeling of electric distribution systems is described, as well as an enhancement to an existing technique to improve the reliability of radial distribution systems under islanded mode of operation through the optimal collocation of DG and addition of feeder inerties. Chapter 3 presents the results of the application of the said enhanced optimizing technique to two distribution test systems including several case studies. Next, in Chapter 4, a methodology to study the impact of PHEVs on distribution systems under islanded mode of operation is proposed, based on optimized charging patterns of an electric vehicle fleet. Finally, Chapter 5 concludes and discusses possible avenues of future work.



## CHAPTER 2

### OPTIMIZATION OF ISLANDED ELECTRIC DISTRIBUTION SYSTEMS

In this chapter, the modeling of electric distribution systems is presented. General reliability concepts are also presented in order to address the redesign of radial distribution systems into partially networked systems with access to distributed resources; this redesign is specifically applicable to islanded distribution systems which may function as *microgrids*. The evolution of such islanded distribution systems are validated by the IEEE standard 1547.4 [70]. The optimization problem addressed is the following: given a radial distribution system, to optimally collocate DG(s) and feeder intertie(s) between feeders at a feasible cost so to improve supply reliability, while satisfying power flow constraints in an islanded mode of operation of the distribution system. For that purpose, an expansion to the Multi Objective Genetic Algorithm (MOGA) methodology described in [20] is proposed in this chapter. The additions to the methods described in [20] are: the simultaneous location of DG and feeder intertie as opposed to assumed locations of DGs, the use of annual load duration curve for expressing the load in the distributed island resource as opposed to average loads alone and the study of the impact of PHEVs.

#### 2.1 Modeling a radial electric distribution system

Electric power distribution systems have traditionally a radial topology as shown in Figure 2.1. The main elements composing a radial feeder are: lines, transformers, buses, and loads. The infinite bus is a theoretical construct for modeling purposes representing the power grid, a large interconnected system with constant voltage magnitude and frequency. Alternatively, the infinite bus may be understood as an ideal voltage source providing the radial feeder with an infinite source of current at zero impedance.

The evolution of electric distribution systems that is addressed in this chapter consists of the optimal addition of both feeder interties between radial feeders and distributed generation units on the distribution end of the grid. The objective is to improve the reliability of the system; however, this must be done within the maximum cost of the project chosen by the candidate utility that owns the distribution system. Figure 2.2 illustrates the idea of evolving a traditional electric distribution system with generation on the consumer side, towards networked or meshed system topologies resembling the topology of the transmission side of the power grid. The distribution planning problem that is dealt with here has strong similarities with the Transmission



Network Expansion Planning (TNEP) and Generation Expansion Planning (GEP) problem [118, 119].

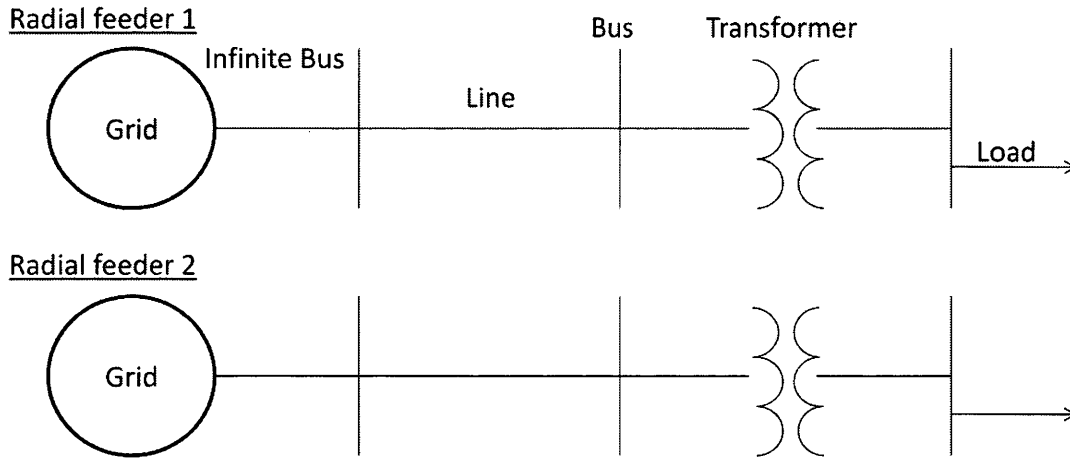


Figure 2.1: Elements of traditional radial feeders in electric distribution systems.

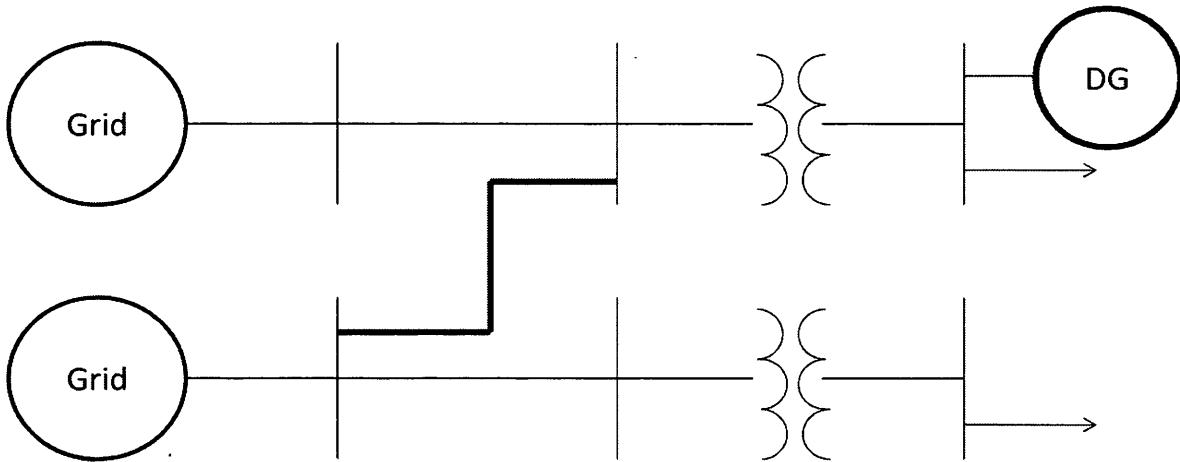


Figure 2.2: Evolution of electric distribution systems towards meshed systems with DG.

### 2.1.1 Modeling of the annual load

The electric power distribution redesign problem presented in this thesis is meant to improve the reliability of a given radial system, measured/quantified annually. In order to do so, the load points in the system have to be modeled by the load occurring annually. For that purpose, the loads can be represented in two modes:

a) Average annual load

In this mode, the annual load is represented by taking the values of the annual average load at every load point throughout the system as shown in (2.1). This representation assumes a fixed average value of the load for a year. The average annual load at load point  $i$   $L_{i,ALoad}$  represents the hourly load  $L_{i,t}$  occurring at that load point, which is a fixed value for the 8760 hours in a year.

$$L_{i,t} = L_{i,ALoad} \quad \forall t = 1 \dots 8760 \quad (2.1)$$

b) Step-load duration curve

In this mode of modeling, the demand includes a time dependency of the load. The time dependency of the load is incorporated by finding the hourly peak demands of the system over a year and convert them into a load duration step-curve [89,103]. This is shown in Figure 2.3, where hourly peak load is represented on the  $y$ -axis and the number of hours is represented on the  $x$ -axis. While it is feasible to obtain the peak load values of every load point for each hour for a one year study period (i.e., 8760 data points), performing a large number of power flow calculations may become computationally prohibitive and redundant. Within a year, each hour maps to exactly one load level  $L_\beta$ , whereas each load level may represent several hours  $\Delta T_\beta$ . To reduce the computational burden and redundancy, a reduced number of data points for the peak load values are chosen arbitrarily. Equation (2.2) defines the step size, which is gives the number of steps or load levels  $N_\beta$  between the maximum peak demand occurring in the system annually  $L_{\beta max}$ , and the annual peak base load  $L_{\beta min}$ . The number of unique values of the peak loads determines the resolution of the hourly component loading profiles. A higher number of steps  $n_\beta$  will increase the computational burden but will result in more accurate load profiles. In summary, the load duration step-curve reorders demands by increasing power levels, and so shows the percent of time that demand equals or exceeds a given power level  $L_\beta$  over a year (note that  $\Delta T_\beta = 8760$  hours). The demand at every load point  $i$  is given by (2.3), where  $L_{i,loadmax}$  is the highest annual peak demand at load point  $i$  and  $L_\beta(\Delta T_\beta)$  is the power level occurring for  $\Delta T_\beta$  number of hours.

$$\delta = \frac{L_{\beta max} - L_{\beta min}}{N_\beta - 1} \quad (2.2)$$

$$L_{i,\beta} = L_{i,PLoad_{max}} * L_{\beta}(\Delta T_{\beta}) \quad (2.3)$$

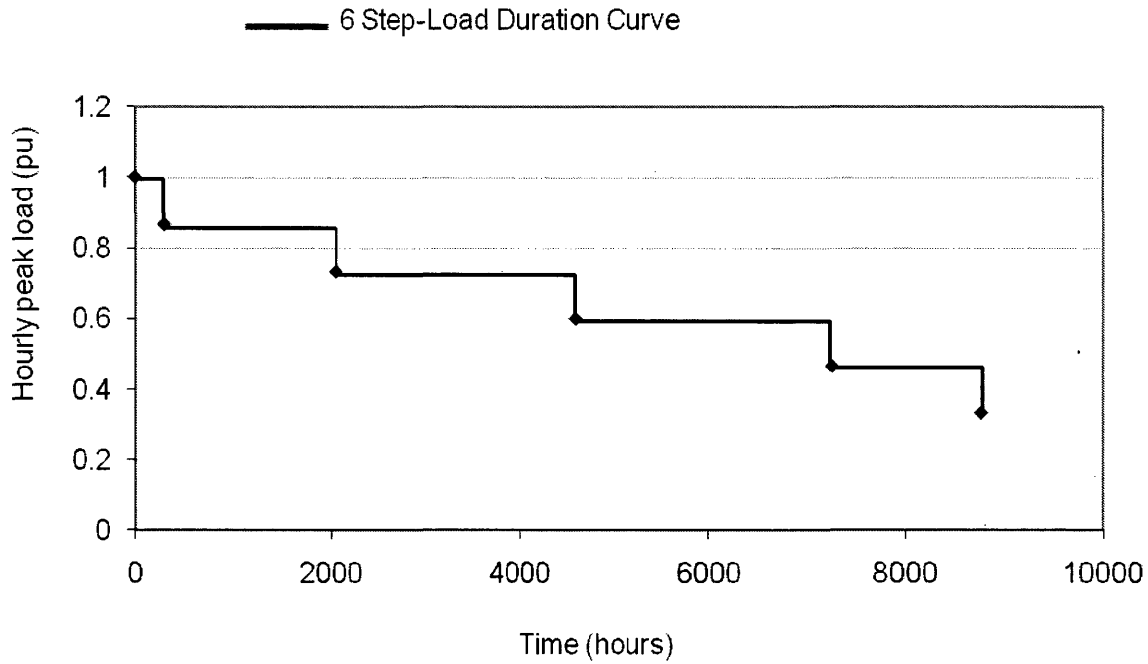


Figure 2.3: Step-load duration curve representing the annual peak load over a year.

### 2.1.2 Modeling of DG

DG is modeled as in [20], where it is proposed that the capacity factor (CF) of the generators is used to represent their power output. CF is the ratio between the actual power output of a generation source during a time period to the output if it had operated at rated power the entire time. CF includes the aggregate outage time for the entire year, without analyzing each separate outage event. The use of the CF to model the power output of DER has been largely used to avoid employing stochastic models for solar and wind generation, which impose the need for stochastic power flows, as well as stochastic load profiles.

The CF of a wind turbine is approximately 25% [120], depending on the wind resource available at the location of installation and 30% was selected for PV installation. The value for the PV installation reflects the CF of PV in Boulder, CO, geographically close to the location of the author. As in [20], it is assumed that the DGs introduced in the system have the adequate control systems in order to curtail or store the excess of generation, should the supply exceed the demand under islanded conditions.

Based on the generation mix identified by an industry survey seeking a definition of a smart distribution system [121], the total system DER power output is given by

$$P_{out} = RE + DS + CDG \quad (2.4)$$

where  $RE$ ,  $DS$ , and  $CDG$  correspond to the contributions from Renewable Energy resources, Distributed Storage and Conventional DG sources, and are calculated using (2.5)-(2.7). Equations (2.4-2.7) are directly taken from [20].

$$RE = R_{RE} * CF_{RE} \quad (2.5)$$

$$DS = ((1 - CF_{RE}) * 0.15 * L_g) \quad (2.6)$$

$$CDG = R_{CDG} * CF_{CDG} \quad (2.7)$$

where the  $R$  represents the total rating of the source listed in the index subscript:  $RE$  for RE resources and  $CDG$  for conventional (or, non-renewable) DG sources.  $CF$  indicates the capacity factor of the subscripted source.  $L_g$  represents the sum of the average installed loads at bus  $g$  where the RE resource backed by storage is installed. Equation (2.5) corresponds to the RE resource generation, while (2.6) describes the contribution of RE resources that are supported by DS and whose output is 15% of the total load at the installation point based on survey responses [20,121]. The rating of the CDG resource is given by  $R_{CDG} = R - R_{RE}$ , which is the rating of the RE resources in the system subtracted from the total DG rating of the system. In this thesis, the  $P_{out}$  is aggregated to known points throughout the test system, as explained in the following Example 1.

#### *Example 1*

*The total DG rating is 10 MW and the contribution from RE generation to the total DG rating is 20% with a capacity factor of 0.28. The capacity factor of CDG is 0.8. Two units, 1 and 2, are placed at two different buses with average annual connected loads of 0.8 MW and 0.9 MW respectively. Calculate the  $P_{out}$  of each DG unit using (2.4).*

$$P_{out} = R_{RE} * CF_{RE} + R_{CDG} * CF_{CDG} + (1 - CF_{RE}) * 0.15 * L_g$$

$$P_{out1} = (0.2 * 10 * 0.28 + 0.8 * 10 * 0.8)/2 + (1 - 0.28) * 0.15 * 0.8 = 3.5 \text{ MW}$$

$$P_{out2} = (0.2 * 10 * 0.28 + 0.8 * 10 * 0.8)/2 + (1 - 0.28) * 0.15 * 0.9 = 3.6 \text{ MW}$$

If the number of units was three, then the first term in the equations above will be divided by three. Note that the maximum number of units to distribute determines the minimum size of a DG unit. In this thesis, it is assumed that the size of a DG unit must be greater than the average annual load of the radial feeder in which the DG unit is located.

### 2.1.3 Basic reliability concepts

The term reliability when used in the context of the utility business usually refers to the amount of time end users are without supply for an extended period of time [122]. This extended period of time is known as an “outage”. Definitions on what constitutes a sustained interruption vary among utilities and end users. In this thesis, existing reliability indices for utility distribution systems will be employed to quantify the reliability. Reliability is affected by system events such as permanent faults on the system that must be cleared before service can be restored. For that reason, introducing DGs on the end user side of the system will increase the reliability of an electric power distribution system under islanded mode of operation while the system event is incipient.

One traditional reliability index that will be used in this thesis is the Average System Availability Index (ASAI) which may be defined as shown below [122]:

$$ASAI = \frac{\text{Customer hours service availability}}{\text{Customer hours service demand}} \quad (2.8)$$

where customer hours service demand = 8760 for an entire year. This index describes time as a fraction of a year for which the system is available.

Next, the load related metric used in this thesis to evaluate the reliability of a power system is the Energy Not Supplied (ENS) which quantifies in kWh the unserved load over a time period, generally one year, and is defined as shown below [123]:

$$ENS = \sum U_i \cdot L_i \quad (2.9)$$

where  $i$  refers to the load point with  $L_i$  average load connected and  $U_i$  annual outage time.

The annual outage time at every load point of the system is a value that is not as commonly available; the ASAI is used to compute the annual outage time of the whole system by subtracting the ASAI from unity as shown in (2.10), which represents the time as a fraction of a year for which the system is not available [20]. In order to obtain the annual outage time in hours,  $U$  in (2.10) is multiplied by the customer hours service demand explained earlier (i.e. 8760 hours).

When moving towards a distribution system with local generation on the consumer end, the average load connected at load point  $i$  is no longer the Power Not Supplied (PNS) of the system. The PNS is given by the demand not met by the generation in the power system under islanded mode of operation. As mentioned earlier, in order to successfully operate a power system under normal balanced three-phase steady-state conditions, generation must equal the demand in the system at all times and this is met through the slack bus construct represented as a generator. The slack bus output  $P_s$  of slack bus  $s$  in kW represents the PNS of a radial feeder; so, the sum of the slack bus outputs is the PNS of a radial distribution system with a slack bus per radial feeder for a given load and generation entered data.

The two ways of modeling the annual load in a power system, presented in section 2.1.1 are used here. The first method models the annual average load as a fixed value of the demand throughout a year. When solving the power flow and extracting the slack bus outputs to obtain the PNS. Multiplying this value by the 8760 hours of a year we obtain the ENS [MWh] as shown in (2.11.a). However, with the second way of modeling the load in the system that uses a step-load duration curve, a power flow computation is performed for each load level  $L_\beta$  in the system. Recall that each load level  $L_\beta$  occurs for  $\Delta T_\beta$  hours in the period of one year; so the slack bus power output  $P_s$  has to be multiplied by the number of hours for which load level  $L_\beta$  occurs. The ENS for the load modeled using a step-load duration curve is given in (2.11.b).

$$U = (1 - ASAI) \quad (2.10)$$

$$ENS_{a)} = U * 8760 * \sum_{s=1}^{N_s} P_s \quad (2.11.a)$$

$$ENS_{b)} = U * \sum_{\beta=1, s=1}^{N_\beta, N_s} \Delta T_\beta * P_s(L_\beta) \quad (2.11.b)$$

where in (2.11.a)  $ENS_{a)}$  is the Energy Not Supplied with annual average loads modeled in the system and there are  $N_s$  slack buses with each  $P_s$  power output. Equation (2.11.b) gives the annual ENS using a step-load duration representation of the loads, in which the power output of a slack bus depends on the load level  $L_\beta$  of the system occurring for  $\Delta T_\beta$  hours and there are  $N_\beta$  loading levels.

#### 2.1.4 Power systems simulation tool

In order to obtain the reliability of a candidate power system, a power flow calculation must be performed. A power flow evaluation is the computation of the voltage at each bus and the loading of the lines and transformers in a power system under balanced three-phase steady-state conditions [111]. Successful power system operation under normal balanced three-phase steady-state conditions, from requires the following [111]:

1. Generation supplies the demand, to control the frequency of the system
2. Bus voltage magnitudes remain close to the rated values
3. Lines and transformers are not overloaded

The power flow computer program is the basic tool for investigating these requirements, and PowerWorld Simulator™ version 14 was chosen as in [20], where it is justified that it performs well solving the power flow of a system with radial feeders compared to other solvers [112]. The solution type used is polar-Newton, which is the Newton-Raphson power flow as described in [111]. The use of PowerWorld™ has the additional benefit that test systems can be built graphically with the relevant component data as shown in Figure 2.4.

The large interconnected grid represented by the theoretical concept of infinite bus explained earlier, is also known as *slack bus* (or *swing bus*) in power flow computations. The slack bus is modeled as a generator that absorbs or supplies generation in order to balance the load, as illustrated in Figure 2.4 where the numbered circled quantities correspond to the requirements listed above. Note that when operating in steady-state conditions, generation and demand are fixed.

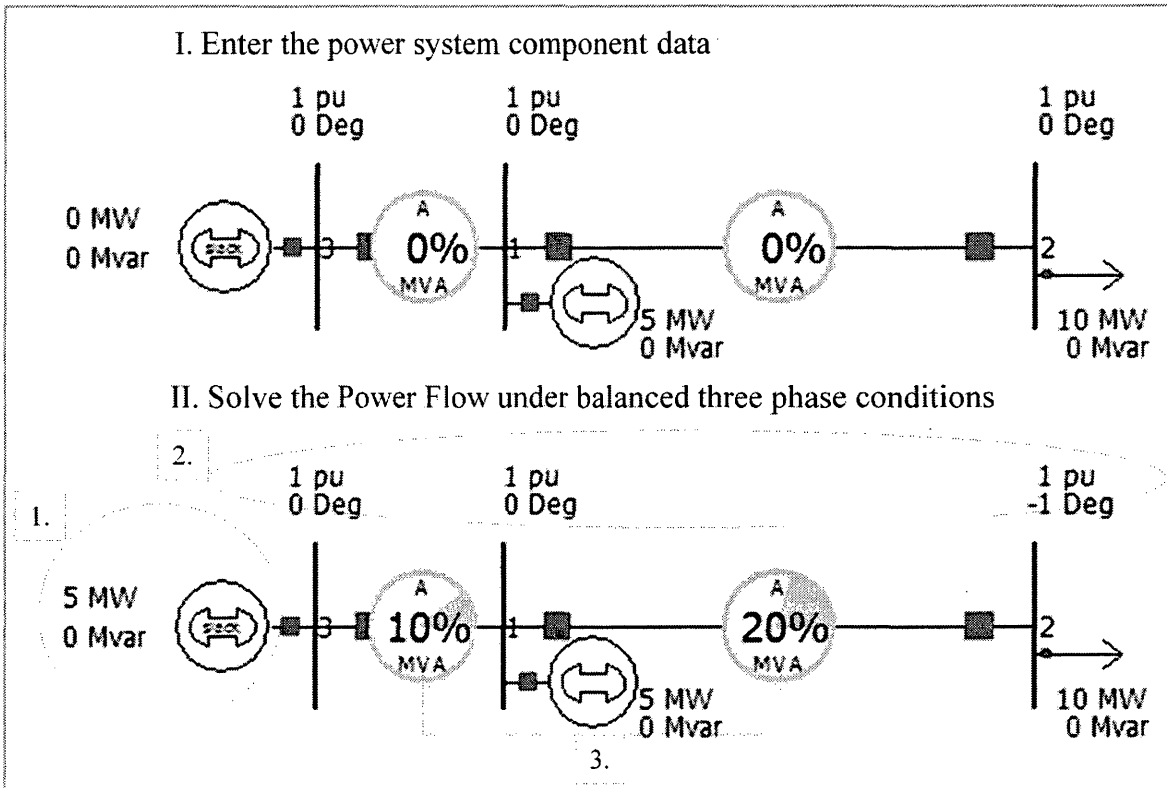


Figure 2.4: Power systems operation under balanced three-phase conditions

## 2.2 Definition of the distribution system redesign problem

The problem of collocating DG sources and networked connections in a given legacy distribution system to improve reliability at a feasible cost does not present the same characteristics as the individual consideration, i.e., DG location in distribution networks or adding networked connections in distribution systems with DGs while improving the desired objective(s).

In fact, when solving the individual problems, i.e., first the optimal sitting of DGs in a given distribution system and, secondly, the addition of optimal networked connections to



increase the system reliability at a feasible cost does not improve the objectives cost and reliability as much as to address the problem as a whole. Empirically, singly handling the optimal location of DG first and optimally locate feeder interties second produces worse objective function values than simultaneously collocate DG units and feeder interties in a radial distribution system.

On the one hand, the optimal DG allocation in a given distribution system is in radial feeders with the highest loads and particularly, at buses where the highest loads are connected. On the other hand, the optimal solution of adding networked connections to improve reliability at a feasible cost is the cheapest available connection between a feeder with DG to one that has no embedded generation. However, the optimal location of a DG in a highly loaded feeder is not necessarily the feeder from where adding a connection has the lowest cost. In addition, the feeders with higher loads might be close to each other and further away from low loaded feeders with no DG. If that is the case, adding networked connections from high load feeders with DGs to the feeders with lower loads and no DGs may not be cost effective.

In the following section, a description of GAs and their adequacy for the problem addressed in this chapter is presented. The optimization problem addressed in this thesis is as follows: *for given a distribution system, collocate DG and networked feeder interconnections at a feasible cost so to improve the reliability while satisfying power flow constraints in an islanded mode operation.* For that, the problem includes the same assumptions regarding the characteristics of the distribution system in question as in [20], where the author addresses the issue of the addition of system feeder interties to maximize the utility of RE resource-based DGs in a legacy radial distribution system that is islanded. These assumptions include also characteristics particular to the problem defined below and are resumed as follows:

- “The protection system allows bi-directional power flow” [20]
- “All connections between feeders are allowed (established rights-of-way)” [20]
- DGs can be placed at every bus of the system, with the exception of slack buses
- “The reliability of existing components will not change as a result of the redesign of the given distribution system and also that the new configuration will have similar reliability as the existing components.” [20]

## 2.3 Genetic algorithm structure

In this section, we will describe the enhanced methodology proposed to address the problem described in previous. A description of how GAs work is made and following that, the mathematical formulation of the GA is presented.

### 2.3.1 Multi-objective Genetic Algorithm (MOGA)

The problem of collocating DGs and feeder inerties in a given distribution system can be stated as a multi-objective (MO) planning problem, where the objective functions which contribute to define a good solution may conflict each other: investment cost versus reliability.

The concept of an optimum for possibly conflicting objectives is described by Pareto optimality [124]. While traditional optimization procedures may result in unique solutions, methods for MO-problem may provide a set of pseudo-optimal solutions. Often, there is no single optimal solution, but rather a set of alternative solutions. These set of points are non-dominated and comprise the Pareto front and the goal of any multi-objective optimization procedure is to identify this Pareto front. The MO planning problem addressed in this thesis is aimed at allowing a utility distribution system designer/planner to choose the “best” solution from candidate topologies. For instances, a redesign solution in a distribution system might increase the reliability by a certain amount at a high cost versus a different redesign solution with lower reliability measure but associated with a lower cost of the project. None of these two solutions can be said to be superior if we do not include preference information of the objectives. Thus if no such information is available, it may be useful to have knowledge about those alternative architectures. A tool exploring the design space for Pareto-optimal solutions can essentially aid the decision maker in at a final design.

In general, a MO optimization problem can be expressed as follows:

$$\min f(x) = \begin{pmatrix} f_1(x) \\ f_2(x) \\ \dots \\ f_n(x) \end{pmatrix}, x \in \Omega$$

subject to

(2.12)

$$x \in \Omega$$

$$c_j(x) = 0, j = 1, \dots, n$$

$$h_k(x) \leq 0, k = 1, \dots, p$$

where  $x$  represents a decision vector,  $\Omega$  is the solution domain,  $f_i(x)$  denotes the objective functions  $c_j(x)$  and  $h_k(x)$  are the equality and inequality constraints, respectively.

GAs have become a viable solution to strategically perform a global search by means of many local searches and have shown to approximate the Pareto front fairly well in power system optimizations [125]. In the literature review provided in this thesis, evolutionary techniques and in particular GAs were used for the reconfiguration problem from an operational perspective, from a design perspective, and for the distribution planning problem of sizing and locating generation on the consumer end of the grid [20], [38, 39], [44-51], [59-63]. Furthermore, GAs have been widely used in power systems for optimal TNEP, GEP, reactive power planning, economic and environmental power dispatch and hydropower operation [118, 119], [125-129].

The basis of the GA methods is derived from the mechanisms of evolution and natural genetics [130]. GAs work by building a population of chromosomes, which are a set of possible solutions to the optimization problem. Within a generation of a population, the chromosomes are randomly altered by means of evolutionary operators in hopes of creating new chromosomes that have better evaluation scores. The next generation population of chromosomes is randomly selected from the current generation with selection probability based on the evaluation score of each chromosome. This is accomplished by looking up the score given by the input fitness function of each gene in the chromosome, adding the scores up, and averaging the score for the chromosome. Each chromosome has a probability of being chosen equal to its score divided by the sum of the scores of all of the generation's chromosomes of that generation. Chromosomes for the next generation are selected using the roulette wheel selection scheme to implement proportionate random selection [131].

Individuals in a generation are modified by evolutionary operators such as crossover and mutation. In order to avoid losing ground in finding the highest-scoring chromosome, elitism is implemented from one generation to another [130]. Elitism reserves two slots in the next generation for the highest scoring chromosome of the current generation, without allowing that chromosome to be crossed over in the next generation. In one of those slots, the elite chromosome will also not be subject to mutation in the next generation. In the crossover phase, all of the chromosomes (except for the elite chromosome) are paired up with a default probability value of

80%, and are crossed over. The crossover is accomplished by randomly choosing a site along the length of the chromosome, and exchanging the genes of the two chromosomes for each gene past this crossover site. After the crossover, for each of the genes of the chromosomes (except for the elite chromosome), the gene will be mutated to any one of the codes with a default probability value of 20%. With the crossover and mutations completed, the chromosomes are once again evaluated with fitness function for another generation, i.e., another round of selection and reproduction follows.

The multi-objective genetic algorithm (MOGA) has been implemented using a Matlab™ toolbox, which is a group of related functions named Genetic Algorithms for Optimization Toolbox (GAOT) [110]. The basic call of the multi-objective GA function which runs the simulated evolution requires an evaluation function unique to the problem at hand. The Matlab™ sub-function to run a multi-objective GA for a user-defined fitness function is *gamultiobj()* [110] and has inbuilt operators for mutation, crossover, and selection. This function has rigid rules on input, and does not accept constraints as defined in (2.12). For that, the constraints are part of the evaluation of the objective fitness function and used to penalize any topology and DG allocation that violated the constraints [20].

### 2.3.2 Objective function and constraints

The objectives to minimize are the cost function  $f_1$  and the reliability of the given distribution system  $f_2$ . Note that improving the reliability is equivalent to minimizing the ENS of a power system.

The set of indexes and parameters used in the mathematical formulation of the optimization problem addressed are presented in Table 2.1.

The first objective function cost is defined in equation (2.13) below. If the binary variable is true (i.e.,  $X_i = 1$  or  $X_g = 1$ ), then connection(s)  $i$  is made and (or) a DG(s) is located at bus  $g$ ; otherwise, no connection is made and (or) no DG is located at that bus.

$$f_1 \sum_{i=1}^{N_c} C_i^C L_i^C X_i + \sum_{j=1}^{N_g} C_g^{DG} P_g^{DG} X_g \quad [\$] \quad (2.13)$$

Table 2.1 Sets, parameters and variables of the MOGA

- Sets
  - $I$ : Set of possible connections,  $1 \dots N_c$
  - $G$ : Set of possible locations of distributed generation,  $1 \dots N_g$
  - $S$ : Set of slack buses,  $1 \dots N_s$
  - $\beta$ : Set of annual load levels,  $1 \dots N_\beta$
  - $B$ : Set of branches (lines) in the system,  $1 \dots N_b$
- Parameters
  - $P_g^{DG}$  = Power output of the DGs located at bus  $g$ ,  $g$  in  $G$  [kW]
  - $C_g^{DG}$  = Cost of the DGs per kW, located at bus  $g$ ,  $g$  in  $G$  [\$/kW]
  - $C_i^C$  = Cost of the possible connection  $i$ ,  $i$  in  $I$  [\$/km]
  - $L_i^C$  = Length of the possible connection  $i$ ,  $i$  in  $I$  [km]
  - $U$  = Annual outage time as a fraction of a year
  - $P_s$  = Power output of slack bus  $s$ ,  $s$  in  $S$  [kW]
  - $\Delta T_\beta$  = Hours in a year with for which the load level is less than or equal to  $L_\beta$ ,  $\beta$  in  $N_\beta$  [h]
- Variables
  - $X_i$  = Connection (s) (binary)
  - $X_g$  = Location of DGs (binary)

The reliability is evaluated using the Energy Not Supplied (ENS) metric introduced in a previous section. As a consequence of the two methods of modeling the load in the candidate power system, there are two distinct computations of the second objective function given by,

$$f_{2a)} = U * 8760 * \sum_{s=1}^{N_s} P_s \quad (2.14.a)$$

$$f_{2b)} = U * \sum_{\beta=1, s=1}^{N_\beta, N_s} \Delta T_\beta * P_s(L_\beta) \quad (2.14.b)$$

where (2.14.a-b) are analogue to (2.11.a-b), corresponding to the ENS over a year when annual average loads and step-load duration curve are used respectively for modeling the load in the system.

The constraints of the problem are to maintain the voltage within  $\pm 5\%$  of the rated value of 1pu for every bus  $a$ , as well as not overload the line(s) between buses  $a$  and  $b$  in the system; these constraints are formulated as:

$$0.95 \leq V_a(x) \leq 1.05 \quad (2.15)$$

$$S_{ab}(x) \leq 1.00 \quad (2.16)$$

The penalty function is a multiplier, proportional to the square of the branch overloading in (2.17) or the square of the voltage deviation from the limits in (2.18). Quadratic penalty functions were chosen as in [20] so that violations would be penalized based on their severity. Equations (2.17) and (2.18) are directly taken from [20] and are only evaluated for buses and branches that violate the constraints: branch loading greater than 100% and bus voltage outside of the  $\pm 5\%$  operating limits. The penalties are:

$$\mathbb{P}_{branch} = \prod_{k=1}^{N_{branch}} |b_{Lk}|^2 \quad (2.17)$$

where  $N_{branch}$  is the number of branch loading violations and  $b_{Lk}$  is the percentage loading on branch  $k$ . The penalties for the voltage violations are

$$\mathbb{P}_{bus} = \begin{cases} \prod_{k=1}^{N_{bus}} |2 - V_k|^2, & \text{if } V_k < 1.0 \\ \prod_{k=1}^{N_{bus}} |V_k|^2, & \text{if } V_k > 1.0 \end{cases} \quad (2.18)$$

In (2.18),  $N_{bus}$  is the number of bus voltage violations and  $V_k$  is the per unit voltage at point  $k$ . The overall penalty is given as

$$\mathbb{P} = \mathbb{P}_{bus} \mathbb{P}_{branch} \quad (2.19)$$

and is applied to the ENS value by multiplying  $f_2$  by the overall penalty.

In addition, the distribution design planner can decide to set a maximum cost of the project  $f_1$  [\$] and/or a desired value of improved reliability so that ENS is at the most  $f_2$  [MWh]. Again, these constraints are included in the fitness function to penalize any individual (a networked topology and set of DG locations) violating the chosen design parameters. This is done

by multiplying the objective function(s) by an artificial factor of  $10^3$  to the one(s) violating the required planning design value- thus, removing it from considerations in future ‘generations’.

2.3.3 Initial population and its importance for convergence

As mentioned earlier in this chapter, a population is comprised of individuals that will be evaluated by a *fitness function*. In the GA applied to the design problem, a chromosome or individual is divided into two components. The first part consists on  $N_c$  binary variables, which are the total number of possible connections and the second part representing the possible locations, the buses in which DGs are connected and is made of  $N_g$  binary variables. Figure 2.5 illustrates the partition a chromosome (individual) which represents a candidate solution.

X (binary)	
$X^c$	$X^g$
Possible Connections	Possible location of DG
0 0 0 1 0 0 1 ..... $N_c$	0 1 0 1 0 0 0 ..... $N_g$

Figure 2.5: Chromosome encoding for  $N_c$  possible connections to be added and  $N_g$  possible locations of DG.

In the conventional GA, the initial population is generated randomly. Yet, selecting an initial population that integrates characteristics of the problem addressed can encourage the convergence to the Pareto front [20], [49]. For that three different ways to input the initial population are explored. Each one of the initial population type leads to better or worse convergence, as proven further in Chapter 3. The three types of initial population configuration are listed below. Based on the knowledge of the problem addressed, an optimal solution has the following characteristics: not a big number of feeder interties additions at feasible cost, and the need of at list one DG unit placed in the system for a connection be able to improve the reliability of the system.

- i. All possible connections between distinct feeders combined with random possible locations of DG within the buses of the system
- ii. All possible connections between distinct feeders combined with random possible locations of DG within the buses in the feeder from which the connection is made

- iii. Possible connections between distinct feeders no longer than 3 km combined with random possible locations of DG within the buses in the feeder from which the connection is made

The three ways of selecting the initial population as listed above are illustrated in Figure 2.6. The three initial population configuration types correspond to a matrix with  $N_c$  rows and  $N_c + N_g$ . The number of possible connections  $N_c$  considered may change from one configuration type to another whereas the number of possible bus locations for DG units  $N_g$  does not.  $N_g$  is always given by the total number of buses in the system, except the slack buses. An individual (row) in configuration type (i) represents one connection matched with one DG unit located randomly.  $N_c$  in type (i) is the total number of possible connections between distinct feeders in a given test system. In configuration type (ii), a chromosome represents one possible connection and one DG unit located at a bus within the feeder form which the possible connection is effected.

The total number of connections  $N_c$  considered is the same as in type (i). The main difference between types (i) and (ii) is that in the former the DG unit is randomly located within the buses of the system. In latter, the location of a DG unit is restricted to the buses in the feeder form where the feeder intertie is issued. Finally, initial population type (iii) is analogue to type (ii), except the total number of possible connections  $N_c$  considered is lower and restricted to feeder interties no longer than 3km.

#### 2.3.4 Evaluation by the fitness function

Finally the algorithm structure is illustrated in Figure 2.7, which shows a flowchart of the fitness function used to evaluate each individual or chromosome contained in the initial population and in the evolutionary ones, and gives the reader an illustrative explanation of the methodology proposed. The fitness function is programmed in Matlab™ and included in the electronic appendix. This function is an extended version of the fitness function proposed in [20] which includes simultaneous collocation of DG and feeder interties versus feeder interties only considered in [20]. Additionally, there are two versions of the fitness function in this thesis, one for each modeling of the annual load in the system.



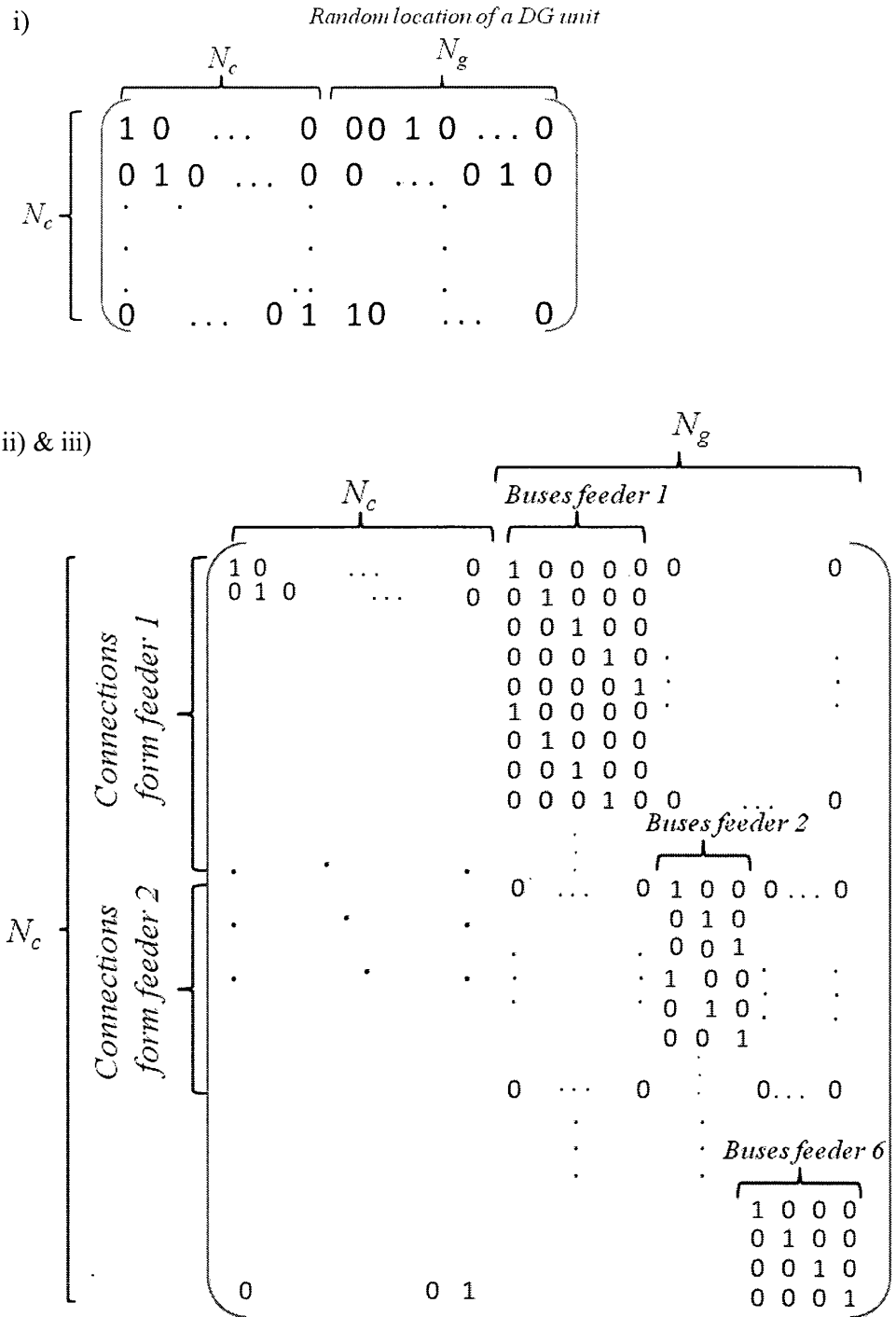


Figure 2.6: Initial population: (i)  $N_c$ = all possible connections between distinct feeders combined with one random possible location of DG unit; (ii)  $N_c$ = all possible connections between distinct feeders combined with possible locations of a DG unit within the buses in the feeder from which the connection is made; (iii) same as (ii) but  $N_c$ = possible connections no longer than 3km between distinct feeders.

PowerWorld Simulator™ 14 introduced in a previous section is chosen to build the radial distribution test system. This software has an add-on called SimAuto™ which allows one to remotely access PowerWorld™ from Matlab™ [20]. SimAuto™ contains most of the functionality available in PowerWorld through the use of script commands such as enter edit mode, run mode, reset the system to flatstart and extract case information.

The typical procedure of the fitness function described in Figure 2.7 includes:

1. Through SimAuto™, transfer the fitness function input information provided by an individual in Matlab™ to the test system built in PowerWorld™, i.e., close the network connection(s) to be added as well as the DG(s) to be located
2. Calculate the cost of the redesign
3. Through SimAuto™, run a power flow calculation in PowerWorld™ from Matlab™
4. Through SimAuto™, extract case system information in order to calculate the reliability metric
5. Through SimAuto™, extract case system information in order to evaluate the constraints and penalize the redesign if required

The steps of computing the fitness function of the MOGA are the same for both load models, with the exception of the ones designed with an asterisk in Figure 2.7. As explained earlier in this chapter, a power flow is run and bus and branch information is extracted for the system. Also, the constraints are verified for each loading level in the system.

Power systems modeling concepts and reliability metrics of distribution systems have been presented under radial and islanded mode of operation. Subsequently, the distribution systems planning problem addressed in this chapter regarding the collocation of feeder interties and DG in a given legacy radial system is described. Finally, an extension to the MOGA methodology proposed in [20] is presented in order to address the problem of simultaneously collocate DG and feeder interties, instead of assuming the number and location of the DG in the available in system. Additionally, two ways of modeling the annual load in the system and three types of initial inputs to the MOGA are explored.

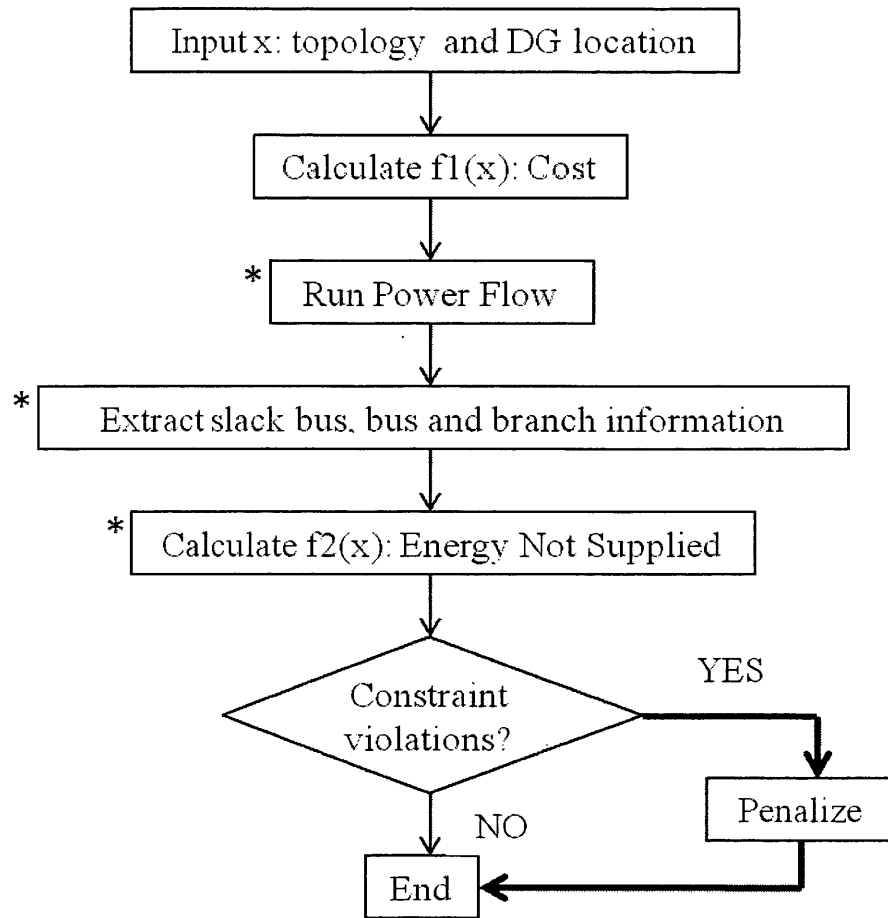


Figure 2.7: Flowchart of the fitness function proposed to evaluate the objective functions of the candidate solutions while satisfying the system and design constraints.

In the next chapter, the extended MOGA methodology is applied first to a three feeder test system, and secondly to a six feeder test system. Several case studies are presented and a discussion on the computational time required by the MOGA depending on the one hand, on the modeling of the load and the second hand, on the initial input to the algorithm is offered.

## CHAPTER 3

### CASE STUDIES OF DISTRIBUTED RESOURCE ISLAND RECONFIGURATION USING THE MULTI-OBJECTIVE GENETIC ALGORITHM

The multi-objective genetic algorithm (MOGA) developed in Chapter 2 is applied first to a simplified three-feeder radial distribution system (3FDR) used as a test system to verify the methodology proposed. Next, the MOGA is implemented in the Roy Billinton Test System (RBTS), developed by the Power Systems Research Group at the University of Saskatchewan as a tool for reliability education and for which data is available [132,133]. Two case studies for the RBTS are solved, differentiated by the approach taken in modeling the annual load in the system. Finally, a discussion on the computational time taken by the MOGA to converge, depending on the choice of the initial population inputted to the algorithm, is presented.

#### 3.1. Simplified three-feeder test system (3FDR)

The simplified three-feeder test system is developed to test the applicability of different optimization methods to the feeder addition problem [20] [40]. The system incorporates three feeders, three transformers and three loads. The advantage of using a simple test system first is to allow the verification of the methodology employed, from the optimization algorithm selected to the software tools utilize for solving and for modeling purposes.

##### 3.1.1. 3FDR test system data

For purposes of completeness, the description of the 3FDR test system is directly reproduced from [20], [40] as follows: “The 3FDR has three feeders, ten buses, and two voltage levels,  $V_1$  and  $V_2$ , where  $V_1$  is greater than  $V_2$ . There are three loads, at buses 3, 6, and 9... Buses 1, 4, and 7 are normally connected to the grid. Since the modeling of this system is under isolated conditions, the grid ties are not shown. Some of the system data for the 3FDR test system were synthesized using example data from [134]. ...It is also assumed that the required loads on ... [the] radial feeders are rated less than the DGs located on those feeders. Each load bus has a non-critical and a critical load component. The critical load is the load that must be served and cannot be interrupted.” The critical demand of the three load points is shown in Table 3.1 and corresponds to annual average loads. Table 3.2 contains the values of the parameters required by

the MOGA as in Table 2.1 in order to obtain the value of the cost of a given configuration as well as evaluate the reliability of the system by calculating the ENS. Note that in the study of the 3FDR, we use annual average loads in the system and the ENS will be calculated as in (2.11.a).

For the purpose of checking the algorithm proposed in a simplified test system, we explore locating only Renewable Energy (RE) DG sources using the capacity factors for wind and solar of 0.25 and 0.3 respectively, as justified in Chapter 2 section 2.1.2. However, the terms for CDG sources and DS in (2.4) are excluded for the modeling of DG in the 3FDR test system. The capital cost of adding RE DG is directly taken from [135] and is included in Table 3.2.

Table 3.1 Annual average load in the 3FDR test system [20]

Load	Critical [kW]
L1	80.2
L2	100.2
L3	50.8

The length of the possible connections to add between feeders is included in Table 3.2. The 3FDR system has two voltage levels  $V_1$  and  $V_2$  and a transformer may be required for a feeder intertie to be added. If that is the case, an impedance of  $0.01 + j0.06$  is assumed on the transformer base [20]. The costs of adding a possible connection in [\$/km] is included in Table 3.2, with the upgrade cost of adding transformer [20]. Finally, the line data for the existing connections of the 3FDR system and the data used for the possible connections to be added between feeders is included in the Appendix. Finally, the annual outage time  $U$  is obtained from and ASAI of 0.999375, value taken from [123].

The 3FDR test system is built in PowerWorld™ using the data provided with the possible connections and DG units to be placed modeled as open lines and generators [112]. In the following sections, the MOGA methodology is applied to the 3FDR system in order to locate first RE DG wind-based generation only and feeder interties, and secondly RE DG solar based generation only and feeder interties in the system.

Table 3.2 Parameters required for implementing the MOGA in the 3FDR test system

<ul style="list-style-type: none"> <li>• <i>Parameters</i></li> </ul>							
<ul style="list-style-type: none"> <li>○ <math>P_g^{DG}</math> = Power output of the DGs located at bus <math>g</math>, based on [20]</li> </ul>							
$G$	2	3	4	5	6	8	9
Wind, $P_g^{DG}$ [kW]	0.091	0.0891	0.1421	0.1421	0.1421	0.1231	0.1231
Solar, $P_g^{DG}$ [kW]	0.1069	0.0891	0.1705	0.1705	0.1705	0.1477	0.1477
<ul style="list-style-type: none"> <li>○ <math>C_g^{DG}</math> = Cost of the DGs located at bus <math>g</math>, directly taken from [135]</li> </ul>							
$C_g^{DG}$ for wind based generation [\$/kW]					1.6		
$C_g^{DG}$ for solar based generation [\$/kW]					5.5		
<ul style="list-style-type: none"> <li>○ <math>C_i^C</math> = Cost of a possible connection <math>i</math>, [\$/km], directly taken from [20]</li> </ul>							
Transformer [\$]				400000			
2.4 kV Line [\$/ft]				50			
12.47 kV Line [\$/ft]				10			
Fixed Line Cost [\$]				100000			
<ul style="list-style-type: none"> <li>○ <math>L_i^C</math> = Length of the possible connection <math>i</math> [km], directly taken from [20]</li> </ul>							
Connection $i$	$L_i^C$ [miles]	Connection $i$	$L_i^C$ [miles]				
Line 1-4	0.1894	Line 3-6	0.4214				
Line 1-5	0.3788	Line 3-7	1.043				
Line 1-6	1.1364	Line 3-8	0.9996				
Line 1-7	0.3206	Line 3-9	1.4330				
Line 1-8	0.3909	Line 4-7	0.1376				
Line 1-9	0.5666	Line 4-8	0.1701				
Line 2-4	0.261	Line 4-9	0.4543				
Line 2-5	0.2841	Line 5-7	0.3588				
Line 2-6	0.3267	Line 5-8	0.3933				
Line 2-7	0.3262	Line 5-9	0.5764				
Line 2-8	0.3551	Line 6-7	0.5687				
Line 2-9	0.5926	Line 6-8	0.4136				
Line 3-4	0.8996	Line 6-9	0.3855				
Line 3-5	0.7576						
<ul style="list-style-type: none"> <li>○ ASAI = 0.999375, directly taken from [20], [123]</li> <li>○ <math>U</math> = Annual outage time as a fraction of a year = (1-0.999375)</li> </ul>							

### 3.2. MOGA applied to 3FDR with RE DG

The extended MOGA algorithm presented in the previous chapter is implemented in a simple 3FDR system. The purpose of testing the methodology in the 3FDR test system is to first, verify the algorithm as already mentioned previously, but also to learn about the redesign solutions obtained.

The problem addressed in the following two sections is to co-locate feeder interties and RE DG units at a feasible cost in order to increase the reliability of the system. The constraints of the system are to maintain the voltage within the acceptable limits of  $\pm 5\%$  and penalize the overloading of the lines in the system. First, wind based DG units are simultaneously located with feeder interties in the 3FDR system, and secondly, solar based DG units are collocated. In the simplified 3FDR test system, the size of the DG units does not depend on the load of the bus in which they are sited, because the DS term in (2.4) is excluded. Consequently, the power output of the DG units is fixed and sized to be higher than the critical load in the feeder in which the unit is located as shown in Table 3.2. The loads in the system are modeled using annual average demand values and thus, equation (2.14.a) is employed to obtain the value of the reliability metric ENS. To calculate the cost of the redesign project, (2.13) is used.

#### 3.2.1. Results of the MOGA applied to 3FDR with wind generation

In this section, the MOGA is applied to the 3FDR system to propose a redesign solution that increases the reliability of the system considering the cost of the project. The reliability metric used is the ENS described in section 2.2 and as a reminder, increasing the reliability of a system corresponds to decreasing the ENS. The results are presented in Table 3.3.

Table 3.3 results of the MOGA applied to the 3FDR test system with wind based DG

Solution #	Connection (s)	DG (s) (wind) bus location #	Cost [ $10^6$ US \$]	ENS [MWh]
1	-	3	0.13	0.83
2	-	6	0.21	0.72
3	-	3 & 6	0.35	0.28
4	Line 4-7	3 & 6	0.52	0.05
5	-	3 & 6 & 9	0.53	0
6	Lines 4-7 & 2-6	3 & 6	0.71	0

The solutions are ordered from in increasing order of cost, which corresponds to a decreasing order of ENS. The cost of the redesign project and the reliability of the system are conflicting objectives. Following the application of the MOGA to the 3FDR test system it is observed that wind based DG is preferably placed in radial feeders where the higher loads have to be supplied. Solution No.1 corresponds to placing one DG unit in feeder 1 where the second highest critical load of 80.2 kW is located. Solution No.2 corresponds to locating one DG units in feeder 2 where the highest load of 100.2 kW is. If placing 2 DG units, feeder 1 and 2 are as shown in Solution No.3. Within a radial feeder, the DG unit is located in buses where the loads are, at buses 3, 6 and 9. Concerning the feeder interties, the MOGA selects the cheapest connection to add between a feeder with a DG unit and a feeder with no generation. Solution No.4 corresponds to co-locating 2 DG units in the highest loaded feeders 1 and 2 where the loads are located (bus 3 and 6) and a feeder intertie between feeders 3-4. However, the ENS of Solution No.4 is 0.05 MWh. The ENS is not reduced to 0 because the excess of energy from the DG unit located in feeder 2 is not sufficient to supply the load of feeder 3. Solution No.5 corresponds to locating 3 DG units, one per radial feeder at the bus where the load is located and reducing the ENS to 0 MWh. Solution No.6 proposes to locate 2 DG units in feeders 1 and 2 respectively, and add feeder interties between feeders 1-2 and 2-3, which reduces the ENS to 0 MWh. The excess of energy produced by 2 DG in feeders 1 and 2 is sufficient to supply the load in feeder 3. However, it is more expensive to add the feeder interties than to place a third DG unit in feeder 3.

The algorithm is verified to provide the Pareto-optimal solutions to the design problem under consideration. The solutions are presented in a look-up table, Table 3.3 and the decision maker, i.e., the utility planning engineer, can choose the best solution to satisfy the set of criteria under consideration. Finally, note that in a that in a radial feeder with critical loads to satisfy in the 100 kW range, i.e., wind based DG sized to generate a power output of around 100 kW per feeder, adding a DG unit in a feeder may be less expensive than adding feeder interties. Solution No.5 which proposes placing 3 DG units, i.e., one DG per radial feeder is less expensive than Solution No.6 which considers locating 2 DG units and building 2 feeder interties between feeders 1-2 and 2-3. Both of these solutions reduce the ENS to 0. Solutions 4 and 5 are sketched in Figures 3.1 and 3.2 respectively.



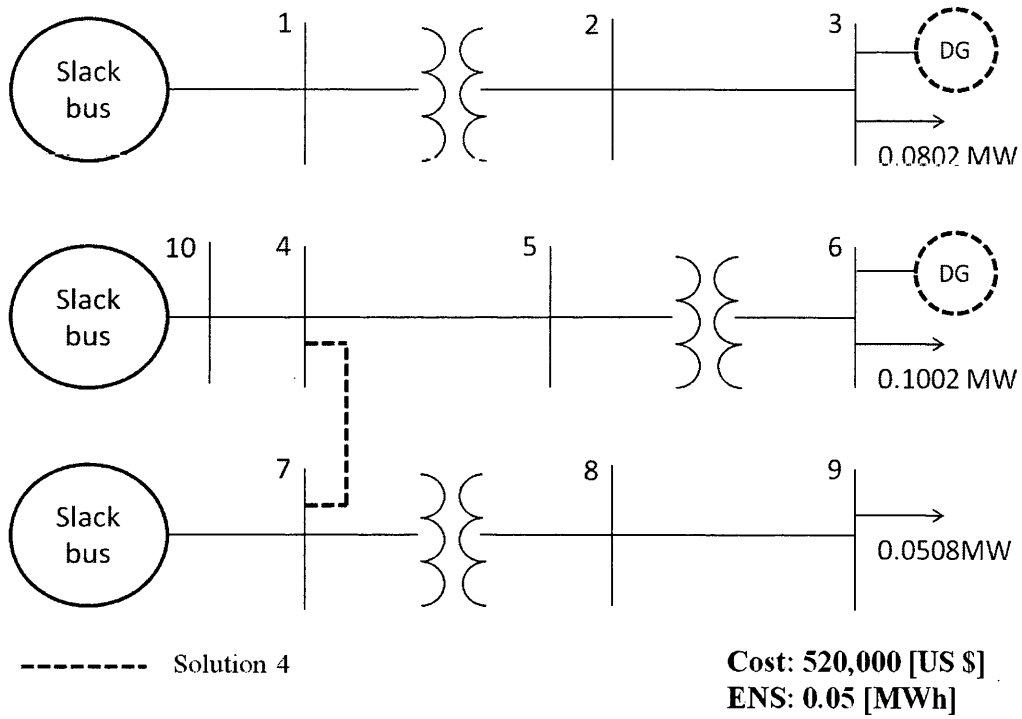


Figure 3.1: Solution 4 for the MOGA applied to the 3FDR system with wind based DGs.

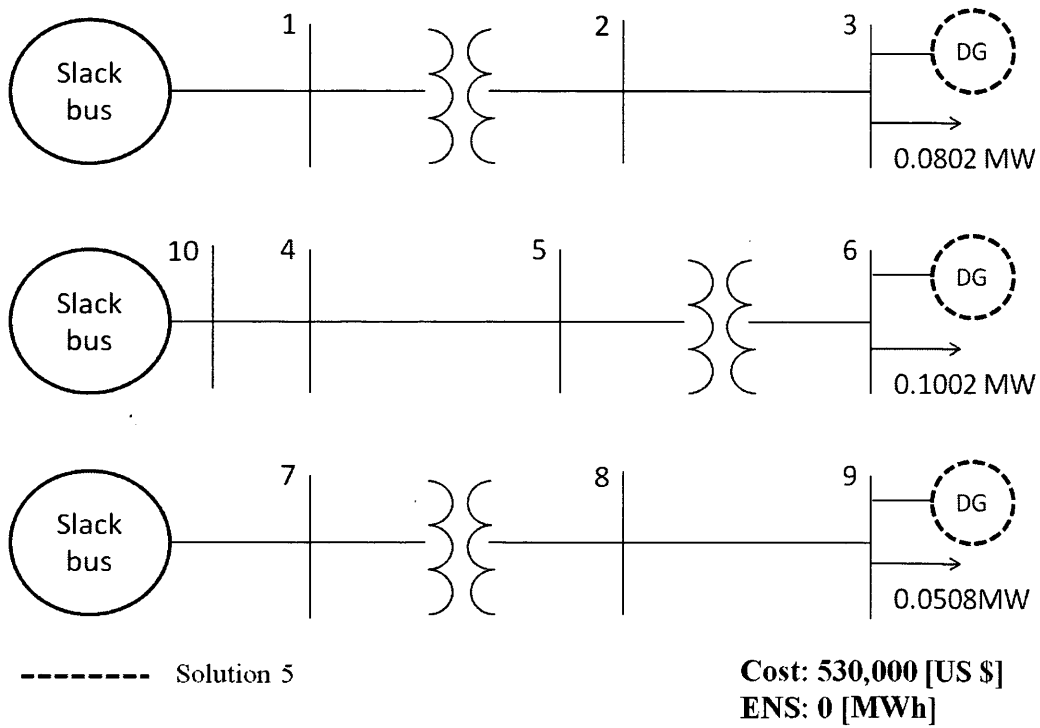


Figure 3.2: Solution 5 for the MOGA applied to the 3FDR system with wind based DGs.

### 3.2.2. Results of the MOGA applied to 3FDR with solar generation

The MOGA is applied to the 3 FDR locating solar based DG, instead of the wind based DG presented in the previous subsection. The capacity factor of solar based DG is 30% and the cost per kW increases to considerable to 5.5 \$/kW compared to DG wind based.

In general, the solutions present the same characteristics as in the previous case, i.e., DG are located at buses with higher loads and networked connections are added between feeders(s) with DG to satisfy the load in the feeder(s) with no DG. The solutions are presented in Table 3.4 in increasing order of cost.

Table 3.4 Results of the MOGA applied to the 3FDR test system with solar based DG

Solution #	Connection (s)	DG (s) (wind) bus location #	Cost [ $10^6$ US \$]	ENS [MWh]
1		3	0.59	0.83
2		6	0.94	0.72
3	Line 4-7	6	1.12	0.33
4		3 & 6	1.21	0.28
5	Line 4-7	3 & 6	1.51	0.0
6	-	3 & 6 & 9	0.23	0

Note that this time, with solar powered DG, the cost of adding feeder interties to increase the reliability of the system is less expensive than adding DG. Solution No.5 and No.6 both reduce the ENS to zero. The former corresponds to locating 2 DG units and adding networked connection between feeders 1-2 and 2-3 is less expensive than the latter, Solution No.6 which corresponds to distributing 3 DG units, one per radial feeder. Additionally, the higher power factor for solar generation based DG placed in feeder 2 is sufficient to supply the loads in feeders 2 and 3 in Solution No.5.

The solution space for the 3FDR system with wind and solar based DG is shown in Figure-3.3. The plot illustrates the concept of Pareto-optimality, in which a range of solutions between lower cost and high reliability and vice versa are included. It corresponds to the decision maker to choose the solution that adapts the best to his subjective preferences.

From implementing the MOGA to a simplified test system such as the 3FDR, preliminary observation of the applicability of the evolutionary optimization methodology proposed in Chapter 2 is obtained. Satisfactory solutions are shown in the Pareto front and are adapted to each

case study with wind and solar DG. For illustrative purposes, solutions 5 & 6 for DG wind based solar based are given in Figures 3.4 and 3.5.

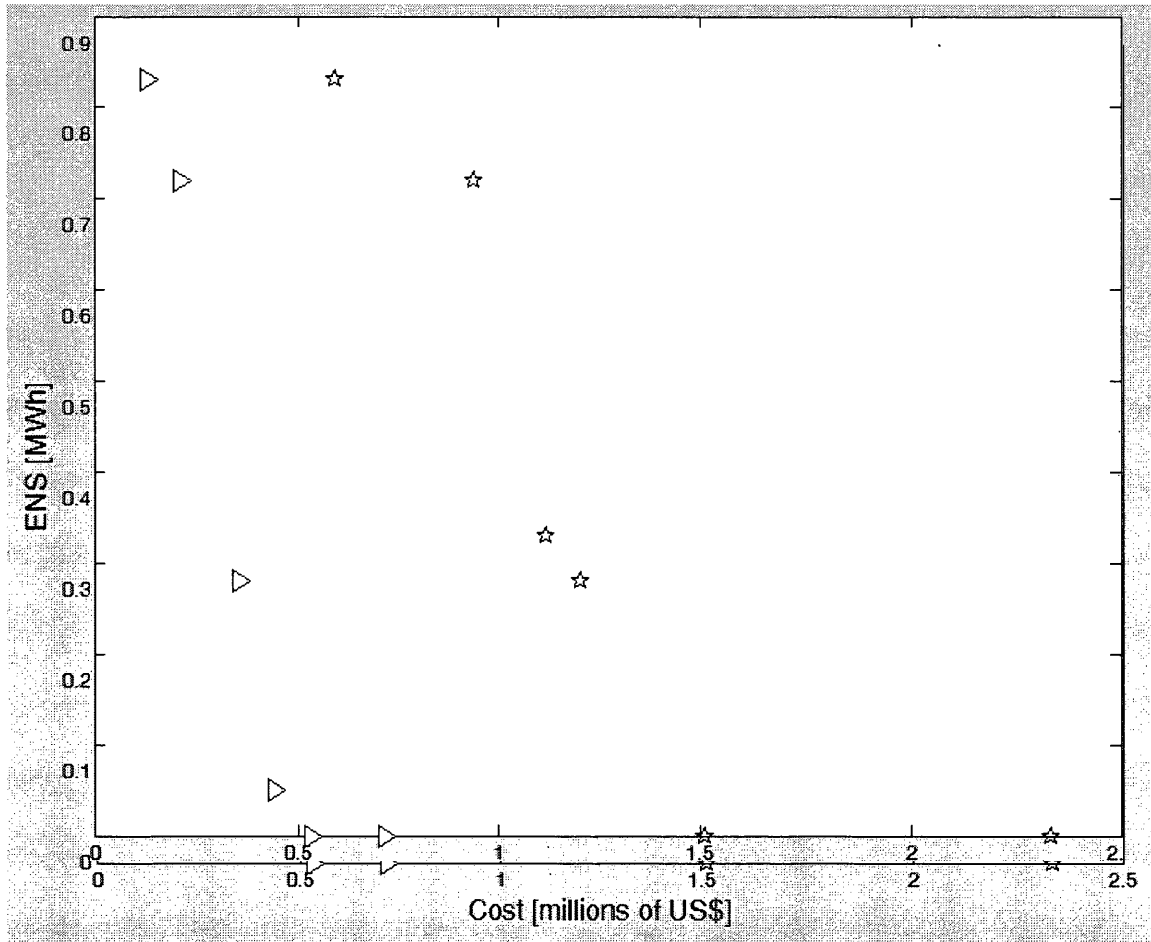


Figure 3.3: Pareto front of the MOGA applied to the 3FDR test system. Triangles are solutions with wind based DG and stars are solutions with solar based DG.

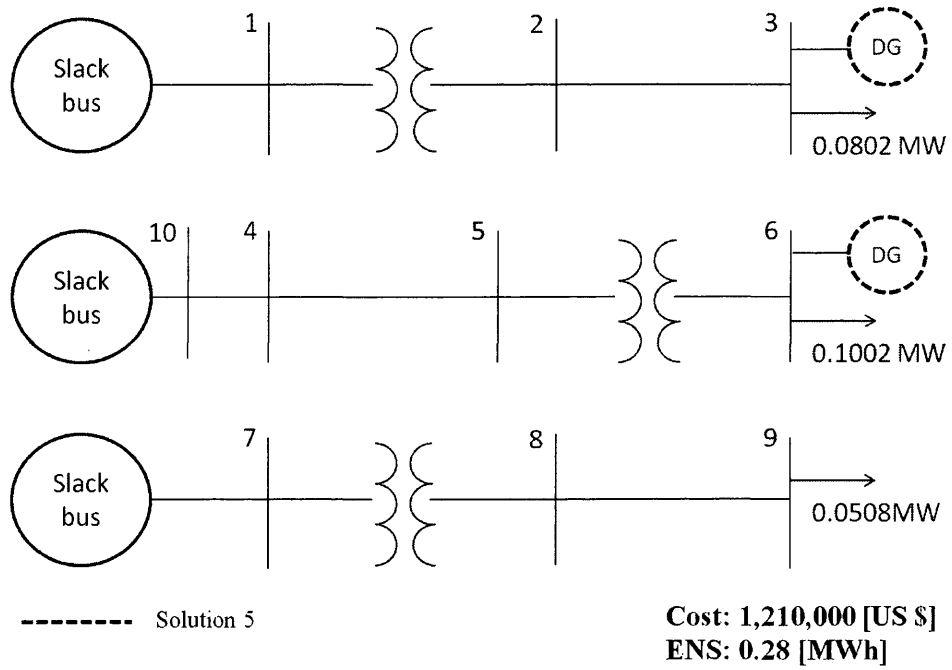


Figure 3.4: Solution 4 for the MOGA applied to the 3FDR system with solar based DGs.

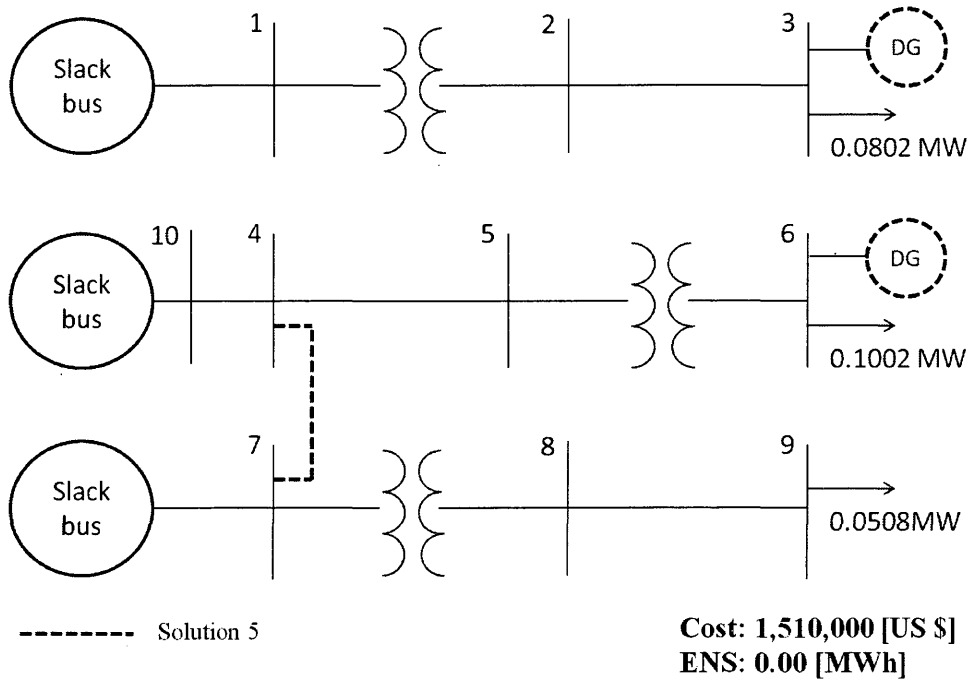


Figure 3.5: Solution 5 for the MOGA applied to the 3FDR system with solar based DGs.

### 3.3. Roy Billinton Test System (RBTS)

The Roy Billinton Test System (RBTS) is a basic reliability test system originated from the reliability education and research programs conducted by the power system research group at the University of Saskatchewan [132]. The basic system data at the transmission level is published in [132], in particular, the annual hourly peak load data is used in this section. Reference [133] develops the distribution networks providing the data at Bus 3, which is the legacy radial distribution test system selected as in [20]. In this section, two test cases with differing modeling of the annual load in the RBTS are explored. The redesign problem is solved for both test cases using the MOGA and the results are given and discussed.

#### 3.3.1. RBTS data

In this section, the same test system as in [20] is chosen. Reference [20] had selected the 11 kV distribution circuits of the bus 3 in RBTS as the candidate system for the purpose of testing the methodology proposed. The distribution network of the RBTS at bus 3 has a peak load of 85 MW. Since two 138 kV feeders were neglected, the peak load of the system shown in Figure 3.6 is 29.5 MW. Under emergency conditions, 20% of the total load of the Bus 3 distribution system is expected to be available for curtailment [133] and it is taken into account by considering only the 80% of the power not supplied, i.e. the sum of the power output of the slack buses of the system by 0.80 [20]. The PowerWorld™ screen shot in Figure 3.6 shows the part of the RBTS bus 3 used as test system with annual average demand representation. There are 27 possible locations for DG units which correspond to the total number of buses in the system, except the slack buses. The possible feeder interties to be added in the system are 302 networked connections and are not included in the figure. The RBTS system shown in Figure 3.6 has normally open tie-switches between buses 1-7, 11-17, and 23-29. The test system in Figure 3.6 corresponds to the legacy radial RBTS system built in PowerWorld™ and “on top” of which the data is changed (closing of feeder interties, sizing of DG units), the power flow is run and the information is extracted. The power output of the slack buses in Figure 3.6 corresponds to the sum of the connected loads in a feeder since the generation units are sized to zero output. The sum of the slack buses adds up to 17.8 MW, which is the annual average power not supplied since annual average loads are modeled in Figure 3.6. The DGs are sized to zero output and the power output of the slack bus per radial feeder is the power not supplied in that feeder. The

topographical information as well as the sizing of the elements (lines and transformers) of the RBTS Bus 3 is taken directly from [20].

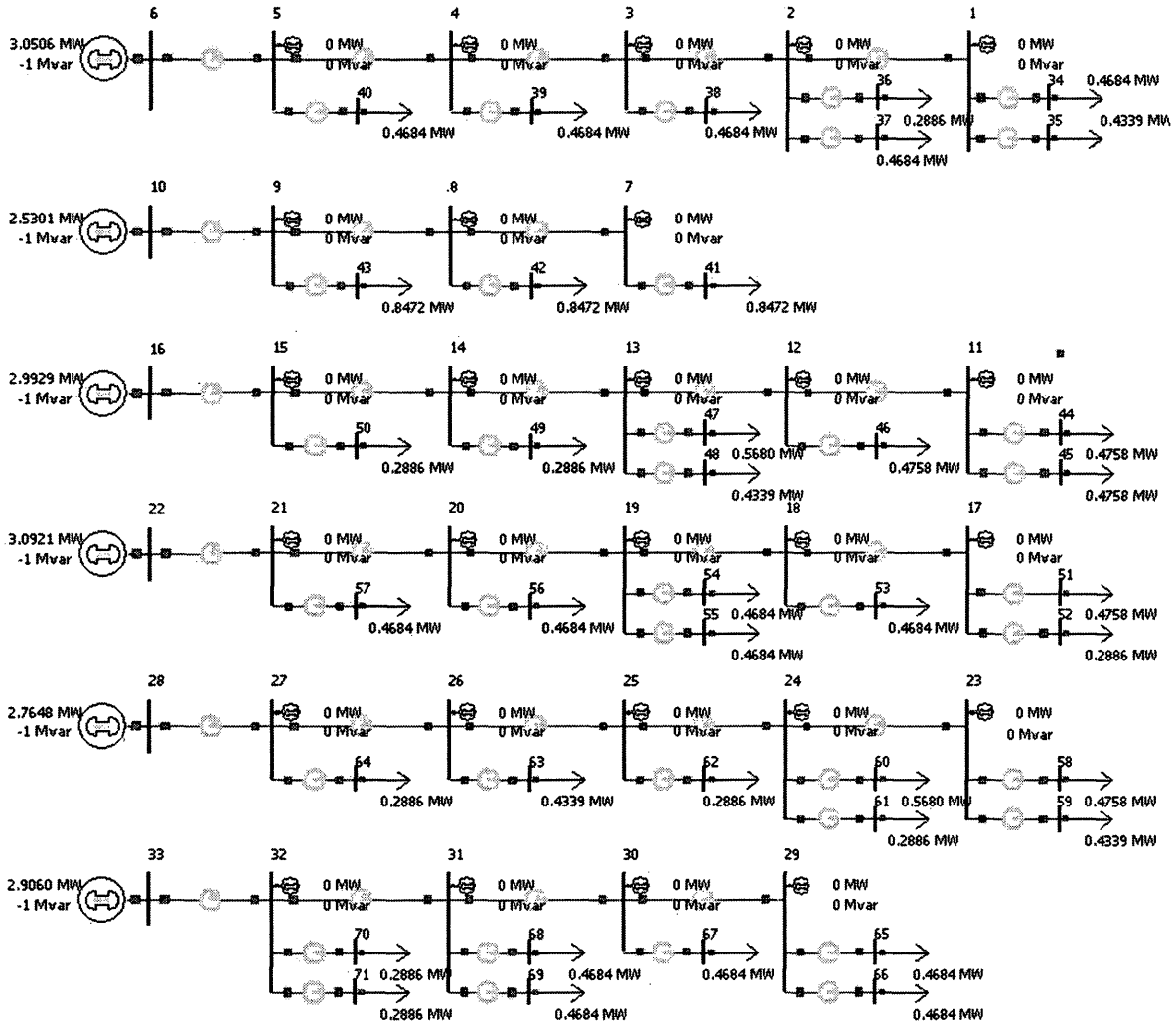


Figure 3.6: RBTS bus 3 test system with annual average loads.

In the following, we do not provide a table containing the required parameters for the implementation of the MOGA as in the 3FDR system because the size of the data is too large.

The DGs size is calculated following (2.4). The power output of a DG located at a given bus depends on the number of units that are being deployed at a time. This parameter is calculated in the fitness function for the given input. The cost in \$/kW of a DG unit is the result of the weighted costs of the generation mix of DGs: Conventional DGs and RE DGs. In this thesis, we have chosen the following design parameters included in Table 3.5 which are based on the survey responses collected and analyzed in [20], [40], [121]. The total rating of DG is 80% of the annual

average load in the system. From that total DG rating, 20% is assumed to be served by RE generation and the remaining 80% is generated by CDG. Finally, from the 20% produced by RE generation, it is assumed that 60% is solar based and 40% is wind based generation. Once more, the capacity factors selected are justified in section 2.1.2 and are the same as the values used for the 3FDR test system. The capacity factor of RE generation is also the weighted individual capacity factors of wind and sun generation based on the percentage contribution of each source.

Table 3.5 Design parameters for DG in the RBTS test system

DESIGN PARAMETERS	
CF: wind, solar, conventional DG	0.25, 0.3, 0.8
Total Annual Average Load	17.95 MW
Total DG penetration	14.36 MW
RE penetration	3.59 MW

The line data from [133] is given in the Appendix, in addition to the transformers that were chosen for system modeling. The lengths of the 302 possible connections are also included in the electronic appendix. In addition, the calculation required in the absence of topographical information of a test system in order to estimate the distance between buses for the possible connections is reproduced from [20] in the Appendix. Next, for all connections the ACSR Flamingo conductor is chosen at a cost of \$200,000 per km, assumed as in [20] on a synthetic cost base for the possible connections. The conductor selection is based on a maximum voltage drop in a feeder of 5% and the methodology is reproduced from [136] and repeated below.

A line-to-neutral equivalent circuit of a three-phase line segment serving a balanced three-phase load is shown in Figure 3.4. The Voltage drop  $V_{drop}$  between the source and the load is defined by (3.1) below, and the “K drop factor”  $K_{drop}$  is defined in (3.2).

$$V_{drop} \cong Re(Z * I) \quad (3.1)$$

$$K_{drop} = \frac{\text{Percent voltage drop}}{KVA * mile} \quad (3.2)$$

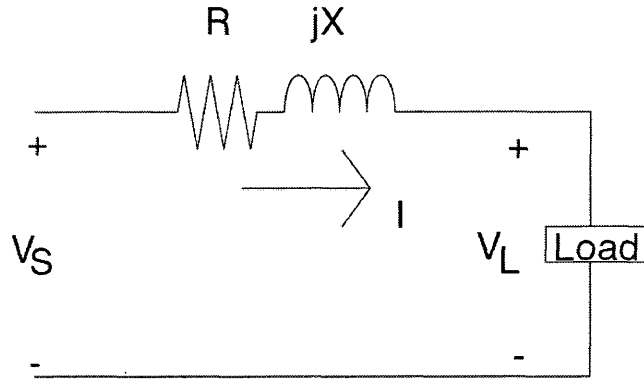


Figure 3.7: Line-to-neutral equivalent circuit of a three-phase line segment serving a balanced three-phase load, taken directly from [136].

The  $K_{drop}$  factor is determined by computing the percent voltage drop as in (3.1) down a line that is one mile long and serving a balanced three-phase load of 1 kVA [136]. The percent voltage drop is referenced to the nominal voltage of the line. In order to calculate this factor, the power factor of the load must be assumed to calculate the current. We assume a power factor of 0.9 lagging is a good approximation for a feeder serving a predominately residential load as in [136]. The  $K_{drop}$  factor can be used to compute the approximate voltage drop down a line section by multiplying  $K_{drop}$  by the KVA value of the load to be served and by the length to the load from the source, i.e. distance from the substation. When line segments are in cascade, the total percent voltage drop from the source to the end of the last line segment is the sum of the percent drops in each line segment [136].

Using this method to compute the total voltage drop in feeder 4, which is the feeder with higher loading, we obtain a total voltage drop of 2%. The parameters of the ACSR Flamingo conductor are included in Table 3.6 as well as the calculated  $V_{drop}$  (for a line one mile long and serving a load of 1 kVA) and  $K_{drop}$  in percentage. The voltage drop value is significantly less than 5%, but we have not considered future load growth and it is a common practice to oversize the maximum loading of the lines. However, it is up to the designer to select the conductor that will determine the cost of the project.

Finally, the ASAI of Bus 3 of the RBTS system used is 0.99964 [133]; this value is used to calculate the annual outage time  $U$  as a fraction of a year as in (2.10).

With the data provided, we can proceed to build the RBTS system in PowerWorld Simulator™ as shown in Figure 3.6 and proceed to implement the MOGA to a six feeder test system.



Table 3.6 ACSR Flamingo data reproduced from [111].

<i>Resistance R</i> [ $\Omega$ /mi]	0.141
<i>Impedance X</i> [ $\Omega$ /mi]	0.412
<i>V<sub>drop</sub></i> (Line 1 mile, Load 1kVA) [V]	0.016086
<i>K<sub>drop</sub></i> [%]	0.00025329
<i>Assumed Cost</i> [\$/mile]	200000

Table 3.7 Annual average load and maximum peak load per load point in the RBTS test system [133].

<i>Customer Type</i>	<i>Load points i</i>	<i>Average Load,</i> <i>L<sub>i,ALoad</sub></i> [MW]	<i>Max. Peak Load,</i> <i>L<sub>i,PLoad<sub>max</sub></sub></i> [MW]
Residential	1, 4-7, 20-24, 32-36	0.4684	0.8367
Residential	11, 12, 13, 18, 25	0.4758	0.8500
Residential	2, 15, 26, 30	0.4339	0.7750
Small Industrial	8, 9, 10	0.8472	1.0167
Commercial	3, 16, 17, 19, 28, 29, 31, 37, 38	0.2886	0.5222
Office Buildings	14,27	0.5680	0.9250

Table 3.8 Load levels in per units form the step-load duration curve and their respective duration in hours, reproduced from [132]

<i>B</i>	<i>Load Level L<sub><math>\beta</math></sub></i> (pu)	$\Delta T_{\beta}$ [hours]
1	1	$3 \cdot 10^{-4}$
2	0.8664	291.71
3	0.7329	1757.26
4	0.5993	2543.03
5	0.4657	2680.56
6	0.3321	1487.45

In the following, two cases of study are developed differing in the way the load is modeled in the system. First, RBTS Case I where the MOGA is implemented to the RBTS test system with annual average load data as shown in Table 3.7. Secondly, RBTS Case II where the annual demand in the system follows the peak loads in the system represented by the step-load duration curve. Table 3.7 includes the maximum peak loads throughout the load points in the system, and Table 3.8 shows the corresponding load level in per unit as well as the hours in a year that the respective load level occurs. The 6 step-load duration data is taken directly from [132] and reproduced in Figure 3.8.

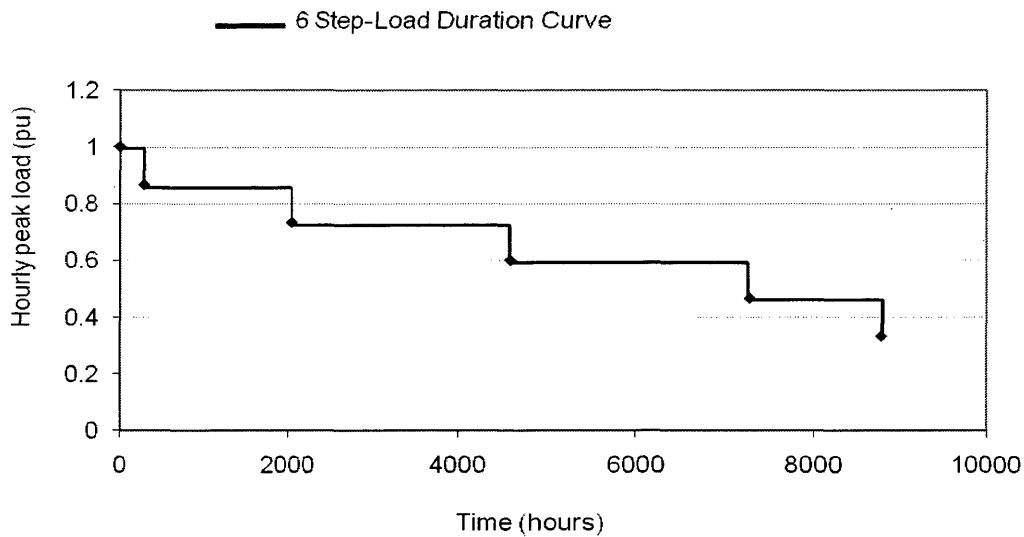


Figure 3.8: Six step-load duration curve reproduced from [132].

As a reminder, the problem addressed is the redesign of the RBTS legacy radial system shown Figure 3.6. The location of DG units and addition of feeder interties is optimized. DG units are modeled as in (2.4)-(2.7) and the design parameters (rating of RE and CDG DG) is given in Table 3.5. It is assumed that a DG unit placed in a radial feeder has a higher power output than the total loading of that feeder. With the design parameters for DG chosen, this assumption corresponds to locating a maximum of 3 DG in the RBTS test system. The constraints of the problem are to maintain the voltage within  $\pm 5\%$  and penalize any overloading the lines and transformers of the system.

### 3.3.2. Results of the MOGA applied to RBTS Case I

We apply the MOGA to the RBTS system with the demand modeled as annual average load data, and using (2.11.a) to calculate the ENS. The most relevant results are shown in Table 3.9 (the actual Pareto front contains 80 solutions), and correspond to the solutions that appear more frequently in the Pareto Front of 5 simulations run for 50 generations. The MOGA is run for 50 generations obtaining satisfying redesign configurations. In general, the number of ideal number of generations is found when the results are replicable from one simulation to another. However, for the redesign problem addressed in this thesis, there are different reconfigurations of the RBTS test system leading to the same or very close values of the objective functions.

To refresh the mind of the reader on GAs, each of the chromosomes in a generation must be evaluated for the selection process. As part of the evaluation process, the elite chromosome of the generation is determined. Within a generation of a population, the chromosomes are randomly altered in hopes of creating new chromosomes that have better evaluation scores. The next generation population of chromosomes is randomly selected from the current generation with selection probability based on the evaluation score of each chromosome. Chromosomes for the next generation are selected using the roulette wheel selection scheme to implement proportionate random selection [137]. In order to avoid losing ground in finding the highest-scoring chromosome, elitism [109] is implemented in this benchmark. Elitism reserves two slots in the next generation for the highest scoring chromosome of the current generation, without allowing that chromosome to be crossed over in the next generation. In one of those slots, the elite chromosome will also not be subject to mutation in the next generation.

In the crossover phase, all of the chromosomes (except for the elite chromosome) are paired up with a default probability value of 80%, and are crossed over. The crossover is accomplished by randomly choosing a site along the length of the chromosome, and exchanging the genes of the two chromosomes for each gene past this crossover site. After the crossover, for each of the genes of the chromosomes (except for the elite chromosome), the gene will be mutated to any one of the codes with a default probability value of 20%. With the crossover and mutations completed, the chromosomes are once again evaluated with fitness function for another generation, i.e., another round of selection and reproduction follows.

The reader can realize the fact that if different reconfigurations of the RBTS test system lead to the same or very close objective function values and the evolutionary operators are

applied randomly, not always the same solutions will appear in the Pareto front. When the MOGA is run for less than 50 generations, it is observed that the Pareto-optimal solution- the cheapest networked connection to add between radial feeders with DG- is not always obtained depending on the initial population type inputted. When the MOGA is run for more than 50 generations, the algorithm yields solutions which point to redesigns of the RBTS within the same range of objective function value; a point to be noted is that even though the two runs- with less than, and with 50 generations- yield solutions within the same range, they differ significantly in the computation time – this is explained in section 3.3.5 in detail.

In solutions 1 through 5 proposed by the MOGA algorithm, the networked connections to add in the system correspond to switching the normally open-tie switches at zero cost. Solution No.1 corresponds to closing the open-tie switch between feeders 3-4, Solutions No.2 and 4 correspond to close 2 open-tie switches between feeders 1-2 and feeders 3-4, and feeders 3-4 and feeders 5-6 respectively. Solutions No.3 and 5 correspond to closing the three open-tie switches. Also, in this set of solutions DG units are located in distinct feeders that cannot be connected by a normally open-tie switch. In this system, it is observed that locating DG units at buses with the higher loads increases the reliability of the system while increasing the cost of the project. This is because the cost of DG is proportional to the power output, modeled with (2.4) which is a linear function of the load. In fact the second term in (2.6) refers to the storage of renewable energy resources and is proportional to the sum of the average loads installed at the bus where the DG unit is located. Equations (2.4) and (2.6) are reproduced below.

$$P_{out} = RE + DS + CDG \quad (2.4)$$

$$DS = (1-CF_{RE}) * 0.15 * L_g \quad (2.6)$$

where  $CF_{RE}$  is the weighted capacity factor of wind and solar RE based DG and  $L_g$  is the average connected load at bus  $g$ .

Looking at Solution 2, a DG unit is located at bus 4 and another DG unit is located at bus 15 with low residential and commercial average annual demand at a cost of \$18.06 million reducing the ENS of the system to 21.96 MWh. Alternatively, Solution 4 has a lower reliability index, ENS of 21.62 MWh, and corresponds to locating DG units on the same feeders as Solution 2 but at bus 13 and 29, respectively, where the highest rated loads are connected, i.e., two

residential customer type loads per bus at a cost of \$18.31 million. Solutions 2 and 4 are drawn in Figures 3.9 and 3.10 respectively. The same reasoning can be applied to understand the difference in cost and reliability improvement for Solutions 3 and 5. Finally, for Solution 6 (shown in Figure 3.11), it is proposed that two DG units be located on the same high loaded feeder 3, and a third DG unit be located on a distant feeder 5 – i.e., one that cannot be connected to the former feeder by closing any existing open tie-switch-, one normally open-tie switch connecting feeders 1 and 2 be closed, and add two new networked connections – one each between feeders 2 and 3, and feeders 4 and 5. This solution corresponds to of the maximum possible improvements of the reliability in the system with an ENS of 21.33 [MWh] a year at a cost of \$18.91 million. The maximum improvement is not zero because first, the rating of the aggregate DG in the RBTS system is 80% of the total annual average load, which corresponds to a capacity generation of 14.24 MW. From the 14.24 MW rating of DG generation, 20% corresponds to RE with 0.28 capacity factor (the weighted capacity factor of wind and solar with 40% and 60% contribution respectively) and 80% of CDG with 0.8 capacity factor. This corresponds to a power output of 10.86 MW. With a maximum of 3 DG units that can be located within the buses of the system, it corresponds to a power output per DG unit of around 3.62 MW each (excluding the DS term which depends on the load where the DG unit is located and contributes in the order of 0.1 MW). As a result, even if 20% of the load is curtailed, i.e., 80% of the power not supplied contributes to the annual ENS, there will always be around 5 MW of unserved load. By adding feeder interties, the unserved load in the system is minimized.

The utility engineer who is tasked with designing the distributed island resource system may decide an apt solution, considering the compromise between the cost of the project and the improvement in reliability of the system, by referring a lookup table of possible solutions such as the one shown in Table 3.9. The decision maker could use other economic metrics such as the Value of Lost Load (VOLL) which estimates the amount that customers receiving electricity with firm contracts would be willing to pay to avoid a disruption in their electricity service [138]. If this value is greater than the difference in costs between the cheaper and expensive solutions, then the expensive solution may be chosen.

Table 3.9 Solutions of the MOGA applied to RBTS Case I, numbered in increasing order of cost of the redesign

Solution #	Connection (s)	DG (s) bus location #	Cost [ $10^6$ US \$]	ENS [MWh]
1	Line 11-17	15	17.97	31.40
2	Line 1-7 Line 11-17	4 & 15	18.06	21.96
3	Line 1-7 Line 11-17 Line 23-29	4 & 15 & 25	18.12	21.88
4	Line 11-17 Line 23-29	13 & 29	18.31	21.62
5	Line 11-17 Line 17-23 Line 23-29	7 & 13 & 23	18.47	21.36
6	Line 1-7 Line 9-15 Line 21-27	11 & 13 & 23	18.91	21.33

### 3.3.3. Results of the MOGA applied to RBTS Case II

In this second case, we execute the MOGA to the RBTS system with the demand modeled with (2.3), tracking a step load duration curve. Again, the solutions collected in Table 3.10 represent those that occur with a higher frequency on the Pareto front of 5 MOGA simulations run for 50 generations.

The solutions proposed are very similar to those occurring in Table 3.9 and previously discussed in subsection 3.2.2; however, it is observed in this case that the value of the ENS obtained is lower. Again, the DG units are placed on feeders with higher rated loads – i.e., feeders 1 and 3 in RBTS - and those that cannot be connected by closing an open tie-switch. Within a feeder, the location that improves the reliability of the system the most is the bus where the higher rated loads are connected; however, this choice may be effected at a higher cost, such as at bus 2 in feeder 1, bus 13 and 11 in feeder 3 and 23 in feeder 5. Solutions No 1 and 3 are the same as is Table 3.9. Solution 2 locates DG at low loaded buses in feeders 3 and 5 and closes the open-tie

switches between those feeders, at a total cost of \$ 18.03 and an ENS of 17.98 MWh. Solution No.3 is an enhancement of Solution No.2, by adding a third DG in feeder 1 and closing the open-tie switch between feeder 1 and feeder 2 reducing the ENS to 17.62 MWh, at a cost of \$ 18.18 Finally, Solutions No. 5 and 6 are variations of Solution No. 3 concerning the location of DG, with generation units located at higher loaded buses such as 11, 13 and 23. However, Solution No.6 proposes to build a feeder intertie between feeders 2 and 3 on top of closing the open-tie switches in the system an corresponding to one of the maximum improvements of the ENS to 18.17 MWh a year, at a cost of \$ 18.62.

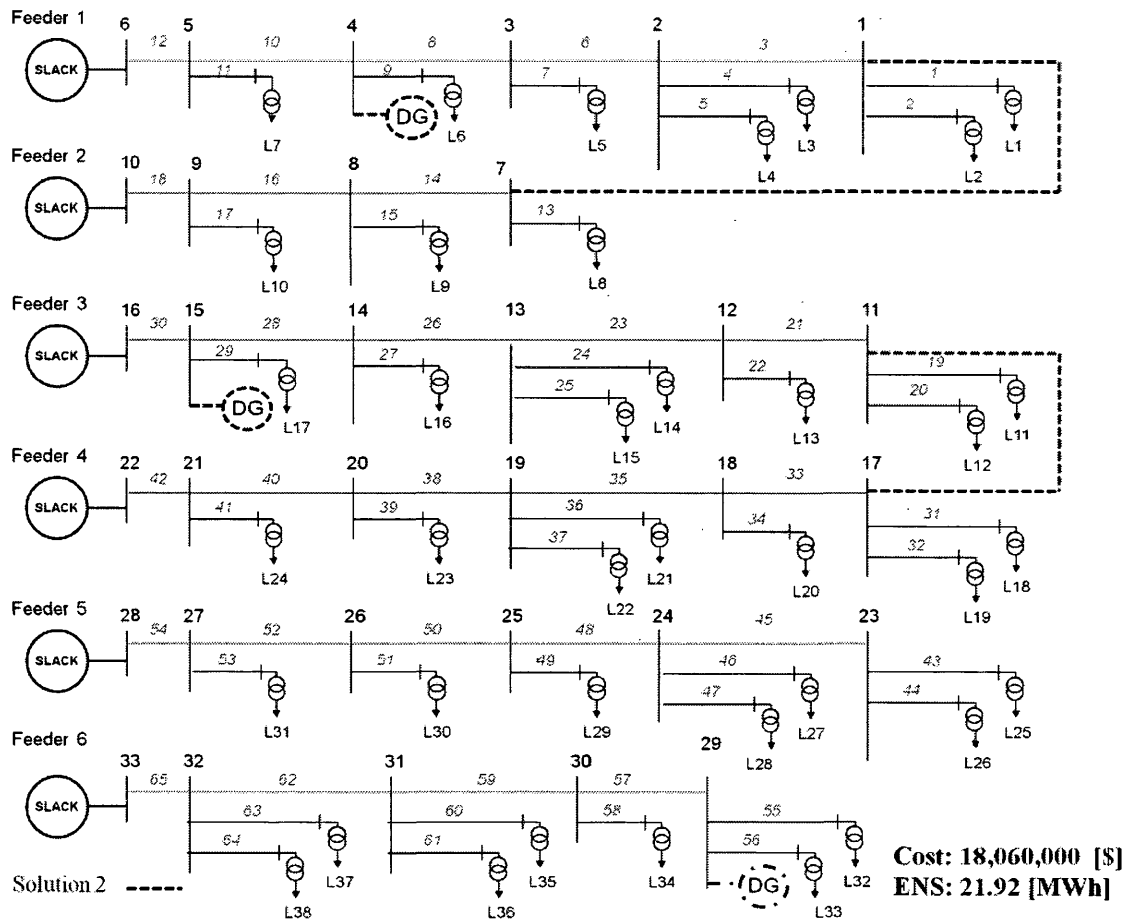


Figure 3.9: Solution 2 of the MOGA applied to RBTS Case I.

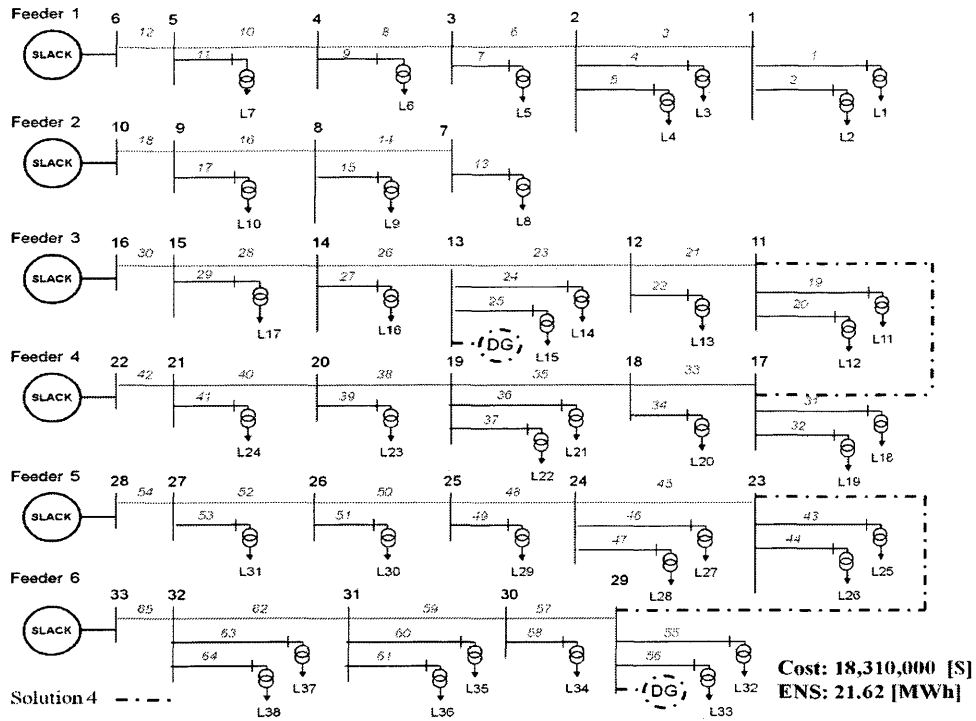


Figure 3.10: Solution 4 of the MOGA applied to RBTS Case I.

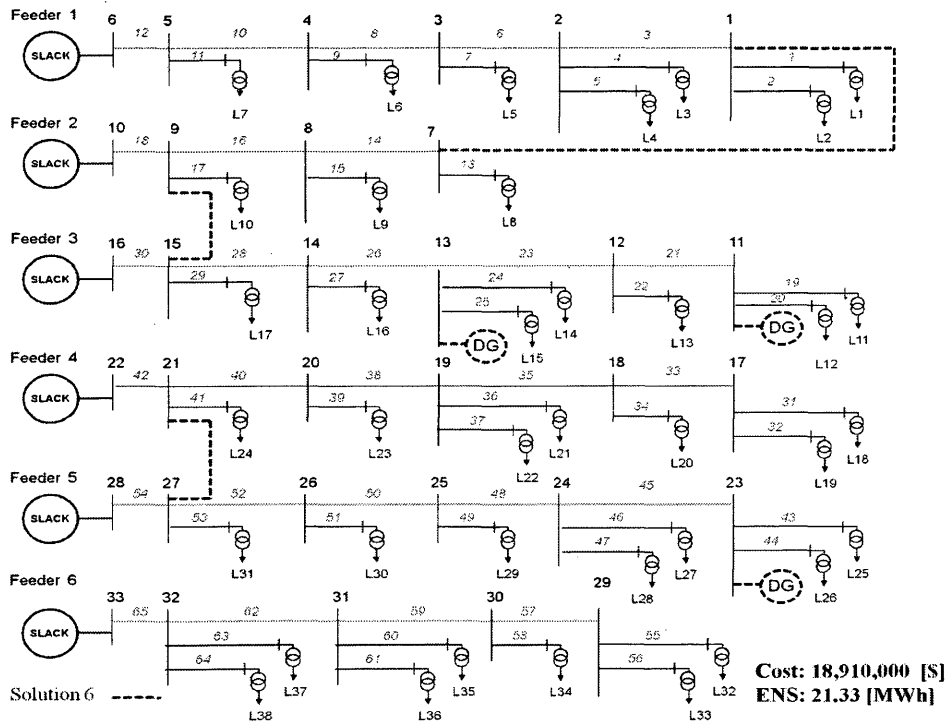


Figure 3.11 Solution 6 of the MOGA applied to the RBTS Case I system corresponding to one of the maximum improvements of the reliability with ENS of 21.33 MWh at a cost of \$18.91 millions of US \$ .



Table 3.10 Solutions of the MOGA applied to RBTS Case II, numbered in increasing order of cost of the redesign

Solution #	Connection (s)	DG(s) bus location #	Cost [ $10^6$ US \$]	ENS [MWh]
1	Line 11-17	15	17.97	28.43
2	Line 11-17 Line 23-29	14 & 25	18.03	19.78
3	Line 1-7 Line 11-17 Line 23-29	2 & 15 & 25	18.18	19.62
4	Line 11-17 Line 23-29	13 & 29	18.20	19.60
5	Line 1-7 Line 11-17 Line 23-29	2 & 11 & 25	18.32	18.37
6	Line 1-7 Line 8-14 Line 11-17 Line 23-29	2 & 13 & 29	18.62	18.17

### 3.3.4. Discussion on the results of RBTS Cases I and II

By modeling the load in the system with average loads as in RBTS Case I, higher values of the ENS in the system for the same redesign solution are obtained than with a more accurate representation of the demand as in RBTS Case II. From this observation we can conclude that modeling the demand in the system with annual average loads may potentially overestimate the ENS when compared to a more accurate representation of the demand over a year. This is not an issue for the redesign when the more accurate value is actually lower. The choice of the type of load modeled may be influenced by the comparison of accuracy versus the computational time for obtaining the Pareto front. In this thesis, a preference of one type of modeling the load over the other is not made.

However, introducing a time dependent characteristic of the load allows introducing more complexity in the model of the candidate power system. Modeling time dependent peak loads for

the solution(s) chosen can provide supplementary information to the designer in order to carry out other studies of an emerging islanded networked distribution system with DG, such as including a more accurate model of DG by taking into account the stochastic nature of RE, adequacy evaluation of the DER in the islanded system, analyzing the future impact of PHEVs, etc. As an example, modeling the system with time dependent load can be interesting to study worst case scenarios of generation and demand. This is the case of very low wind and solar radiation based DGs combined with high demand, (or vice versa), high power output of RE DG and very low demand in the system.

### 3.3.5. Computational time of the expanded MOGA applied to the RBTS

The computational time required by the MOGA applied to the RBTS depends on two factors: the initial population input to the algorithm; and, the modeling of the demand in the system.

Figure 3.7 shows the average computational time required by RBTS Case I and II as averaged over 5 simulations of 50 generations for the three ways of inputting the initial population as explained in Chapter 2 and repeated below:

- i. one possible connection between distinct feeders combined with one random possible location of a DG unit within the 27 buses of the system. The total number of possible connections between distinct feeders is 302.
- ii. one possible connections between distinct feeders combined with one possible location of a DG within the buses in the feeder from which the connection is made. The total number of possible connections between distinct feeders is 302.
- iii. one possible connections between distinct feeders no longer than 3 km combined with one possible location of a DG unit within the buses in the feeder from which the connection is made. The total number of possible connections between distinct feeders no longer than 3 km is 164.

As the reader can appreciate in Figure 3.12, the computational can be reduced by up to 60% by carefully selecting the initial population. Figure 3.12 illustrates the computational times required by the MOGA for 50 generations, and Figure 3.13 to the MOGA run for 25 generations. Fifty generations of the MOGA with initial population configuration types (i), (ii), (iii) converge to a satisfactory Pareto-front. However, if the MOGA is run for 25 generations with initial

population types (i) and (ii), it is observed that the Pareto-optimal solution- the cheapest networked connection to add between radial feeders with DG- is not always obtained. In Figure 3.14, the Pareto front of the MOGA with initial population types (ii) and (iii) run for 25 generations for RBTS Case I (average annual demand in the system) are compared.

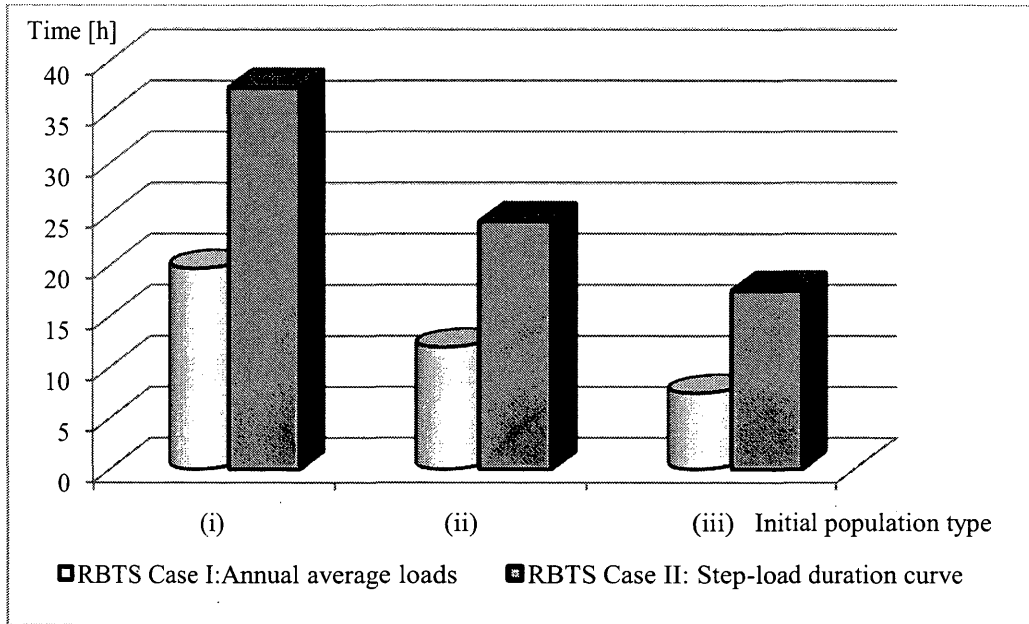


Figure 3.12: Computational time of RBTS Case I (cylinder) and II (box) for 50 generations and three types of configuration of the initial population.

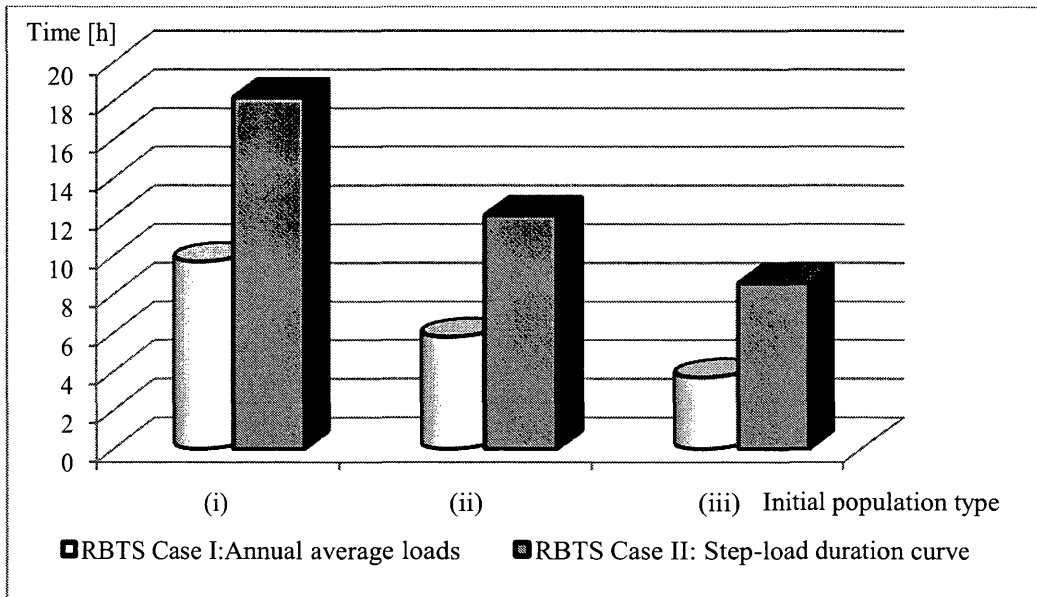


Figure 3.13: Computational time of RBTS Case I (cylinder) and II (box) for 25 generations and three types of configuration of the initial population.

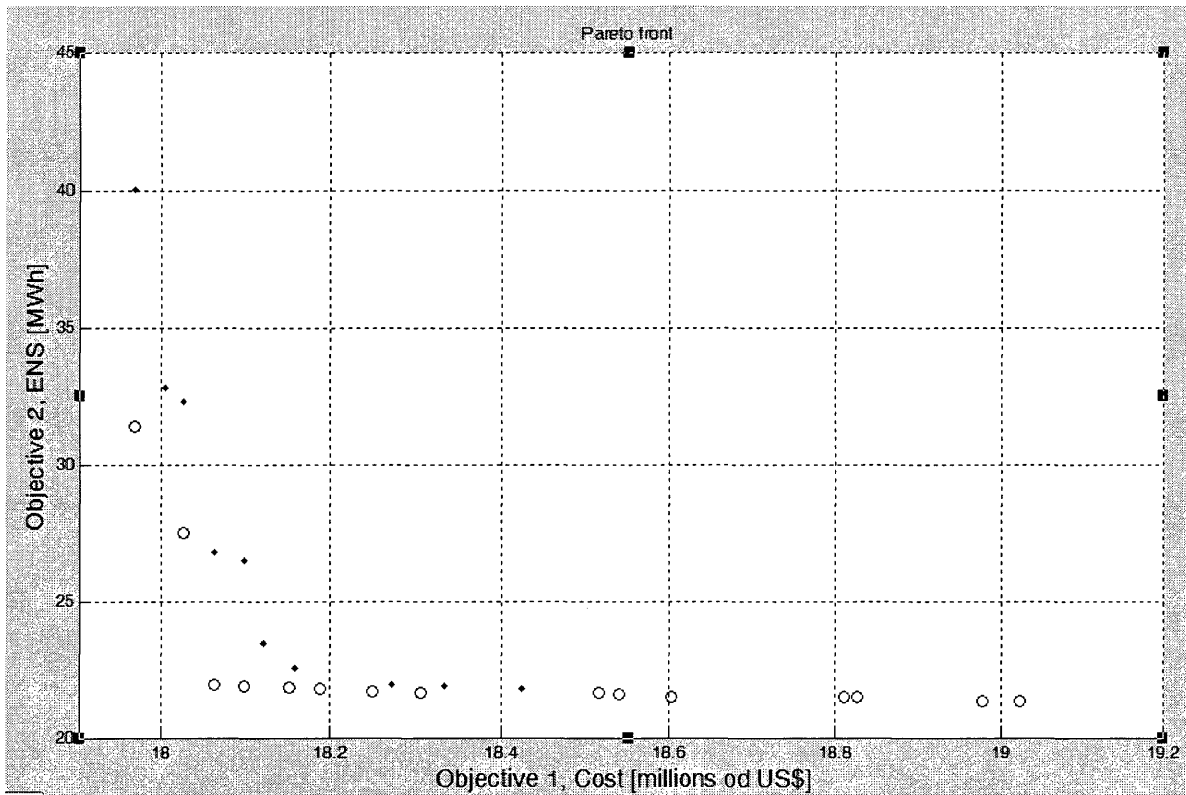


Figure 3.14: Pareto front of the MOGA applied to RBTS Case I with initial population type (ii) (rhombus) and initial population type (iii) (circles)

The extended MOGA applied to RBTS Case I for 25 generations corresponds to the most rapid implementation of the MOGA with average annual loads in the system and it is still a large value of 3 h and 40 min on a dedicated Intel® Core 2 CPU 4300 1.8 GHz machine. This increased computational time is due mainly because the fitness function of the MOGA evaluates only one individual of a population each time a population within a generation is evaluated, which adds to the run time. The main component of additional computational time is due to the fact that each time the fitness function is evaluated a power flow must be solved in order to obtain the reliability of the system and verify system constraints violations. For that, the connection from Matlab™ to SimAuto™ must be established and the PowerWorld™ system file opened. For Matlab™ to access PowerWorld™ through SimAuto™ takes approximately 10 s. This procedure has to be repeated for the evaluation of each candidate solution within a population. For a population size of 164 individuals, evaluating each of the individuals takes 18 minutes. This is the time required to obtain the fitness of the entire population within only one generation. For RBTS Case II, 50 generations of the MOGA take between 17 and 18 hours with initial population type (iii). In this case, the power flow has to be evaluated for each loading level of the system in order

to extract the slack buses power outputs and verify the systems constraints, which more than doubles the computational time required by the MOGA to solve RBTS Case II compared to RBTS Case I.

Finally, when the expanded MOGA described in this thesis is compared to the MOGA proposed in [20], the number of generation required for convergence is increased. In [20], the problem addressed is to optimally add feeder interties in the RBTS system with DGs arbitrarily located within the buses of the system. The number of generations required by the MOGA in [20] is 15. Adding the complexity to the original problem of co-locating feeder interties and DG in the system considerably increases the number of generations required by the MOGA to converge to Pareto-optimal solutions.

In the next chapter, a study of the contribution of PHEVs is performed for a fleet of PHEVs with V2G, i.e. enabling bi-directional charge/discharge capabilities of a vehicle from/to the grid. The impact is quantified by simulating the behavior of a vehicle as a load and as a generator for every day of a year. For that, an hourly peak load representation of the load is necessary. In fact, a PHEV hourly load is added or subtracted to the hourly peak load at the load point where the PHEV is located if it is charging or discharging respectively for the 8760 hours of a year. The data for hourly peak load for the RBTS test system is reproduced using [145]. Next, the annual average loads and a step-load duration curve are computed so that a similar application of the MOGA as described in this chapter may be performed for quantifying the impact of PHEV additions to a test system and to its design.

## CHAPTER 4

### IMPACT OF PLUG-IN HYBRID ELECTRIC VEHICLES ON AN ELECTRIC DISTRIBUTION SYSTEM ISLAND

PHEVs sales are expected to significantly increase in the car and light-truck market primary due to their potential to lower fuel cost, reduce petroleum consumption and decrease harmful emissions. In addition, the light vehicle fleet and the power grid can be complementary systems for managing energy and power through V2G technology. With the existing policies in the US, 1 million PHEVs are projected to be on the road in 2015, and between 2015 and 2020, PHEV sales are projected to be sustainable without requiring federal aid [139, 140]. As a consequence of the increasing number of PHEVs, their impact on the electric grid must be fully understood. The impact depends on a number of factors that are unknown yet such as design characteristics and market penetration rates. In this chapter, a methodology is proposed to determine the impact of PHEVs in distribution systems based on optimized charging patterns of a PHEV fleet. For that purpose, a probabilistic vehicle fleet simulation is performed in order to model the size and driving behavior of a PHEV fleet in the RBTS test system. Subsequently, the charging patterns of the PHEV fleet that may interact with the grid in V2G mode are optimized for utility peak shaving purposes and for the profit of the owner of the vehicle, when operating in V2G mode, and are compared to uncontrolled and delayed charging of the battery vehicles. The charging patterns of the RBTS PHEV simulated fleet are used to determine the impact of PHEVs in the RBTS system under islanded mode of operation and two case studies are presented.

#### 4.1 PHEVs in electric distribution systems

The deployment of PHEVs has the potential positive impact on the electric power system from the point of view of enabling new ways of electric energy management technologies as well as offsetting use of petroleum fuels with other energy sources. It is essential to realize that the existing power system infrastructure may not be adequate to deal with the increased demand and new patterns of consumption and power flows in the grid. For that reason, an increasing number of studies are focusing on the impact that PHEVs will have on the loading of distribution systems [89, 90], [102-108]. Yet, system-wide impacts of PHEVs in emerging distribution systems can only be understood when these vehicles are considered as both new loads and new distributed resources [79].

To the knowledge of the author, research related to the impact of PHEVs in distribution systems does not incorporate V2G capabilities of such vehicles. The contribution of PHEVs with V2G capabilities to the existing generating capacity of the grid is being currently explored from a technical to an economic point of view, but has not been included so far in the studies on the impact of the additional load on the distribution power grid.

#### 4.1.1 PHEVs with V2G technology

The concept of V2G is that an electric vehicle can provide electric energy back to the grid while not engaged in transportation. Perhaps, the most relevant to V2G among the many possible electric vehicle types is the hybrid type, which produces electricity on board from an internal combustion (IC) engine turning a generator. Specifically, PHEVs which have a grid connection allowing recharge from the grid as well as from fuel, and larger electrical components are the most suited for V2G purposes [15], [94], [100],[141,142]. PHEVs are designed with large capacity battery packs and a control algorithm such that operation is intended to be charge depleting, thus substituting stored electric energy in the battery for petroleum-based fuel. A PHEV power train runs under a charge-depleting control algorithm until the defined lower limit on the state of charge (SOC) is reached, and then runs under a charge-sustaining algorithm. Such control algorithms are also to be developed and are an open problem on the same level of importance to continued development of components such as battery chemistries, power electronic controllers, and electric machines [90], [102]. The two modes of charge operation of a PHEV battery will be further described and extended in the next section, since it plays a crucial role to determine the energy required per vehicle.

Research on V2G potential of PHEVs has concluded that the regulation, spinning reserves and peak power markets are the most suited for vehicle generation [15], [95]. In this chapter, we look at PHEVs as DER with specific battery energy requirements and constraints. For that, several enabling technologies must be developed and are considered as assumptions to this work. Reference [36] documents the enabling technologies for customer-driven DER and has inspired the important ones for PHEVs with V2G. The unique ones to PHEVs with V2G are based on the literature research [15] [90], [99]. Principally, some of the enabling technologies for PHEV with V2G integration are: a) adaptive protective system with bidirectional power flow; b) existence of a market structure that recognizes the PHEVs with V2G as a fully participating entity; c) proliferation of smart power electronic devices to control charging patterns and interconnection of electric vehicles under grid connected and islanded mode of operation; d)

agent like technology for enabling communication architectures serving the grid system operator; e) availability of dynamic pricing of electricity and load management; and f) presence of smart meters .

#### 4.1.2 Key assumptions to determine the impact of PHEVs

In order to fully understand the impact of PHEVs in distribution systems, key unknown and difficult to predict variables such as likely market penetration and design characteristics rates must be assumed. Concerning the former, many analytical approaches that attempt to model the customer acceptance and purchasing decisions of new and used vehicles have been developed [139], [141-144]. The methodology described in the following sections assumes a 30% penetration of PHEVs as in [89, 90], [104], and can be applied to other levels of penetration. Another issue is the availability of charging stations at work, at shopping locations or along streets and roads. In this thesis we consider that vehicles can charge at the respective owner residence and that a worker of commercial and office buildings can recharge PHEVs at work. However, in the probabilistic simulation of daily behaviors it is not considered whether a vehicle leaving from a residential load point is the same vehicle that recharges in a commercial or office building. This takes into account the fact that not all people arriving to work in a commercial building are from the same geographical area. In addition, an added factor that will influence the impact of PHEVs is the charging rate, i.e., the power at which the vehicle connects to the grid. In the United States, a 40-mile-range PHEV might take six hours to charge at 120 V or three hours to charge at 240 V [78]. At 120 V, the utility and the homeowner may not require any upgrades to the electrical service whereas at 240 V, the homeowner and perhaps the utility may have to perform service upgrades [78]. In this chapter, 50% of the vehicles charge at home at level 1, corresponding to 1.8 kW charge rate per hour, with a 120 V at 15 A connections. The other 50% does it at level 2 of charging with an electrical connection of 240 V and 30 A, drawing at an hourly charge rate of 7.2 kW. Vehicles in commercial and office buildings are considered to charge at level 2.

Pertaining to the design characteristics of the PHEV fleet, vehicle operational characteristics of a vehicle fleet published in [90] are used.

In the following section a methodology to quantify the impact of a PHEV vehicle fleet in a distribution system is presented. The methodology proposed in this chapter is depicted in Figure 4.1. Firstly, the methodology estimates a vehicle fleet size and annual behavior using a



probabilistic methodology proposed in [90], to obtain the daily energy required by the fleet over a year and the behavioral daily time parameters of the PHEV fleet; secondly, a linear programming approach is used to optimize the driving patterns of the vehicle fleet in order to determine the hourly increased load due to PHEVs over a year; finally, the impact on the annual reliability of a distribution system can be quantified by obtaining the ENS in the system with new annual loading that includes the PHEVs.

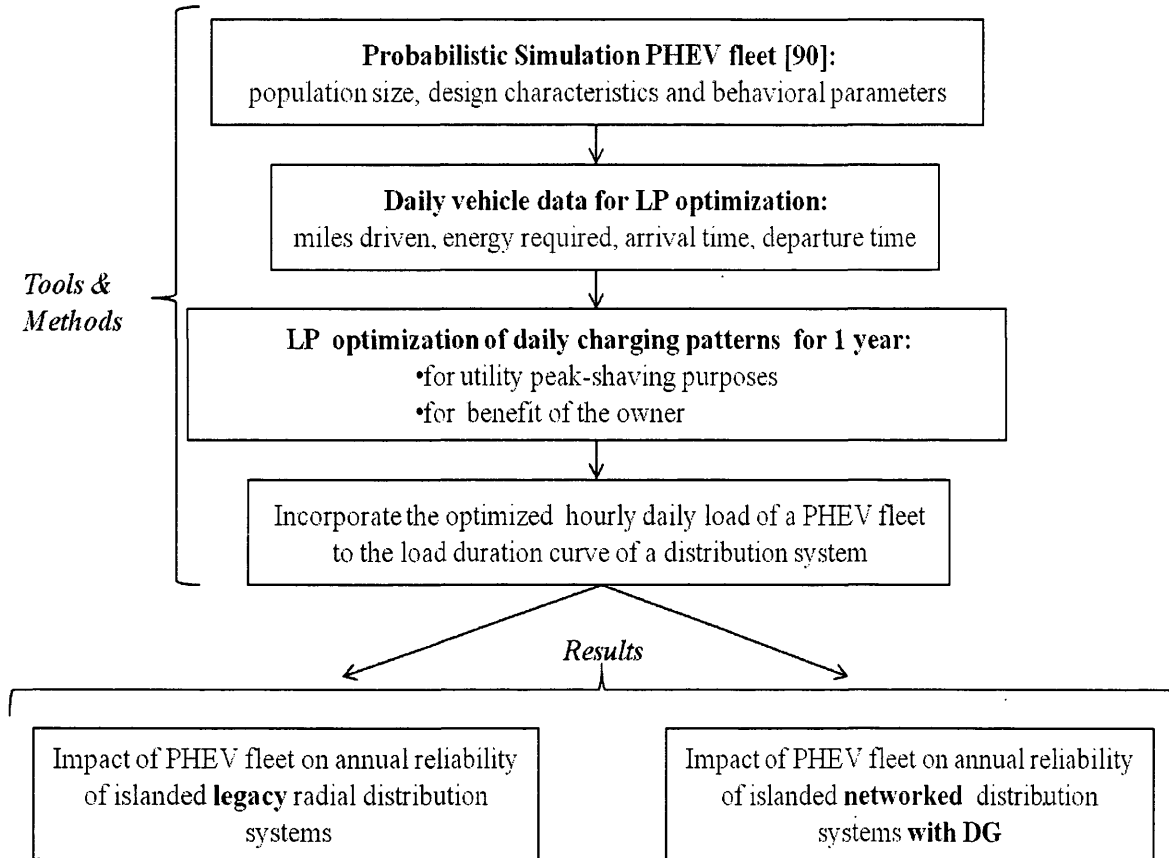


Figure 4.1: Methodology proposed to determine the impact of a PHEV fleet on the annual reliability of distribution systems under islanded mode of operation. The probabilistic vehicle fleet simulation methodology in [90] is used to generate daily data of a PHEV fleet unique to the distribution system under consideration. The LP algorithm is solved and the new annual loading of the distribution system is obtained. Finally, the impact of the PHEV fleet on the annual reliability can be quantified.

## 4.2 Probabilistic simulation of a PHEV fleet

The probabilistic PHEV fleet simulation used in this thesis is proposed in the final report titled “Power System Level Impacts of Plug-In Hybrid Vehicles” of the Power Systems Engineering Research Center (PSERC) [90]. The parts of the methodology used in this thesis are presented in this section and Equations (4.1)-(4.8) and Tables 4.1- 4 are directly taken from the PSERC final report. This is done for the completeness of the thesis. The probabilistic PHEV fleet simulation methodology is programmed in Matlab™ in a function named *PHEVSim()* using [90]. *PHEVSim()* and other auxiliary functions specific to the probabilistic PHEV fleet simulation are included in the electronic appendix.

The vehicle fleet characteristic design parameters are computed in [90] based on vehicle simulations performed using Powertrain System Analysis Toolkit (PSAT) version 6.2, developed by DOE's Argonne National Labs [81] and documented in [90]. Four vehicle classes were arbitrarily selected by the authors in 2009, to provide a diverse vehicle fleet representative of what a real vehicle fleet could look like. In 2011, the future vehicle fleet does not correspond to the one the authors of [90] predicted with regards to the vehicle brands. However, the design characteristics (i.e. battery size and efficiency) are still representative of actual and upcoming designs of PHEVs [78], [139].

Once the complete vehicle models are selected, PSAT simulates the operation of the modeled vehicles over specified driving schedules. Three drive schedules Highway Fuel Economy Test (HWFET), Urban Dynamometer Driving Schedule (UDDS), and the updated federal test driving cycle (US06) are selected in [90] to generate varied results representative of an entire vehicle fleet. PSAT simulations are performed for each vehicle class over each drive cycle and varying the amount of drive energy supplied from the battery obtaining discrete results per vehicle class.

The variable amount of driving energy supplied from the vehicles is defined in [90] as “ $k_{phev}$ , such that  $k_{phev}=0$  represents a charge sustaining mode in which on average all the drive energy is comes from gasoline and  $k_{phev}=1$  represents a charge depleting mode, i.e., all of the drive energy comes from electricity”. The vehicle simulation methodology utilizes randomly generated vehicle design parameters including  $k_{phev}$ . To facilitate simulating PHEV operation without a priori knowledge of the exact value of  $k_{phev}$ , performance characteristics such as the required energy per mile driven are approximated in [90] based on the discrete PSAT results as,

$$E_c = a_c^E (kphev_c)^{b_c^E} \quad (4.1)$$

where  $E_c$  is the required energy per mile driven [kWh/mi.] and  $a_c^E$  [kWh/mi.] and  $b_c^E$  are values of the approximated function parameters for each vehicle class (type)  $c$ . The function parameters shown in Table 4.1 are directly taken from [90]. Reference [90] estimates these parameters from the discrete PSAT results using a weighted nonlinear least squares approximation method.

Table 4.1 Parameters of the approximated function (4.1), taken directly from [90].

Vehicle class $c$	$a_c^E$ [kWh/mi.]	$b_c^E$
1	0.3790	0.4541
2	0.4288	0.4176
3	0.6720	0.4040
4	0.8180	0.4802

As mentioned earlier, the benefits of PHEVs for a driven distance can be optimized through the control strategy adopted in the two driving modes: charge depleting and charge sustaining modes. At the start of a trip, the charge depleting mode is used when the vehicles battery is fully or almost completely charged. On trips longer than the depleting driving distance, after the battery is depleted to a specified lower level determined by the state of charge (SOC) in the battery, the control strategy is switched to the charge sustaining mode. The charge sustaining mode relies on gasoline to maintain a constant average SOC where on average all the energy used to drive the PHEV comes from gasoline. The driving distance in the charge depleting mode is called in [90] the *charge depleting distance*,  $M^D$  (miles). The charge depleting distance for each vehicle  $v$  and class  $c$  is calculated as a function of the useable battery capacity  $B_c$  [kWh], and the vehicles required grid energy per mile  $E_c$  as in (4.1). The useable battery capacity is assumed to be a random variable (RV) within the battery capacity ranges of SOC defined in Table 4.2 for each vehicle class. The distribution of the battery capacity of each vehicle class  $c$  is explained in section 4.2.2. By assuming a depleting distance  $M^D$  of 40 miles for every vehicle class in [90], the *kphev* parameter range per class can be obtained from rearranging (4.1) and (4.2) and are shown in Table 4.2. The limits of the *kphev* parameter represent the percentage of energy per mile on average which comes from a battery on board a PHEV, within the assumed vehicle control strategy. The two-mode vehicle control strategy is dictated by the required SOC during the charge depleting mode.

$$M_c^D = \frac{B_c}{E_c} \quad (4.2)$$

Once the operational ranges of the four vehicle types have been selected, the design and behavioral parameters can be simulated. The following three vehicle parameters are based on random distributions in [90]: PHEV vehicle class population size, PHEV design parameters and battery capacity and finally daily behavioral parameters such as driving distance, departure time, and arrival time. To produce the random parameters of a vehicle fleet, the PSERC final report uses the Box-Muller method [145] to generate normally distribute random variables  $N$  which are recurrently used in this section and given by (4.3).

$$N = \sqrt{-2 * \ln(U_1)} * \cos(2 * \pi * U_2) \quad (4.3)$$

where  $N$  is a standard normal value (a normal RV with a mean of zero and a variance of one), and  $U_1$  and  $U_2$  are independent and identically distributed pseudo random numbers distributed uniformly over the range (0,1]. A Matlab™ inbuilt function *rand()* is used to obtain  $U_1$  and  $U_2$ .

Table 4.2  $K_{phev}$  ranges per class assuming  $B_c$  SOC ranges, reproduced from [90]

Vehicle class $c$	$B_c$ [kWh]		$k_{phev_c}$	
	Max	Min	Max	min
1	12	8	0.5976	0.2447
2	14	10	0.6151	0.2750
3	21	17	0.5428	0.3217
4	23	19	0.4800	0.3224

#### 4.2.1 PHEV class population size

Four vehicle types are selected by the PSERC report. The vehicle class probability distribution  $p_c$  is 0.2 for classes 1 and 4 and 0.3 for classes 2 and 3 [79]. The first random parameter to determine is the number of PHEVs in each class. As already mentioned in the previous section, the level of penetration assumed in this thesis is 30%. The total number of PHEVs is given by  $0.3 * N_t$ , with  $N_t$  being the total number of cars in the area power system of

interest. The number of PHEVs in each class is normally distributed where mean is  $0.3*Nt*Pc$  and standard deviation of 1% of the mean. It is justified in [79] that the normal distribution is selected because it “often occurs naturally and realistically models random customer behavior”. The vehicle class population is then computed as,

$$N_{phev} = \mu_c + \sigma_c * N \quad (4.4)$$

where  $N$  is given by (4.3),  $\mu_c$  is the mean and  $\sigma_c$  is the standard deviation per vehicle class  $c$ .

#### 4.2.2 PHEV design parameters and battery size

The next probabilistic parameters that need to be simulated are the vehicle design characteristics  $k_{phev_c}$  and usable battery capacity  $B_c$  [kWh]. “The random vehicle design parameters are assumed to be distributed according to a bivariate normal distribution with mean vector  $\mu$  and covariance matrix  $\Sigma$ ”, [90]. The justification stated in [90] for the assumed distribution is the ability of the bivariate normal to include parameter correlation. Using the specified ranges of  $k_{phev_c}$  and  $B_c$  simulated in Table 4.2,  $\mu$  and  $\Sigma$  are calculated. The correlation between  $k_{phev_c}$  and  $B_c$  is arbitrarily set to 0.8 by the authors of the PSERC report. “This correlation represents the intuitive relationship between the design parameters  $k_{phev_c}$  and  $B_c$ ”, [90]. The correlation coefficient is arbitrarily selected with added consideration that it be positive definite so that a Cholesky decomposition of  $\Sigma$ ,  $L$ , can be computed. Next, a vector of two standard normal values is generated using (4.3). Finally, the desired multivariate normal distribution is given by,

$$\vec{x} = \begin{bmatrix} k_{phev_c} \\ B_c \end{bmatrix} = \vec{\mu} + L * \vec{N} \quad (4.5)$$

where  $\vec{\mu}$  is a two dimensional mean vector  $L$  is the lower triangular matrix from the Cholesky decomposition of  $\Sigma$ , and  $\vec{N}$  is a two dimension vector of standard normal values. This procedure is repeated for each vehicle class, obtaining the values shown in Table 4.3 (for more details on this calculation see *PHEVSim()* in the electronic appendix).

Table 4.3 Random battery size and  $kphev$  parameter obtained from *PHEVSim ()*

Vehicle class $c$	$BC [kWh]$	$kphev_c$
1	14.3015	0.5976
2	14.1827	0.6151
3	19.1516	0.5428
4	21.3211	0.4800

#### 4.2.3 PHEV daily data

The next random parameter that needs to be generated is the daily vehicle performance, i.e., the miles driven per vehicle  $M_{d,v}$  [mi.]. The log normal distribution is according to the recommendation in [90]. This distribution has been verified in [90] by comparing sample generated results with known driving pattern statistics. “The known driving statistics are average yearly total miles driven of 12,000 miles, 50% of drivers drive 25 miles per day or less, and 75% of drivers drive 45 miles or less [146]”, [90]. Sample results computed in [90] using 328,500 log normal random variables with mean  $\mu_m = 3.37$  and standard deviation  $\sigma_m = 0.5$ , show that the total yearly driving distance average is 12,018 miles, 48% of the vehicles drive 25 miles or less each day, and 83% of the vehicles drive 45 miles or less each day, which closely approximate the driving performance results from [146]. Once more, the log normal RVs are generated using the standard normal random variable (RV)  $N$  in (4.3) and computed using (4.6).

$$M_{d,v} = e^{(\mu_m + \sigma_m * N)} \quad (4.6)$$

where  $M_{d,v}$  is the distance driven by vehicle  $v$  per day  $d$ , and  $\mu_m$  and  $\sigma_m$  are the mean and standard deviation respectively of the log normal distribution.

Knowing the battery size capacity available per vehicle class  $B_c$ , the required energy per mile driven per vehicle class  $E_c$ , the charge depleting distance  $M_c^D$  per vehicle class and finally the daily driving distance  $M_{d,v}$  per vehicle, the daily recharge energy required from the grid per class and vehicle can be computed,  $DE_{d,c,v}$  as in (4.7). The daily recharge energy required from the grid depends on whether the charge depleting distance has been reached in a daily trip. If the daily driving distance of a PHEV  $M_{d,v}$  is smaller than the charge depleting distance, the energy required from the grid when the vehicle arrives home is the energy requirement per mile by the vehicle class  $E_c$  multiplied by the driven distance that day. Conversely, if the charge sustaining

mode has been reached, meaning that the charge depleting distance that day has been exceeded, then the SOC of the battery has been maintained within the assumed limits in Table 4.2 and the required energy that day is the full battery capacity per vehicle class  $B_c$ .

$$DE_{d,c,v} = \begin{cases} B_c & , \quad \text{if } M_{d,v} \geq M_{d,c} \\ M_{d,v} * E_c & , \quad \text{if } M_{d,v} \leq M_{d,c} \end{cases} \quad (4.7)$$

Finally, the time performance parameters, departure time and arrival time are modeled using Gaussian distributions, as the best estimate of random residential consumer behavior [79]. Different timing distributions are used to model the potential different consumer behaviors on weekdays versus weekends. As before a standard normal value  $N$ , is computed using (4.3). Then, the time values are given as,

$$T_{d,v}^{res} = \mu_t + \sigma_t * N \quad (4.8)$$

where the result  $T_{d,v}$  is a normally distributed integer with mean  $\mu_t$  and standard deviation  $\sigma_t$ . The values for  $\mu_t$  and  $\sigma_t$  are given in Table 4.4. The value  $T_{d,v}$  represents either the arrival time or the departure time depending on the values used for the mean and standard deviation. The arrival time  $A_{d,v}$  for vehicle  $v$ - on day-  $d$  must occur after the departure time  $D_{d,v}$  for vehicle- on day- . To achieve this specification, an acceptance-rejection method is used in [79]. Let  $A_{d,v}$  be a particular generated arrival time and  $D_{d,v}$  be a particular generated departure time. Each generated pair is checked, and if  $A_{d,v} \leq D_{d,v}$ , then a new pair is generated and the process is repeated until and the generated pair is accepted. The number of pairs  $(A_{d,v}, D_{d,v})$  are generated for the number of vehicles in a residential PHEV fleet.

Table 4.4 Time parameters mean and standard deviation for weekday and weekends reproduced from [90]

Parameter	Departure (am)		Arrival (pm)	
	Weekday	Weekend	Weekday	Weekend
$\mu_c$	7	9	6	15
$\sigma_c$	1.73	2.45	1.73	2.45

The daily time parameters given by (4.8) are representative of residential loads, which is the type of loading studied in [90]. However, in the RBTS test system there are five office building and two commercial building type of loading. For that reason, (4.9) is proposed in this thesis as simulating the time characteristics for office and commercial type of loads. The procedure followed is to first generate a number of arrival and departure residential times using (4.8) equal to the size of the office and commercial building PHEV fleet. After that, the values are used in (4.9.a) and (4.9.b) to determine the actual time characteristics of the office and commercial building PHEV fleet.

$$A_{d,v}^{non-res} = D_{d,v}^{res} + \frac{M_{d,v}}{S} \quad (4.9.a)$$

$$D_{d,v}^{non-res} = A_{d,v}^{res} + \frac{M_{d,v}}{S} \quad (4.9.b)$$

where  $A_{d,v}^{non-res}$  and  $D_{d,v}^{non-res}$  are the arrival and departure times respectively of office and commercial type of load points,  $D_{d,v}^{res}$  and  $A_{d,v}^{res}$  are residential departure and arrival times generated using (4.8) and  $M_{d,v}$  is the miles driven by vehicle  $v$  per day computed by (4.6). Finally,  $S$  is the average urban driving speed assumed to be 25 miles per hour [147].

With the probabilistic simulation method described in this section by referring to the original work done in [90], data for daily energy requirements per vehicle and arrival and departure behaviors of a PHEV fleet can be generated for a year, and used as parameters for the linear optimization method presented in the next section in order to determine the annual loading of a distribution system with PHEVs.

#### 4.3 LP algorithm for the PHEV fleet charging problem

Towards modeling the impact that a simulated PHEV fleet with V2G capabilities may have on a given distribution system, an imperative question to answer is: for how long does a PHEV behave as a load and for how long it behaves as a generator? From a utility perspective, a PHEV fleet in an area may be used for peak shaving purposes. From a customer point of view, the PHEV may be used to reduce the hourly energy consumption, i.e. reduce the owner's energy bill.



With these two motivations as possible driving factors of a PHEV charging pattern behavior, a LP algorithm is proposed to determine the expected annual loading of the RBTS test system.

#### 4.3.1 Mathematical formulation

Once the PHEV fleet is simulated with the method explained in section 4.2, an LP algorithm can be formulated in order to resolve the charging patterns of a given number of vehicles in a distribution system. First, the LP for peak shaving purposes is presented and secondly, the one for minimizing the vehicle owner's energy bill. These two algorithms are handled separately in this thesis. Future work may warrant an algorithm for co-optimization purposes.

##### 4.3.1.1 LP algorithm for peak shaving purposes

The algorithm is described by introducing first the sets of indexes used in the algebraic notation of the mathematical formulation of the LP, followed by the parameters required in the model. Next the variables which need to be determined by the algorithm in order to obtain the objective value, the objective function and finally the constraints to the problem.

- Sets: The sets represent the index notation used in the mathematical formulation of the algorithm.
  - $I$  = set of load types , from  $1 \dots N^I$
  - $C$  = set of PHEV classes, from  $1 \dots N^C$
  - $V$  = set of PHEV per class, from  $1 \dots N^V$
  - $D$  = set of days in a year, from  $1 \dots N^D$
  - $T$  = set of hours in a day, from  $1 \dots N^T$
- Parameters: The parameters are the required data in order to determine the variables and constraints of the problem
  - $N^I, N^C, N^V, N^D$  and  $N^T$  are the total number of load types  $i$ , vehicle classes  $c$ , vehicles  $v$  per class, days  $d$  in a year and hours  $t$  in a day respectively
  - $B_c$  = Battery size per vehicle class  $c$  [kWh]

- $C_c^{max}$  = Maximum hourly charge rate per vehicle class  $c$  [kW]
  - $DE_{d,c,v}$  = Daily energy required per day  $d$ , vehicle class  $c$  and vehicle  $v$  [kWh]
  - $A_{d,c,v}$  = Daily arrival time per day  $d$ , vehicle class  $c$  and vehicle  $v$  [h]
  - $D_{d,c,v}$  = Daily departure time per day  $d$ , vehicle class  $c$  and vehicle  $v$  [h]
  - $L_{d,i}^{av}$  = Average base load (without PHEVs) on day  $d$  and load type  $i$  [kW]
  - $L_{d,i,t}^{peak}$  = Peak base load (without PHEVs) on day  $d$ , load type  $i$  and hour  $t$  [kW]
- Variables: The variables in the system are determined by the LP algorithm. The first two variables  $C_{d,c,v,t}^+$  and  $C_{d,c,v,t}^-$  represent the daily energy charged and discharged per vehicle per hour. Note that because of the hourly time period resolution of the variables, power and energy have the same value. Yet,  $C_{d,c,v,t}$  is the energy stored in the battery by the end of time period  $t$  and is analogous to an inventory variable, keeping track of the energy in the battery. The next two variables  $V_{d,c,v,t}^+$  and  $W_{d,c,v,t}^+$  are mathematical constructs to sense the variation between charging and discharging within one day, and are used to constraint the cycling occurring in a battery per day. At last,  $L_{d,i,t}$  is the total hourly daily load per load type with PHEVs and  $Z_{d,i,t}$  is the absolute difference of the mentioned load and the average base load.
    - $C_{d,c,v,t}^+$  = Amount charged on day  $d$ , vehicle class  $c$ , vehicle  $v$  and time  $t$  [kW]
    - $C_{d,c,v,t}^-$  = Amount discharged on day  $d$ , vehicle class  $c$ , vehicle  $v$  and time  $t$  [kW]
    - $C_{d,c,v,t}$  = Energy stored on day  $d$ , vehicle class  $c$ , vehicle  $v$  and time  $t$  [kWh]
    - $V_{d,c,v,t}^+$  = Positive difference between  $C_{d,c,v,t}^+$  and  $C_{d,c,v,t}^-$  on day  $d$ , vehicle class  $c$ , vehicle  $v$  and time  $t$  [kW]
    - $W_{d,c,v,t}^+$  = Absolute value of the difference between  $V_{d,c,v,t}^+$  and  $V_{d,c,v,t+1}^+$  [kW]
    - $L_{d,i,t}$  = Load at day on day  $d$ , load type  $i$  and hour  $t$  [kW]
    - $Z_{d,i,t}$  = Absolute value of the difference between  $L_{d,i,t}$  and  $L_{d,i}^{av}$  [kW]

- Objective function: For peak shaving purposes, the objective is to minimize the sum of the absolute difference of the actual hourly daily load to the average daily load. Because the actual daily average load with PHEVs is unknown and depends on the uncertain variables in the system, the average base load is used instead.

$$Peak\ shaving = Minimize \left\{ \sum_{d,i,t} Z_{d,i,t} \right\} \quad (4.10)$$

- Constraints: The constraints are the restrictions to the problem and limit the feasible region of the problem, i.e., the solution space where the values of the variables can be found.
  - Battery restrictions: Equations (4.11) and (4.12) set the maximum charge rate of the battery of a vehicle per hour and (4.13) expresses the energy left in the battery when the vehicle arrives home. If the charge sustaining mode has not been reached, the energy left in the battery will be the battery size minus the energy required to bring it to full charge. If the charge depleting distance has been exceeded, then the energy in the battery when the vehicle arrives home will be 0. Equation (4.14) states the hourly inventory balance in the battery per day and it is equal to the energy available in the battery in the previous hour added to the charge or discharge occurring in the present hour. In (4.15), the requirement is that the vehicle is fully charged by the daily departure time of the vehicle. Finally, (4.16-18) are constraints related to the cycles of charge and discharged allowed per day during the charging period, i.e. between the arrival and departure time of the vehicle. Equation (4.16) measures the positive difference between charging and discharging; when positive charging occurs and when it is zero discharging occurs. Next, (4.17) subtracts the values of the positive variation in (4.16) and hour  $t$  to the one occurring at  $t+1$ ; if the absolute value of the difference is not zero then it accounts for a variation between charge and discharge or vice versa and if the difference is zero, it represents no variation between charging and discharging or vice versa. At last, the number of non zero values allowed in  $W_{d,c,v,t}^+$  is 3. Suppose that a two charge/discharge cycles occur during a charging period: the first non-zero value accounts for a variation between the first charge and discharge; the

second non-zero value accounts for the first discharge and the second charge; and finally the third non-zero value accounts for the variation between the second charge and the second discharge. The sum of the absolute difference between two time periods of the variation between charging and discharging should be less than or equal to three times the maximum charge rate. Equation (4.18) constraints the battery to have a maximum of 2 battery cycles, which are defined as a complete discharge, followed by a complete charge of a battery [148].

$$C^+_{d,c,v,t} \leq C_c^{max} \quad \forall d, c, v, t \quad (4.11)$$

$$C^-_{d,c,v,t} \leq C_c^{max} \quad \forall d, c, v, t \quad (4.12)$$

$$C_{d,c,v,t} = B_c - DE_{d,c,v} \quad \forall d, c, v \text{ and for } t = A_{d,c,v} - 1 \quad (4.13)$$

$$C_{d,c,v,t} = C_{d,c,v,t-1} + C^+_{d,c,v,t} - C^-_{d,c,v,t} \quad \forall d, c, v \text{ and } A_{d,c,v} \leq t \leq D_{d,c,v} \quad (4.14)$$

$$C_{d,c,v,t} = B_c \quad \forall d, c, v \text{ and for } t = D_{d,c,v} \quad (4.15)$$

$$V^+_{d,c,v,t} \geq C^+_{d,c,v,t} - C^-_{d,c,v,t} \quad \forall d, c, v \text{ and } A_{d,c,v} \leq t \leq D_{d,c,v} \quad (4.16)$$

$$-W^+_{d,c,v,t} \leq V^+_{d,c,v,t} - V^+_{d,c,v,t+1} \leq W^+_{d,c,v,t} \quad \forall d, c, v \text{ and } A_{d,c,v} \leq t \leq D_{d,c,v} - 1 \quad (4.17)$$

$$\sum_{d,c,v,t} W^+_{d,c,v,t} \leq 3 * C_c^{max} \quad \forall d, c, v, \text{ and } A_{d,c,v} \leq t \leq D_{d,c,v} - 1 \quad (4.18)$$

- Load in the system with PHEVs: (4.19) calculates the load in the system with PHEVs which is the daily base load at load type  $i$  added to the sum of the charging or discharging of the vehicles present at that load type. Equation (4.20) gives the absolute value of the difference between the occurring daily load at load type  $i$  and time  $t$  and the daily average base load value  $L^{av}_{d,i}$ .

$$L_{d,i,t} = L_{d,i,t}^{peak} - \sum_{j=1}^{N^V} (C_{d,c,v,t}^- + C_{d,c,v,t}^+) \quad \forall d, i, t \quad (4.19)$$

$$-Z_{d,i,t} \leq L_{d,i,t} - L_{d,i}^{av} \leq Z_{d,i,t} \quad \forall d, i, t \quad (4.20)$$

- Non-negativity constraints: (4.21) states that all the variables are positive or equal to zero.

$$C_{d,c,v,t}^+, C_{d,c,v,t}^-, C_{d,c,v,t}, V_{d,c,v,t}^+, W_{d,c,v,t}^+, L_{d,i,t} \text{ and } Z_{d,i,t} \geq 0 \quad (4.21)$$

#### 4.3.1.2 LP algorithm for minimizing the vehicle owners consumption

The mathematical formulation of the optimization problem in order to minimize the costumers energy bill is very similar to the one presented in the previous section 4.3.1.1. For that reason, only the differences to the model discussed above will be presented in this section.

The parameter required to determine the new objective function is the daily price per hour  $P_{d,t}$  [\$/kWh]. A TOU pricing scheme is chosen and synthetic data is created, inspired by the residential TOU pricing currently offered in [149] and shown in Figure 4.2, and adapted to the residential rates offered by a candidate utility in [150] and shown in Figure 4.3.

The objective function for the LP algorithm for the customer benefit is then given by,

$$\text{Energy bill} = \text{Minimize} \left\{ \sum_{d,i,t} P_{d,t} * L_{d,i,t} \right\} \quad (4.22)$$

where  $P_{d,t}$  is the hourly daily rate of energy consumption and  $L_{d,i,t}$  is the load in the system with PHEVs

The set of constraints that define the optimization problem to minimize (4.22) are the same as the ones required for peak shaving purposes, except for (4.20) which is irrelevant to minimizing the customers energy bill.

### 4.3.2 LP algorithm implementation

The LP algorithms to optimize the charging patterns of a PHEV fleet are coded in AMPL™ language [151]. AMPL™ is a language designed to make the formulation of an optimization problem easy to the user. The language closely resembles the symbolic algebraic notation that many modelers use to describe mathematical programs and similar to the one used in section 4.3.1. Yet, it is regular and formal enough to be processed by a computer system. The solver used is IBM ILOG CPLEX™ which is a mathematical programming solver for linear programming, mixed integer programming, quadratic programming, and quadratically constrained programming problems installed in a machine named cross-country in Colorado School of Mines with the following specifications: Dell PowerEdge R410, dual-quadcore Intel E5520 with HyperThreading enabled, 12GB of RAM, pair of 160GB drives in a RAID1 [152].

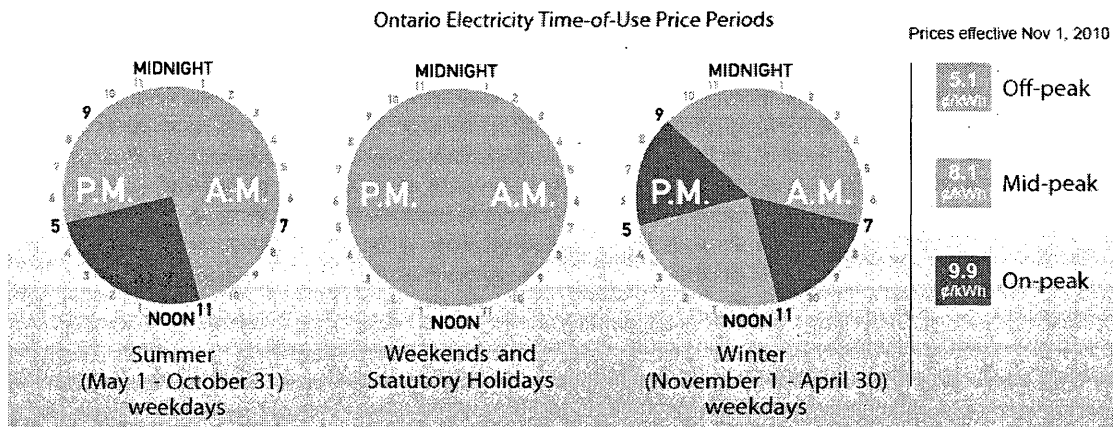
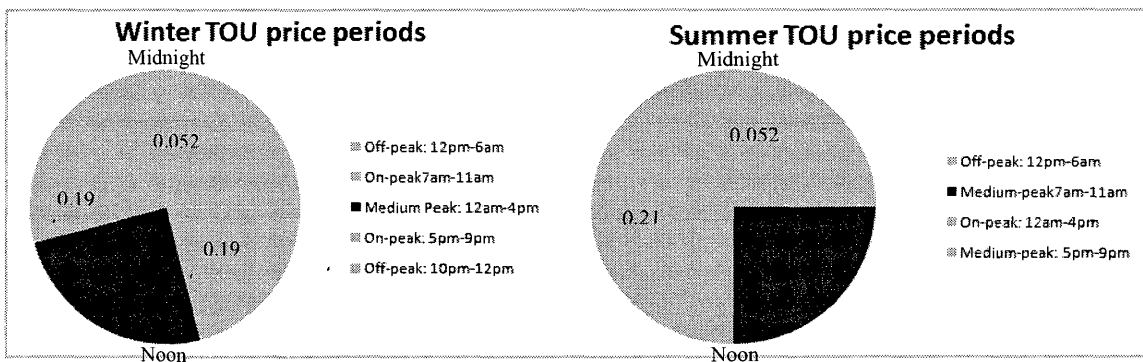


Figure 4.2: Ontario Electricity TOU price periods for the summer and winter weekdays, and for the weekends and holidays, directly taken from [149].



\*the numbers inside the pie charts express the energy rate in \$/kWh

Figure 4.3: Synthetic data of TOU price periods for the summer and winter weekdays.

#### 4.4 Application of the PHEV fleet probabilistic simulation and LP algorithms to the RBTS test system

First, the PHEV fleet simulation method [79] presented in the previous section is applied to the RBTS test system to generate the required parameters for the optimization model. Secondly both of the LP algorithms are applied to the characteristics of the RBTS test system and the charging patterns of the PHEV fleet are determined. The charging patterns of the battery vehicles obtained from the LP solver CPLEX<sup>TM</sup> are given in the electronic appendix.

##### 4.4.1 PHEV fleet simulation applied to the RBTS test system

In order to use the probabilistic simulation of a PHEV fleet presented in 4.2 to the RBTS test system, a number of assumptions must be held.

First, to determine the total number of cars  $N_t$  and apply (4.4) to calculate the PHEV vehicle class population size, the load types with PHEVs must be chosen. For that purpose, the residential, commercial and office building load types are selected to have customers with PHEVs. The RBTS test system is described in section 3.1.1 and Table 3.7 shows the load types in the system.

The total base load of residential load points adds up to 19.9 MW.  $N_t$  is calculated based on an average consumption of energy per customer of 2 kW and 1.5 vehicles per electric customer [89,90], [104] such that the total number of cars in the residential area of the RBTS is 14,925. Using (4.4), the PHEV class population size is shown in Table 4.5. The total number of PHEVs in the RBTS test system with 30% of penetration is 4,474. The PHEV fleet is uniformly distributed throughout the residential loads in the system, i.e., every residential load point in Table 3.7 is assumed to be 186 PHEVs. The 24 residential load points in Table 3.7 are classified into 3 types of residential loads differentiated by their power demand. The total number of vehicles for which annual daily behavioral data is generated for each residential load type, is 186 cars. It would be time prohibitive to generate daily data (energy required, arrival and departure times) for the 24\*186 vehicles in the residential area of the RBTS test system. Nevertheless, the size of the vehicle fleet chosen allows generating 67,704 values of probabilistic daily energy required, arrival and departure times. These daily parameters for each vehicle within the four classes of study and for a year time period are included in the electronic appendix due to their large dimensions. Residential charge rates are chosen to be level 1 (120V, 15A) for vehicle class 1 and 2, and level 2 (240V, 30A) for types 2 and 4.

Table 4.5 Probabilistic results of population size per vehicle class

<i>Vehicle class</i> <i>c</i>	Vehicles per load point type		
	Residential	Office building	Commercial
1	44	15	7
2	48	18	9
3	45	14	6
4	49	19	8

Concerning commercial and office building type of loads, the size of the vehicle fleet depends on the number of workers in the buildings. According the Energy Information Agency (EIA) of the US Department of Energy (DOE), there are in average 38 and 17 workers per office and commercial building respectively. If each one of the workers owns 1.5 vehicles, with 30% of penetration the total number of PHEVs per office and commercial building is 17 and 8 PHEVs respectively. Each commercial load point is assumed to serve four commercial buildings and each office building load type serves two. In addition, the working schedule for office buildings is from Monday through Friday, whereas commercial buildings are assumed to be functional all days of the week.

Finally, the PHEV design and battery capacity characteristics are the ones presented in section 4.2.2, which depend only on the PHEV type and not on the distribution system where the vehicle is located.

#### 4.4.2 LP algorithm applied to the RBTS test system

The LP algorithm is applied to the loading and PHEV fleet characteristics of the RBTS test system. The AMPL<sup>SM</sup> program used to run both LP algorithms is included in the electronic appendix, including the data file, model file and the run file. Table 4.6 includes the dimensions of the sets indexes of the problem and gives the reader an idea of the size of the problem given by the number of variables and constraints. The number of vehicles is approximated to the average of the average number of vehicles per load type (three residential types, one commercial and one office building). The size of a variable related to the battery charge is *4 vehicle classes x 33*



vehicles per class  $\times$  364 days in a year  $\times$  24 hours per day  $\sim 1.15 \times 10^6$  per variable. The size of a variable related to the new load in the system is 5 load types (3 residential and 2 non-residential)  $\times$  364 days in a year  $\times$  24 hours per day  $\sim 4.37 \times 10^4$ . The total number variables  $n$  required to determine the objective function value is: 5 battery related variables  $\times 1.15 \times 10^6$  (size a battery variable) + 1 load variable  $\times 4.37 \times 10^4$  (size of a load variable)  $\sim 5.79 \times 10^6$  variables. The size of the problem is the product of the number of variables  $n$  and the number of constraints  $m=10$  and is approximately  $5.79 \times 10^7$ .

Table 4.6 Size of the sets of indexes of the LP in the RBTS test system

Sets	Dimensions
I	$N^I = 5$
C	$N^C = 4$
V	$N^V \sim 33$
D	$N^D = 364$
T	$N^T = 24$

In the previous chapter, the results published in [132] were used to build the load duration curve of the RBTS Bus 3 test system. A load duration curve described by 100 data points is given in [132] for the RBTS system in per unit of the peak load and study periods. However, in this chapter, the LP algorithms require the daily load curves per load type of the system for a period of 1 year as input parameters. For that purpose, the data on weekly peak in percent of the annual peak load, daily peak load in percent of the weekly peak, and at last hourly peak load in percent of the daily peak load of the RBTS test system are used. These data for the RBTS test system are the same as that of the IEEE Reliability Test System (RTS) [145]. The IEEE RTS system was published by the IEEE Subcommittee on the Application of Probability Methods and provides a set of data that can be used in system reliability evaluation [132]. The weekly and daily data is shown in Table 4.7-8 respectively and the hourly load profile of the yearly seasons, in percent of the daily peak load is drawn in Figure 4.4. With these data, hourly annual data ( $24 \text{ hours} \times 52 \text{ weeks} \times 7 \text{ days a week} = 8736 \text{ load data}$ ) can be computed.

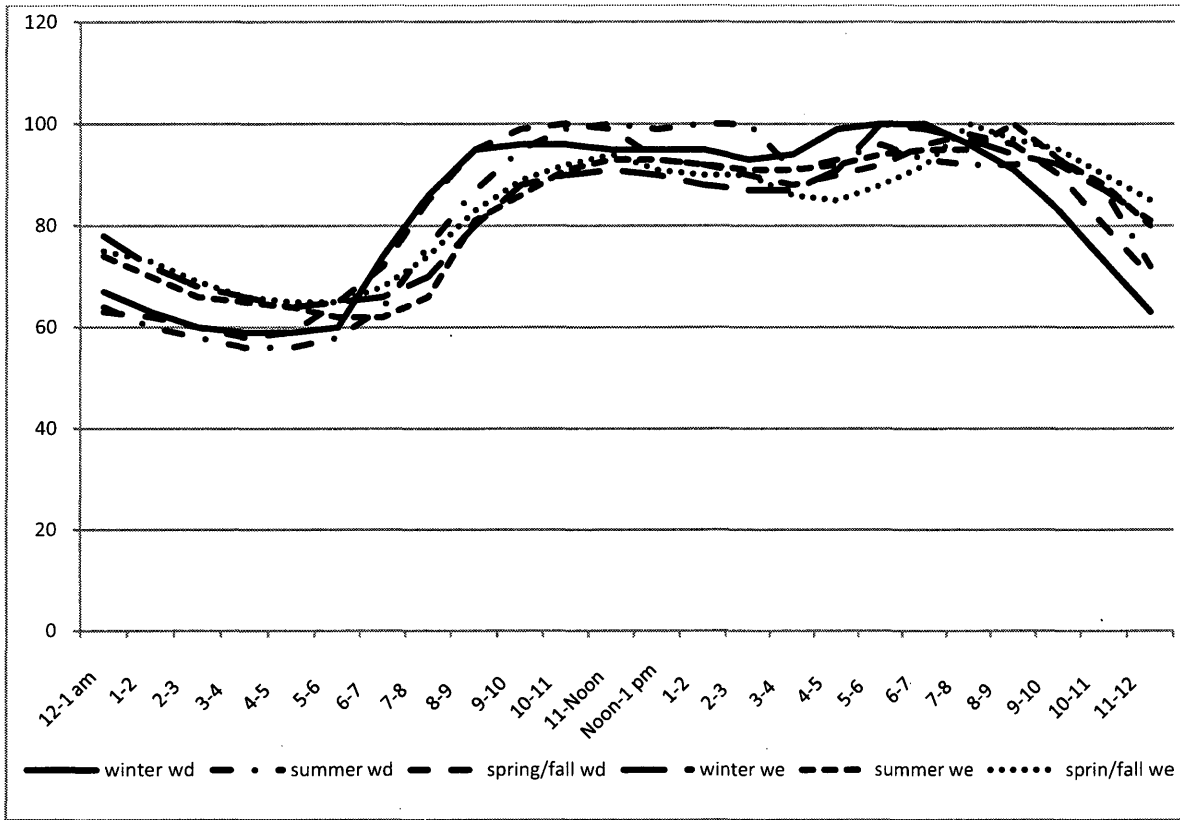


Figure 4.4: Seasonal hourly load in percent of the daily peak load for weekdays (*wd*) and weekends (*we*) reproduced from [145].

Table 4.7 Weekly peak load in percent of annual peak load, taken directly from [145]

Week	Peak Load	Week	Peak Load	Week	Peak Load	Week	Peak Load
1	82.2	14	75	27	75.5	40	72.4
2	90	15	72.1	28	81.6	41	74.3
3	87.8	16	80	29	80.1	42	74.4
4	83.4	17	75.4	30	88	43	80
5	88	18	83.7	31	72.2	44	88.1
6	84.1	19	87	32	77.6	45	88.5
7	83.2	20	88	33	80	46	90.9
8	80.6	21	85.6	34	72.9	47	94
9	74	22	81.1	35	72.6	48	89
10	73.7	23	90	36	70.5	49	94.2
11	71.5	24	88.9	37	78	50	97
12	72.7	25	89.6	38	69.5	51	100
13	70.4	26	86.1	39	72.4	52	95.2

Table 4.8 Daily load in percent of weekly load directly taken from [145]

Day	Peak Load
Monday	93
Tuesday	100
Wednesday	98
Thursday	96
Friday	94
Saturday	77
Sunday	75

Furthermore, in this chapter, a more accurate representation of office and commercial building daily load profiles has been computed using synthetic data. In the previous chapter, the load duration curve is computed from the data available in [132] and in which the load points of the RBTS system are approximated to behave as residential loads. In this chapter, the winter hourly load profile of commercial and office buildings is computed as in Figure 4.5 in order to simulate the charging patterns of vehicles occurring during work hours. The summer load is considered to be 15% more than the winter and the spring and fall hourly loads are considered to be 15% less than the winter loads. These values may be aptly modified for various geographical regions as needed.

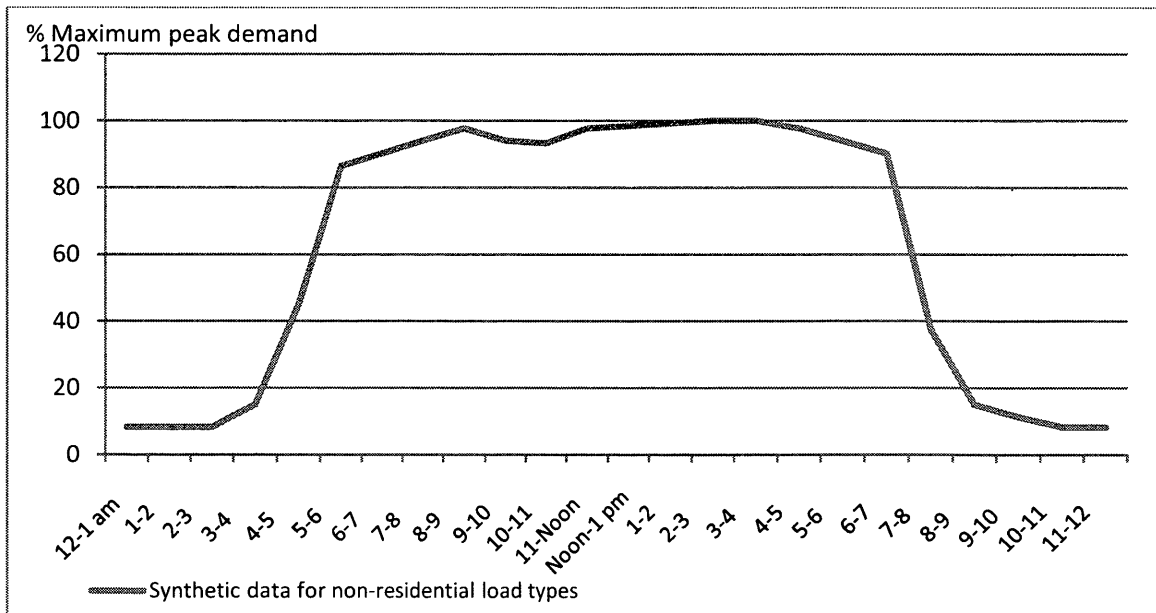


Figure 4.5: Winter hourly load profile for non-residential type of load (synthetic data).

Due to the large size of the problem, the memory of the cross-country machine used to run the LP charging pattern algorithms was not enough to solve the problem. For that reason, the algorithms are solved for the three residential load types first and for a vehicle class at a time. Furthermore, due to the similar population size of vehicles per class, the average of the population size per class is considered, which means that every class has the same number of vehicles equal to 46 in a residential load point. With that assumption, the dependence of the vehicle index on the class is avoided. After running the algorithms for the individual four vehicle classes, the base load is subtracted from the determined new load of the residential load types with one class of PHEVs, obtaining the added load of the PHEV fleet per class. This quantity is summed for the four classes and added to the base load, obtaining the contribution of the four vehicle classes to the base load. Next the algorithms were solved for commercial and office building type of load separately, for all types of vehicle classes obtaining the new loading of non-residential load types with PHEVs directly.

The results of the optimized PHEV fleet patterns in the loading of the RBTS system are shown in Figure 4.6. The load duration curve is computed, representing the annual loading ordered by decreasing power demand of all the load points 1-38 of the RBTS system. Curve (1) corresponds to the RBTS base load, curve (2) to the RBTS with PHEVs optimized for peak shaving purposes and at last curve (3) is drawn and illustrates the RBTS loading with PHEVs optimized for the benefit of the customer.

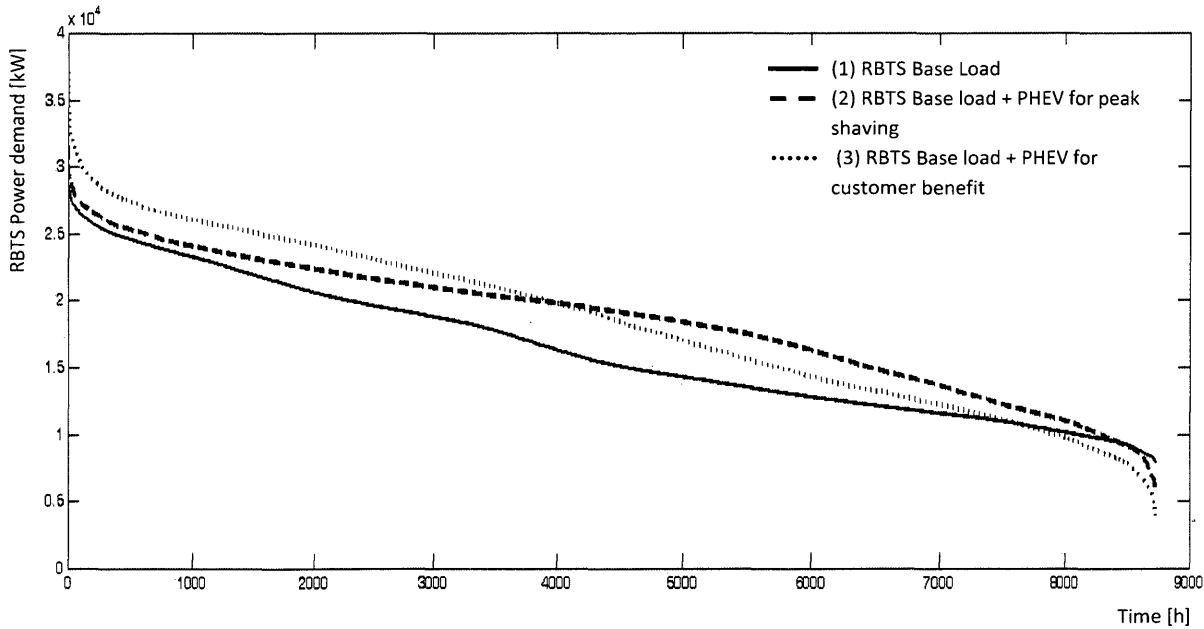


Figure 4.6: Load duration curve of the RBTS system base load, base load and PHEVs optimized for peak shaving purposes, base load and PHEV loads optimized for customers profit.

Concerning the loading of the RBTS with PHEVs optimally charged for utility peak shaving purposes curve (3) in Figure 4.6, the peak demand of the system increases by 2.4 MW. From the perspective of the utility serving such new loading characteristics, it means that the capacity demanded by the RBTS distribution system area is slightly increased. In addition, the annual energy consumed by the RBTS power system area with PHEVs optimized for peak shaving purposes is greater than without PHEVs, i.e. the area under curve (2) is greater than the area under curve (1). Using a trapezoidal approximation to calculate the annual energy of curves (1) and (2), the annual energy consumed by the RBTS base load system is  $1.43 \cdot 10^5$  MWh, versus  $1.62 \cdot 10^5$  MWh consumed by the RBTS system with an optimized PHEV fleet loading for peak shaving purposes. To summarize, the peak demand increases by 2.4 MW corresponding to an 8 % increase with respect to the RBTS base load system and the annual energy consumption is increased by 13.3 %.

Four vehicle charging patterns obtained from the LP algorithm solved with IBM CPLEX™ solver are plotted in Figures 4.7 and 4.8. Note that the axis in Figure 4.7 starts in the afternoon hours (pm), when residential drivers arrive home. On the contrary, Figure 4.8 begins in the morning hours (am), corresponding to the arrival period of time to non-residential buildings.

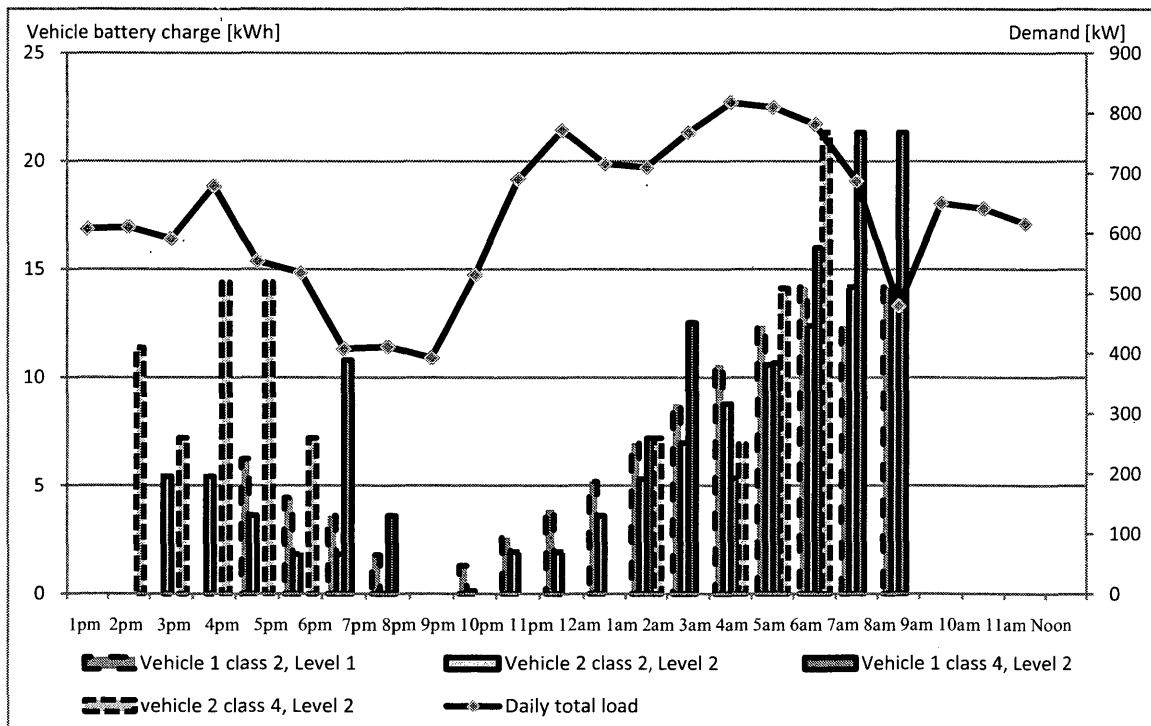


Figure 4.7: Individual optimized PHEV battery charging patterns of four vehicles and total daily load for a weekday residential demand for peak shaving purposes.

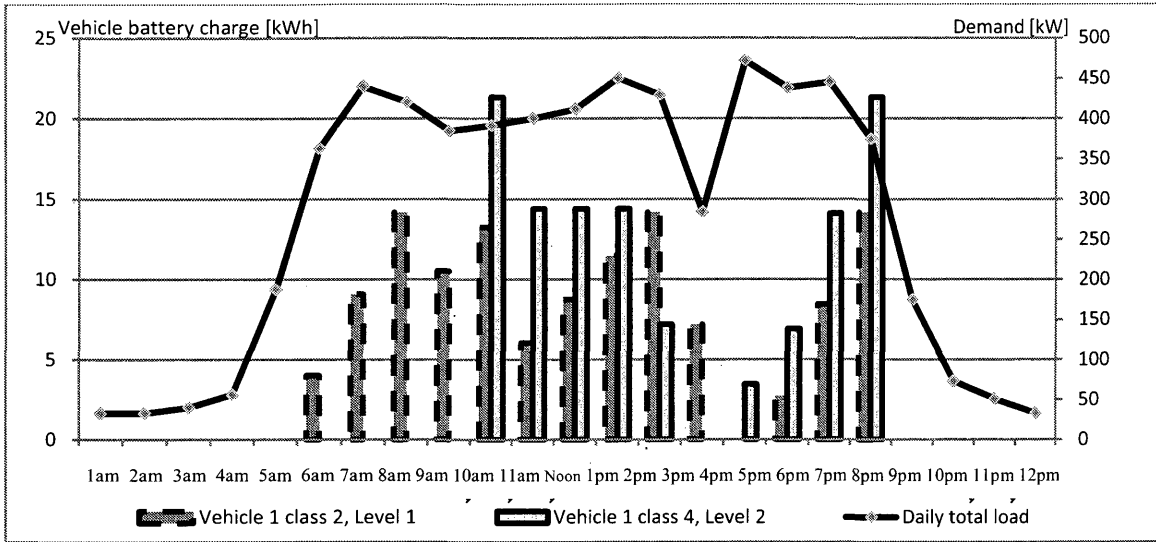


Figure 4.8: Individual optimized PHEV battery charging patterns of two vehicles and total load for a weekday commercial demand for peak shaving purposes.

The charging patterns of four vehicles within the PHEV fleet for a winter day are shown for illustrative purposes, as well as the total load for that day for a residential load type 1 in Figure 4.7 and for two vehicles for commercial load type of demand in Figure 4.8. The peak demand in residential load types is shifted from the late afternoon (6-8 pm) in Figure 4.4 to the night (2-4 am) with 30% of penetration in residential areas. Looking at the individual charging patterns of the vehicles, four are selected in order to illustrate the peak shaving charging strategy. The four column graphics illustrate the energy stored in the battery of a PHEV per hour. The first series corresponds to a vehicle class 2, charging at level 1 and arriving home at 5pm. At arrival time, it fully discharges the available energy in the battery during peak demand, and waits to start charging at 10 am to be completely charged again by 6 am. The vehicle leaves at 8 am, and has discharged for an hour before leaving. The second vehicle class 2 charging at level 1 has arrived at 3 pm, waits until 5 pm to start a complete discharge of the 5.2 kWh of available energy during the following two hours and once more, starts the charging periods at 10 pm. The same recognizable behavior of discharging and charging patterns can be observed in the third and fourth column series, in which the vehicles charge/discharge at level 2 at a higher rate: vehicles discharge during peak time hours of the base load, and charge during the night. If the vehicle arrives home before 5 pm approximately, the general strategy is to wait until the load of the system increases during peak demand periods after 5 pm, and then discharge for peak shaving purposes.

For commercial and office buildings, the daily peak demand normally occurring at 3 pm is reduced, and the strategy followed is to charge the vehicle when the vehicle arrives to the work place before noon, discharge during the afternoon hours and charge again to be have full capacity when driving back home as shown in Figure 4.8 for a weekday.

With regards to the loading of the RBTS with PHEVs optimally charged for the benefit of the customer shown in curve (3), the peak demand of the system increases considerably from 29.1 MW to 37.4 MW. A capacity demand increase of 8.3 MW is a significant raise of 25.8 % with respect to the power required by the RBTS base load system. In addition, the energy consumed by the RBTS with PHEV fleet optimized for the costumers benefit is also  $1.62 \cdot 10^5$  MWh a year, the same as the energy consumed by a the RBTS with a PHEV fleet optimized for peak shaving purposes. The optimized objective function given by (4.22) is 16.72 millions of US \$. It corresponds to the sum of the hourly energy bill for a year for the entire RBTS system with PHEVs optimized for customer benefit. We computed (4.22) for curve (2) (PHEVs for peak shaving) and the annual energy bill would be of 17.0 millions of US \$ a year. This difference is due to the TOU pricing method employed. First, the TOU pricing off-peak, medium-peak region and on-peak time frames where created in function of the RBTS daily base load profile, without considering PHEVs in the system. Secondly, the optimization algorithm minimizes the energy consumption in the on-peak and medium-peak time frames, shifting the charging of the PHEVs to off-peak TOU pricing regions, see Figure 4.9. Utilities should be aware of this matter, and should carefully offer appropriate TOU pricing schedules to reduce the energy consumption of the distribution system, as well as the peak demand with respect to the new load daily pattern with PHEVs.

Optimized charging patterns with TOU pricing of individual vehicles obtained from the LP solved with CPLEX<sup>TM</sup> are plotted in Figure 4.9 for a residential type of load, and for a type commercial in Figure 4.10. The column graphic illustrates the energy stored in the battery of a PHEV. The first series corresponds to a vehicle class 3, charging at Level 2 and with the following time characteristics: arrival time 8 pm and departure time 8 am. The charging strategy determined by the LP algorithm is to discharge the 11 kWh available in the battery during the on-peak price period and charge during the off-peak pricing frame. Finally, it discharges at the maximum discharge rate for Level 2 at 7 am during on-peak and charges back on hour later so that the battery is fully charged by departure time. The following question might come to the mind of the reader: is it worth for the owner of the PHEV to discharge at 7am to charge at back again at 8 am? This question cannot be answered without the individual loading of the owners as

available data. The available data in the RBTS is the demand at a load point, which is the aggregate of several individual customers. So it happens to be worth according the LP algorithm to discharge and charge back again the following hour in function of what the other customers charging patterns are within that load point because the aggregate load at 7 am and 8 am during on-peak hours is reduced in Figure 4.9. The LP algorithm optimizes the charging patterns with respects to the electric demand at a load point, but it could be extended to individual charging patterns if the required data is available. The second series corresponds to a vehicle class 3 and level 2 of charging arriving at 3 pm and leaving at 3 am. The charging strategy followed this time is to fully charge when the vehicle arrives home during medium-peak TOU price period , discharge during on-peak hours and charge back again during off-peak hours. The third and fourth column graphs correspond to two vehicles class 1 charging at level 1, and following the same strategies as for the first and second series respectively.

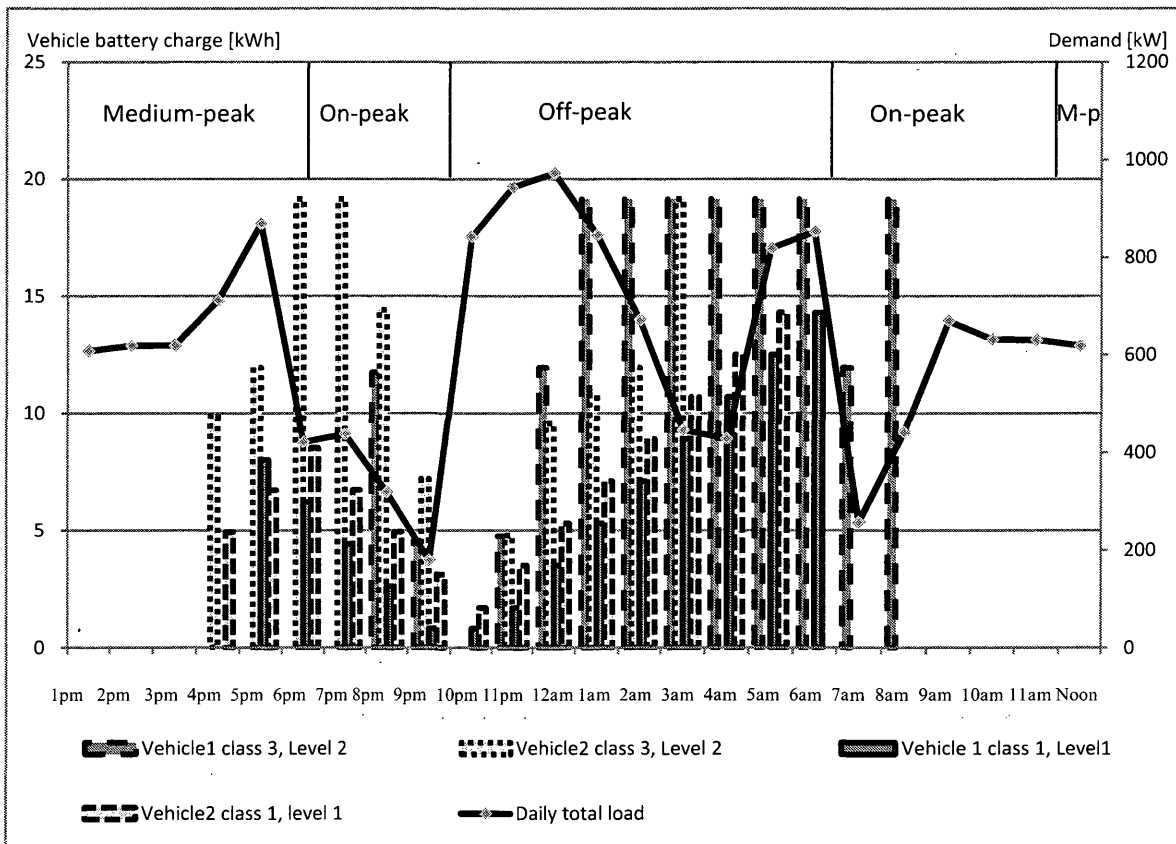


Figure 4.9: Individual optimized PHEV battery charging patterns of four vehicles and total load for a weekday in winter with TOU pricing.



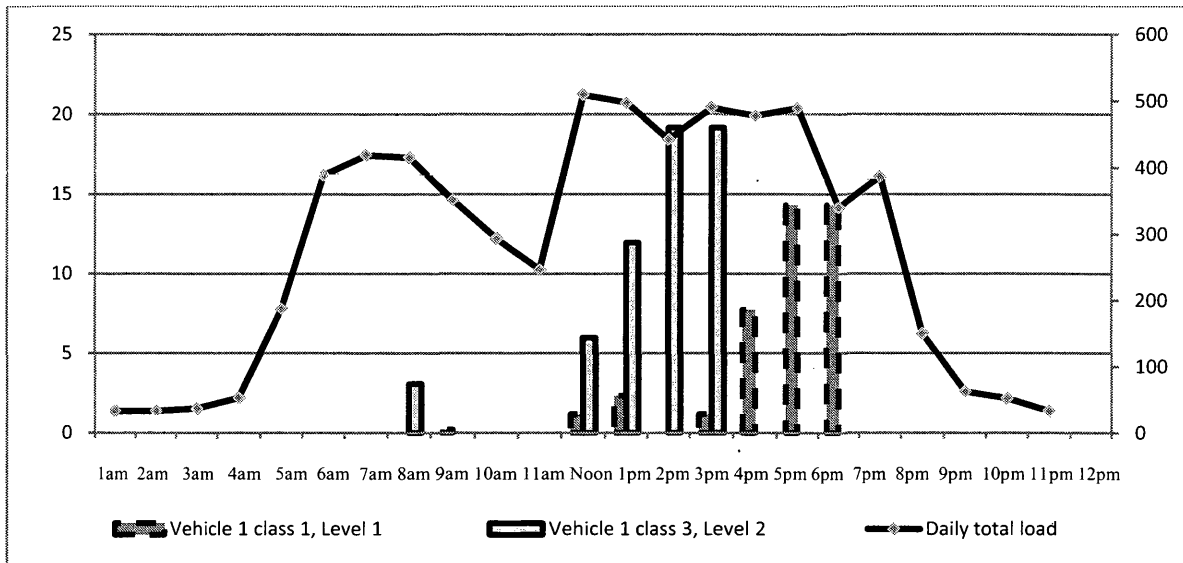


Figure 4.10: Individual optimized PHEV battery charging patterns of two vehicles and total commercial load for a weekday in winter with TOU pricing.

Finally, the line curve in Figure 4.9 represents the total residential load type 1 for that day. The total residential load type 1 for that day is in accord with the TOU price periods selected in this thesis, i.e., the charging patterns of the PHEV fleet have lowered as much as possible the loading during on-peak price periods. Yet, the variability of a residential load point at the medium voltage (11kV) level is increased, creating steeper ramps due to the charging/discharging of the vehicles, but also due to the periods where a big number of vehicles don't charge/discharge and the demand decreases or increases to base load values.

#### 4.4.3 Impact of uncontrolled and delayed charging strategies without V2G in the RBTS test system

In this section, we compare both of the optimized loadings of the RBTS system with a PHEV fleet of 30% of the total transportation fleet, to uncontrolled and delayed charging of the same size PHEV fleet with no V2G. Uncontrolled charging of a PHEV means that the vehicle plugs in to recharge its battery when it arrives home. Delayed charging of a PHEV is a strategy allowing the vehicle to start charging as late as possible, i.e. the beginning of the charging period starts with a delay equal to the time difference between the required charging time at a level of charging and the available charging time.

Figure 4.11 shows the load duration curve of the RBTS base load system, the RBTS with and uncontrolled charged PHEV fleet and finally the RBTS loading with a PHEV fleet delayed

charging strategy. The impact on the RBTS test system of the PHEV fleet with uncontrolled charging is especially dramatic. The annual capacity demand in kW rises to 39.9 MW, which correspond to percentage increase of 37 % with respect to the power demanded by the RBTS base load area. The annual energy demand of the area is increased to  $16.5 \cdot 10^5$  MWh, which represents an increase of 15.5 % in energy demand. However, the impact of the same PHEV fleet with delayed charging control is mitigated considerably. The annual energy demand of the area is the same as with uncontrolled charging of PHEVs, however, the peak demand of the area is slightly increased from 29.1 MW to 29.7 MW.

#### 4.5 Reliability impact of PHEVs in the RBTS system

Once the size, design and behavioral characteristics of the PHEV fleet are modeled for the RBTS test system and the optimized charging patterns have been determined in order to obtain the expected new annual loading of the system, the annual reliability can be evaluated. First the reliability impact is quantified in the RBTS radial distribution system and secondly, in the RBTS redesigned distribution system with networked interties between feeders and DG units.

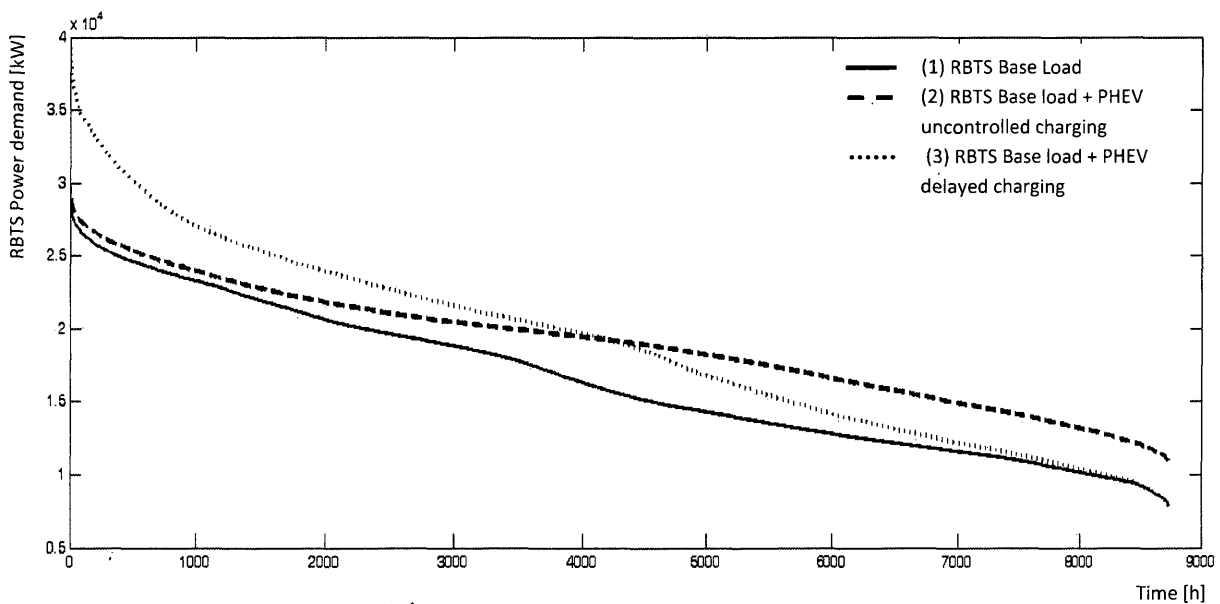


Figure 4.11: Load duration curve of the RBTS base load (1), base load and PHEV uncontrolled charging fleet (2), base load and PHEV delayed charging fleet (3).

#### 4.5.1 Reliability impact of PHEVs in the RBTS radial system

To evaluate the impact of the new loading with PHEVs on the reliability of the RBTS system, we compute the step-load duration of curve as explained in chapter 2, section 2.1.1. Figure 4.12 shows the step-load duration curves for the RBTS base load, base load and PHEVs for peak shaving and base load and PHEVs for customer benefit.

Curve (1) in Figure 4.12 does not correspond precisely to the step-duration curve computed for the RBTS test system in the previous chapter. In this chapter, a more accurate representation of office and commercial building daily load profiles has been computed using synthetic data presented in Figure 4.5, where the new daily profile of non-residential loads is shown in percentage of the annual peak demand. For that reason, the annual peak demand of office and commercial building load types is the same in Chapter 3 and in Chapter 4; yet, the annual average load of non-residential load types is different. The hourly daily data for residential loads is computed using the hourly, daily and seasonal characteristics in [145] and reproduced earlier in this chapter.

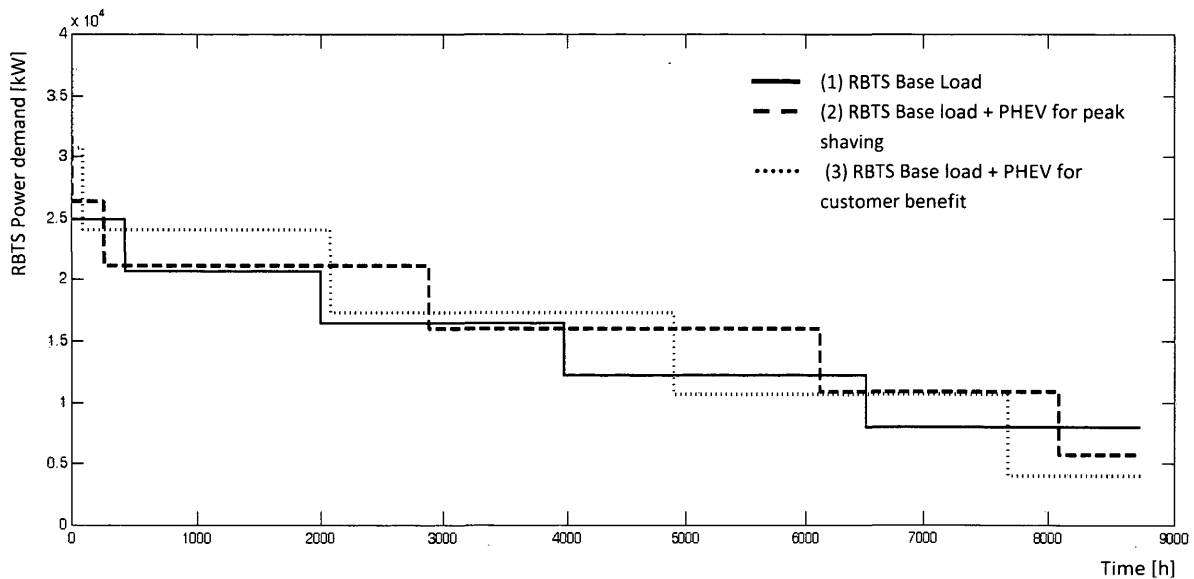


Figure 4.12: Step-load duration curve of the RBTS test system without PHEVs (base load (1)) and with PHEVs optimized for peak shaving (2) and for customer benefit (3).

The new loading characteristics by type of demand are given in Tables 4.9-11. Table 4.9 shows that the annual average demand per load point for the RBTS system with PHEVs is the same for the vehicles optimized for utility peak-saving and for the benefit of the customer, with a tolerance of  $10^{-3}$ . However, with a more accurate representation of the annual demand as in

Tables 4.10-11, the annual loading characteristics of the RBTS with PHEVs optimized for peak-shaving and with TOU pricing are different.

Table 4.9 Annual average demand per load point in the RBTS base load system and the RBTS with PHEVs

<i>Customer Type</i>	<i>Load points i</i>	<i>Annual average load, <math>L_{ALoad}</math> [MW]</i>		
		<i>Base load</i>	<i>Base load + PHEVs peak shaving</i>	<i>Base load + PHEVs TOU pricing</i>
Residential	1, 4-7, 20-24, 32-36	0.4684	0.4939	0.4940
Residential	11, 12, 13, 18, 25	0.4758	0.5011	0.5012
Residential	2, 15, 26, 30	0.4339	0.4606	0.4607
Small Industrial	8, 9, 10	1.0167	1.0167	1.0167
Commercial	3, 16, 17, 19, 28, 29, 31, 37, 38	0.1889	0.2024	0.2024
Office Buildings	14,27	0.3345	0.4778	0.4778

Table 4.10 Annual maximum peak load per load point in the RBTS base load system and the RBTS with PHEVs

<i>Customer Type</i>	<i>Load points i</i>	<i>Max. peak load, <math>L_{i,PLoadmax}</math> [MW]</i>		
		<i>Base load</i>	<i>Base load + PHEVs peak shaving</i>	<i>Base load + PHEVs TOU pricing</i>
Residential	1, 4-7, 20-24, 32-36	0.8367	0.9143	0.9857
Residential	11, 12, 13, 18, 25	0.8500	0.9275	0.9986
Residential	2, 15, 26, 30	0.7750	0.8532	0.9258
Small Industrial	8, 9, 10	1.0167	1.0167	1.0167
Commercial	3, 16, 17, 19, 28, 29, 31, 37, 38	0.5222	0.6143	0.6468
Office Buildings	14,27	0.9250	1.219	1.1976

Table 4. 11 RBTS load levels in per unit from the step-load duration curves and their respective duration in hours (base load and with PHEVs)

$B$	Base load		Base load + PHEVs peak shaving		Base load + PHEVs TOU pricing	
	Load Level $L_{\beta}$ (pu)	$\Delta t_{\beta}$ [hours]	Load Level $L_{\beta}$ (pu)	$\Delta t_{\beta}$ [hours]	Load Level $L_{\beta}$ (pu)	$\Delta t_{\beta}$ [hours]
1	1	$3 \cdot 10^{-4}$	1	$3 \cdot 10^{-4}$	1	1
2	0.8546	422	0.8359	249	0.8212	87
3	0.7092	1583	0.6719	2632	0.6424	1992
4	0.5639	1974	0.5078	3235	0.4636	2817
5	0.4185	2531	0.3438	1965	0.2849	2783
6	0.2731	2225	0.1797	654	0.1061	1056

Computing the ENS with (2.11.a) using annual average demand values to represent the loading of the system, the impact of PHEVs with V2G technology on the reliability of the RBTS system is quantified. Note again that in this chapter, the *base load* system is computed using synthetic data for non-residential load types and thus, the values of ENS differ from the ones obtained in the previous chapter. The results of ENS for the RBTS base load system and for the RBTS with PHEVs are shown in Table 4.13. The annual average demand of the RBTS test system with PHEVs optimized for peak-shaving purposes and with TOU pricing is the same and thus, the annual ENS of the RBTS test system with PHEVs optimized for peak-shaving purposes and with TOU pricing is the same. The annual ENS of the RBTS base load system is 44.52 MWh, versus the ENS of 47.45 MWh a year of the RBTS with PHEVs.

Using (2.11.b) to compute the ENS with step-load duration modeling of the RBTS base load and the RBTS base load with PHEVs, the impact on the reliability of the RBTS with 30% penetration of PHEVs with V2G technology is computed. The results of the annual ENS are shown in Table 4.13 for the RBTS legacy system. In addition, the *PNS* for each loading level in the system is also provided.

Table 4. 12 ENS of the RBTS radial legacy system with average annual demand

	Base load	Base load + PHEVs
ENS [MWh]	44.52	47.45

Table 4. 13 PNS per load level in the RBTS radial legacy system and annual ENS

<i>B</i>	Base load		Base load + PHEVs peak shaving		Base load + PHEVs TOU pricing	
	$\Delta t_{\beta}$ [hours]	<i>PNS</i> [MW]	$\Delta t_{\beta}$ [hours]	<i>PNS</i> [MW]	$\Delta t_{\beta}$ [hours]	<i>PNS</i> [MW]
1	$3 \cdot 10^{-4}$	23.64	$3 \cdot 10^{-4}$	26.27	1	27.85
2	2225	20.20	249	21.96	87	22.86
3	2531	16.76	2632	17.64	1992	17.88
4	1975	13.32	3235	13.33	2817	12.90
5	1583	9.88	1965	9.21	2783	7.92
6	422	6.45	654	4.71	1056	2.95
<b>ENS [MWh]</b>	<b>39.88</b>		<b>45.87</b>		<b>39.26</b>	

Using a more accurate representation of the annual load of a distribution system, it is observed that the reliability of the system is not the same for the RBTS radial system with PHEVs optimized for peak-shaving and with TOU pricing. The *ENS* for the RBTS with PHEVs optimized for peak shaving purposes is 45.87 MWh a year. The annual *ENS* increases by 6 MWh compared to the *ENS* of the RBTS base load system, due principally to the increase of the base load of the system for peak-shaving purposes. Looking at Figure 4.16, the energy under the step-load duration curve (2) is over curve (1) for load levels number 4 and 5, to provide power to help balance loads by valley filling (charging at night when demand is low). In lower load level numbers (higher loading in the system), curve (2) stays closer to curve (1), which corresponds to the peak shaving strategy of sending power back to the grid when demand is high. The valley filling strategy creates a higher energy demand during the majority of the time in a year period, in detriment of the reliability that decreases. However, in the RBTS radial legacy system with PHEVs optimized with TOU pricing rates, the annual reliability of the system is increased

compared to the reliability of the RBTS radial system base load. Minimizing the energy bill corresponds to minimizing the energy consumption of the system, in particular during on-peak price periods. The second decrease observed in the daily load curve during the night with TOU price periods in Figure 4.9, does not occur that pronouncedly for valley filling purposes in Figure 4.7, and reduces the *PNS* in load levels 4-6. These load levels occur during more than 75% of the hours in a year. The fact that the power demanded during more than 75% of the year is reduced with TOU pricing has a direct consequence in increasing the annual reliability of the system. As a consequence, the annual reliability of a radial legacy distribution system may be increased with PHEVs if an adequate charging strategy is in place. Modeling the demand in a distribution system with annual average loads may not allow quantifying precisely the impact of different charging strategies of PHEVs to the reliability of distribution systems. However, using a step-load duration curve to represent the annual loading in a distribution system enables to include more detail into the study of the impact of different charging strategies to the reliability of distribution systems.

#### 4.5.2 Reliability impact of PHEVs in the RBTS redesigned test system

In this section, the impact of PHEVs is quantified in the redesign solutions proposed in the previous chapter in section 3.3.3, and presented in Table 4.12. Note that the redesign solutions proposed in Chapter 3 are obtained with the load data given in [132, 133] and reproduced in Table 3.7. However, the PHEV impact is quantified using different load data for non-residential type of loading. The redesign solutions are still valid for the new RBTS base load data. Only office building and commercial type of load data is different. Office buildings are 2 of the 38 load points in the system and their change in annual loading characteristics will not affect the redesign solutions. With regard to commercial type of demand, there are 9 load points in the RBTS system. Yet, in the data used in Chapter 3, office building load points have the lowest value of demand with respect to the other types of loading and are even lower in the data used in Chapter 4. This means that if a redesign involved adding feeder interties and DG between buses with office building type of loading, this was due to the low value of this type of demand, which is even lower with the data used in this chapter.

The power output of the DG in the system is sized with respect to the total annual average load in the RBTS base load system with synthetic data used for non-residential load types. Considering the same design characteristics as in Chapter 3, i.e., the total contribution of DG is 80% of the total annual average demand in the system, the total DG rating in the RBTS system with synthetic data used for non-residential load is 10.33 MW (with the load considered in

Chapter 3 as in [132], the total rating of DG was sized to 14.24 MW). The ENS of the redesigned RBTS test system with base load and with PHEVs is computed in Table 4.14 using (2.14.a), i.e., with average annual loads in the system.

Table 4.14 ENS of the RBTS system for redesign solutions of the RBTS test system

Solution		ENS [MWh]	
Connections from bus-to bus	DG bus location	Base load	Base load + PHEVs
11-17	15	29.10	30.72
1-7 & 11-17	4 & 15	20.25	21.55
11-17 & 23-29	14 & 25	20.35	21.65
11-17 & 23-29	13 & 29	19.95	21.19
1-7 & 11-17 & 23-29	2 & 15 & 25	20.14	21.43
1-7 & 11-17 & 23-29	7 & 13 & 23	19.69	20.93

The reader can appreciate that the redesigned RBTS system is more reliable than the RBTS legacy system by reducing the *ENS* from 40 to 60 %. However, the algorithm in the previous chapter found optimal solutions for the base load of the RBTS system without PHEVs and the cost and reliability are directly influenced by the demand per load point which has changed. In this chapter, the PHEV distribution per load point is uniform, i.e. every load point has increased the demand by a similar amount. Yet, if the distribution is not uniform and different penetrations of PHEVs are expected per load point, the ENS of the redesign may be affected in a manner different to the results presented in this thesis.

#### 4.5.3 Redesign of the RBTS test system with PHEVs

In this section, we implement the MOGA methodology proposed in Chapter 2 to the RBTS system with PHEVs. The redesigned solutions, i.e. feeder interties and DG units to be added to the system will be optimized with the new loading with PHEVs occurring in the system. DG units are sized in function of the annual average load in the system as in the previous chapter. When compared to the RBTS base load test system, the total annual average demand has



increased only by 13% from 12.91 MW to 14.54 MW in the RBTS system with PHEVs. This increment affects insignificantly the size of the power output of the total DG in the redesigned system that is increased from 10.33 MW to 11.63 MW, considering the same design characteristics as in Chapter 3, that is, the total contribution of DG is 80% of the total annual average demand in the system. The results of the MOGA applied to the RBTS test system with PHEVs are shown in Table 4.14. The redesign of the RBTS system with PHEVs is done using annual average loads in the system. As discussed in Chapter 3, the results are very similar to modeling the demand with annual average loads as using a step-load duration curve. Additionally, the computational time required with step-load duration curve modeling is doubled when compared to the annual average load modeling. At last, the annual average loads in the RBTS test system with PHEVs optimized for peak-shaving and with TOU pricing are the same, and therefore, the redesign solutions with annual average loads are valid for both charging strategies.

Hence, the MOGA with annual average loads modeled in the system is used for the redesign of the RBTS test system with PHEVs. The solutions are shown in Table 4.15. Once the redesign solutions are obtained, the ENS of such solutions is computed using (2.11.b), with step-load duration curve representation of the annual demand, in order to obtain a more accurate value of the ENS for the solutions and is presented in Table 4.16.

Concerning the solutions proposed by the MOGA, they follow the same criteria as the redesigns of the RBTS base load system. Again, DG units are placed on feeders with higher rated loads – i.e., feeders 1 and 3 in RBTS - and those that cannot be connected by closing an open tie-switch. Within a feeder, the location that improves the reliability of the system the most is the bus where the higher rated loads are connected. The rated loads connected have changed but are classified in the same decreasing order of demand in the RBTS with PHEVs as in the RBTS base load system, with the exception of the second residential load type. As a consequence, buses with low connected demand such as 14 and 15 appear as possible locations for DG in Solutions No. 1,2 and 4 in the redesign solutions of the RBTS base load and the RBTS with PHEVs because they corresponds to the lowest demands in both systems. However, bus 11 in Solutions No. 3 and 5, where load points 11 and 12 are located and correspond to the second residential load type, is the new highest load connected in feeder 3. As a consequence, bus 11 is chosen over bus 13 in the RBTS redesign solutions with PHEVs.

Again, the redesign solutions proposed by the MOGA in this section are considering a uniform distribution of PHEVs per load point and different results would be obtained if a non-uniform distribution of PHEVs per load point is expected.

Table 4.15 Redesign solutions of the MOGA applied to the RBTS test system with PHEVs and annual average demand modeled in the system.

Solution #	Connection (s)	DG (s) bus location #	Cost [ $10^6$ US \$]	ENS [MWh]
1	Line 11-17	15	17.60	30.72
2	Line 1-7 Line 11-17	5 & 14	17.70	21.55
3	Line 1-7 Line 11-17	5 & 11	17.87	21.31
4	Line 1-7 Line 11-17 Line 23-29	4 & 14 & 23	18.64	21.62
5	Line 1-7 Line 11-17 Line 17-24	5 & 11 & 19	18.33	21.00



## CHAPTER 5

### CONCLUSIONS AND FUTURE WORK

This chapter is organized as follows: first, conclusions derived from the research done in this thesis are presented, and secondly, avenues of future work are described.

#### 5.1 Conclusions

At first, conclusions derived from implementing the expanded MOGA presented in Chapter 2 and applied to tests systems in Chapter 3 are discussed. Next, conclusions from the study of the impact of PHEVs to the reliability of distribution systems are presented.

##### 5.1.1 Conclusions to the extended MOGA

An extended methodology to design emerging distribution systems under islanded mode of operation proposed in [20] is presented in the first part of this thesis, Chapters 2 and 3. The additions are on the one hand, to simultaneously co-locate feeder interties and DG in a legacy radial distribution system in order to improve the reliability under islanded mode of operation, and on the other hand, to explore a more accurate modeling of the annual load of the distribution system with a step-load duration curve and analyze its impact on the planning of such systems.

Primarily, as a consequence of increasing the complexity of the problem to simultaneously co-locate DG and feeder interties in a given radial distribution system, the number of generation required by the MOGA is considerably increased from 15 to at least 25. For that reason, the computational time is increased. The exact values of the time required for the MOGA in [20] and the expanded MOGA in this thesis are not comparable because the algorithms were run on different machines. Secondly, a more accurate representation of the annual load in the system to be designed leads to very similar redesign solutions of a given distribution system. However, the computational time required by modeling the demand with a step-load duration curve representation versus one unique annual load level (annual average demand) is at least doubled. In addition, the value of the annual ENS with annual average loads modeled in the system is over-estimated when compared to a more accurate representation of the demand. This consideration is not an issue for the planning stage of a distribution system.

### 5.1.2 Conclusions to the study of the impact of PHEVs

First, the conclusions to the impact of PHEVs in distributions systems are valid under the assumptions considered in Chapter 4, subsection 4.1.2, concerning the percentage of PHEV penetration, charging locations, charging levels and operational and design characteristics of PHEVs. However, the methodology proposed in Chapter 4 can be adjusted to modifications made in the assumptions.

The impact of 30% of penetration of PHEVs in the RBTS radial legacy system using synthetic data for non-residential load types is:

- Under peak shaving and TOU pricing charging strategies, the daily peak demand is shifted to 3-5 am and increased from 8-25% depending on the charging strategy with respect to the RBTS without PHEVs.
- Under delayed charging strategy of PHEVs without V2G, the peak demand is insignificantly increased and shifted to 3-4 am.
- Under uncontrolled charging of PHEVs without V2G, the peak demand increases 37% with respect to the RBTS without PHEVs.
- PHEVs with V2G increase the annual energy consumption of the RBTS test system by 13%, compared to PHEVs without V2G that increase the annual energy consumption to 16%
- TOU pricing rates can significantly increase the peak demand if no “demand charges” are applied.

The impact of 30% of PHEV penetration to the reliability and design of the RBTS test systems is:

- Step-load duration modeling of the annual load allows depicting differences in the impact of distinct charging strategies to the reliability of distributions systems under islanded mode of operation. However, annual average load modeling of the demand does not reveal such differences in the annual reliability of the new loading of the RBTS test system with PHEVs optimized with different objectives.

- Charging strategy for utility peak shaving purposes increases the energy consumption for valley filling purposes and thus, decreases the annual Energy Not Supplied of distribution systems.
- Charging strategy with TOU pricing periods for the benefit of the customer increases the annual reliability of distribution systems under islanded mode of operation due to the decrease in energy consumption to reduce the energy bill.
- RBTS redesign solutions without considering PHEVs increases the reliability of the system with PHEV penetration
- The redesign solutions of the RBTS system considering PHEVs in the system may vary with respect to the solutions proposed without PHEVs and it depends on the probability distribution used to model PHEVs in a test system

## 5.2 Future work

Several open topics for further exploration are available from the research presented in this thesis.

With regards to the modeling of DG, time dependency on the power output of such machines can be explored. In this thesis, DG is modeled using the capacity factor of the different types of DG contributing to the total rating. However, as it has been explored in this thesis with the respect to the annual load, the time dependency of the power output of DG throughout a year may or may not affect the redesign solutions of radial legacy distribution systems. Considering the large computational time required by the extended MOGA to converge into Pareto-optimality, a pre-conditioned search methodology to cut down the computation time can be explored. For instance, an acceleration technique for filtering potentially infeasible and/or suboptimal inputs, based on machine learning may potentially reduce the number of input candidate solutions that require a power flow evaluation. If a significant fraction of the inputs tested, it is possible that the input from that fraction is either infeasible or the values for the objective functions are sub-optimal, a *filter* based on machine learning can potentially alleviate the number of power flow evaluations, by identifying features of inputs that will lead to infeasibility or sub-optimal objective values [153].

Concerning the methodology proposed to quantify the impact of PHEVs with V2G capabilities in distributions systems, potential expansions are: first, develop a study a survey on how a future vehicle fleet in distributions systems will look like, and secondly, run software simulations with the results from the first study to obtain an accurate model of a PHEV fleet.

Pertaining to the LP algorithms, the modeling of a vehicle battery can be extended and more detail on the operation of such devices included. Finally, a probabilistic based methodology can be developed to model the distribution of PHEVs throughout the load points of a medium voltage system.

## REFERENCES

- 
- [1] 110th Congress of the United States, "Title XIII (Smart Grid)," in *Energy Independence and Security Act of 2007*. Washington, DC: Dec. 2007, pp. 292 - 303.
  - [2] "The Smart Grid – an Introduction," *US Department of Energy*, 2008.[Online]Available: <http://www.oe.energy.gov/SmartGridIntroduction.htm>.
  - [3] "Green paper - a European Strategy for Sustainable, Competitive and Secure Energy," *European Energy Commission*, 2006.[Online]Available:[http://europa.eu/documents/comm/green\\_papers/pdf/com2006\\_105\\_en.pdf](http://europa.eu/documents/comm/green_papers/pdf/com2006_105_en.pdf)
  - [4] "Vision and Strategy for Europe's Electricity Networks of the Future," European SmartGrids Technology Platform, 2006.
  - [5] J. Lu, D. Xie, and Q. Ai, "Research on Smart Grid in China," in *Transmission Distribution Conference Exposition: Asia and Pacific*, pp. 1 – 4, Oct. 2009.
  - [6] S. Suryanarayanan, P.F Ribeiro and M.G Simões, " Grid Modernization Efforts in the USA and Brazil- Some Common Lessons Based on the Smart Grid Initiative," in *IEEE Power and Energy Society (PES) General Meeting*, Minneapolis, pp. 1-5, Jul. 2010.
  - [7] "China's Energy Conditions and Policies," *Information Office of the State Council of the People's Republic of China*, Dec. 2007.
  - [8] "National Electricity Policy," *Ministry of Power of India* published by authority No. 23/40/2004-R&R Vol.II, Feb. 2005.
  - [9] M. Smith. (September 2009). *Overview of the U.S. Department of Energy's Research & Development Activities on Microgrid Technologies*. Available:<http://der.lbl.gov/presentations>
  - [10] S. Suryanarayanan, *et al.*, "Achieving the Smart Grid through Customer-driven Microgrids supported by Energy Storage," in *IEEE International Conference on Industrial Technology*, Viña del Mar, Chile, 2010.
  - [11] Institute of Electrical and Electronics Engineers (IEEE), "Draft Guide for Design, Operation, and Integration of Distributed Resource Island Systems with Electric Power Systems,," in *IEEE Draft Standard 1547.4*,, 2008.
  - [12] N.Hatziargyriou, H.Asano, R.Iravani, and C.Marnay "Microgrids," *IEEE Power & Energy Magazine*, pp.78-94, July/Aug. 2007.
  - [13] "American Reinvestment and Recovery Act 2009, " presented at the One Hundred Eleventh Congress of the United States of America, Washington, part 5, sec. 1141, Sep. 2009.



- 
- [14] "Benefits and Challenges of Achieving a Mainstream Market for Electric Vehicles Final Report," *U.S. Department of Energy (DOE)*, Jun. 2010. [Online] Available: <http://info.ornl.gov/sites/publications/files/Pub24143.pdf>
- [15] Kempton, W. and J. Tomic, "Vehicle-to-grid power fundamentals: Calculating capacity and net revenue," *Journal of Power Sources*, vol. 144, no. 1, pp. 268-279, 2005.
- [16] M. D. Galus, R. La Fauci, and G. Andersson, "Investigating PHEV Wind Balancing Capabilities using Heuristics and Model Predictive Control," in *IEEE Power & Energy Society (PES) General Meeting*, Minneapolis, Minnesota, USA, 2010.
- [17] M. Kezunovic, S.T Waller, I. Damnjanovic, "Framework for Studying Emerging Policy Issues Associated with PHEVs in Managing Coupled Power and Transportation Systems," in *IEEE Green Technologies Conference*, Grapevine (TX ), pp. 1-8, Apr. 2010.
- [18] H. Brown and S. Suryanarayanan, "Improving Reliability of Islanded Distribution Systems with Distributed Energy Resources via Optimal Addition of Feeder Interties." *IEEE Transactions on Industrial Electronics Special Issue on Optimization for Smart Grids (under revision)*, 2010, pp. 1-9.
- [19] J.M. Armas and S. Suryanarayanan "A Heuristic Technique for Scheduling a Customer-Driven Residential Distributed Energy Resource Installation," *Intelligent System Applications to Power Systems (ISAP '09)*, Nov.2009.
- [20] H.Brown, "Implications on the Smart Grid Initiative on Distribution System Engineering: Improving Reliability on Islanded Distribution Systems with Distributed Generation Sources," M.S dissertation, Dept. Elec. Eng., Colorado School of Mines, 2010.
- [21] Office of Electric Transmission and Distribution, "Grid 2030: A National Vision for Electricity's Second 100 years," United States Department of Energy [Online].Available: [http://www.oe.energy.gov /DocumentsandMedia/Electric\\_Vision\\_Document.pdf](http://www.oe.energy.gov /DocumentsandMedia/Electric_Vision_Document.pdf) [Accessed Apr. 20, 2009].
- [22] F. Gonzalez-Longatt, C. Fortoul, "Review of the Distributed Generation Concept: Attempt of Unification," Presented at the International Conference on Renewable Energies and Power Quality (ICREPQ'06) Annu.Meeting, Palma de Mallorca, Spain, 2006. [Online] Available: <http://www.icrepq.com/full-paper-icrep/275-GONZALEZ.pdf>
- [23] T.Ackermann, G. Andersson and L. Söder, "Distributed generation: a definition," *Electric power Systems Research*, Vol.57, No.3,pp.195-204, Apr.2001.
- [24] G. Pepermans, J.Driesen, D. Haeseldonckx, R. Belmans, and W.D'haeseleer "Distributed Generation: Definition, Benefits and Issues," *Energy policy*, Vol.33, pp. 787-798, 2005.

- 
- [25] R. E. Brown, "Impact of Smart Grid on Distribution System Design," presented at IEEE Power and Energy Society General Meeting, Pittsburgh, PA, 2008
- [26] J. Fan and S. Borlase, "The Evolution of Distribution," *IEEE Power and Energy Magazine*, vol. 7, pp. 63-68, 2009.
- [27] R.S. Thallam, S. Suryanarayanan, G.T. Heydt and R. Ayyanar, "Impact of Interconnection of Distributed Generation on Electric Distribution Systems – A Dynamic Simulation Perspective," IEEE PES General Meeting 2006, June 23-27, Montreal.
- [28] A. Vojdani, "Smart Integration," *IEEE Power and Energy Magazine*, vol. 6, pp. 71-79, November/ December 2008.
- [29] A. Ipakchi and F. Albuyeh, "Grid of the Future," *IEEE Power and Energy Magazine*, vol. 7, pp. 52-62, March/April 2009.
- [30] S. Karnouskos, O. Terzidis, and P. Karnouskos, "An Advanced Metering Infrastructure for Future Energy Networks," in *New Technologies, Mobility and Security*, 2007, p. 597-606.
- [31] S. Borenstei, M. Jaske and A. Rosenfeld, "Dynamic Pricing, Advanced Metering and Demand Response in Electricity Markets," Center for the Study of Energy Markets Working Paper, University of California at Berkeley, Oct. 2002
- [32] J. McDonald, "Adaptive Intelligent Power Systems: Active Distribution Networks," *Energy Policy*, vol. 36, pp. 4346-4351, 2008.
- [33] R.P Gupta and R.K Varma, "Power Distribution Automation: Present Status," *Academic Open Internet Journal*, vol. 15, 2005
- [34] N.S Wade, N.S. P.C Taylor, P.D Lang and P.R Jones, "Evaluating the Benefits of an Electrical Energy Storage System in a Future Smart Grid," *Energy policy*, vol. 38, n. 11, pp. 7180-7188, 2010.
- [35] A. Oudalov, R. Cherkaoui and A. Beguin, "Sizing and Optimal Operation of Battery Energy Storage System for Peak Shaving Application," in *Power Technology Conference Proceedings*, Lausanne (Switzerland), Jul. 2007.
- [36] Armas, J.M. and Suryanarayanan, S., —A Heuristic Technique for Scheduling a Customer-driven Residential Distributed Energy Resource Installation, *Proc. 15th Int'l Conference on Intelligent Systems Applications to Power Systems*, pp. 1-7, 2009.
- [37] A. Goikoetxea, J. A. Barrena, M. A. Rodriguez, and G. Abad, "Benefits of Distributed Energy Storage Working in Parallel to Distributed Energy Resources," in *ICREPEQ Valencia (Spain)*, 2009.

- 
- [38] M. A. N. Guimaraes, C. A. Castro, and R. Romero, "Reconfiguration of Distribution Systems by a Modified Genetic Algorithm," in *IEEE Power Tech 2007* Lausanne, 2007, pp. 401-406.
- [39] C. C. Chu, M. S. Tsai, and C. Y. Lee, "Applications of Hybrid GA-ACO on Feeder Reconfiguration for Distribution System Scheduled Maintenance Outage under Load Variations," in APAP2009, Jeju (Korea), , Oct. 2009
- [40] H. Brown, D.A Houghton, G.T Heydt, S. Suryanarayanan, "Some Elements of Design and Operation of a Smart Distribution System," Transmission and Distribution Conference and Exposition, 2010 IEEE PES , vol., no., pp.1-8, 19-22 April 2010.
- [41] T. P. Wagner, A. Y. Chikhani, and R. Hackam, "Feeder Reconfiguration for Loss Reduction: An Application of Distribution Automation," *IEEE Transactions on Power Delivery*, vol. 6, pp. 1922-1933, October 1991.
- [42] T. E. McDermott, I. Drezga, and R. P. Broadwater, "A heuristic nonlinear constructive method for distribution system reconfiguration," *IEEE Transactions on Power Systems*, vol. 14, pp. 478-483, May 1999.
- [43] F. V. Gomes, S. Carneiro, J. L. R. Pereira, M. P. Vinagre, P. A. N. Garcia, and L. R. d. Araujo, "A New Distribution System Reconfiguration Approach using Optimum Power Flow and Sensitivity Analysis for Loss Reduction," *IEEE Transactions on Power Systems*, vol. 21, pp. 1616-1623, November 2006.
- [44] M. A. N. Guimaraes, C. A. Castro, and R. Romero, "Reconfiguration of Distribution Systems by a Modified Genetic Algorithm," in *IEEE Power Tech 2007* Lausanne, 2007, pp. 401-406.
- [45] Enacheanu, B., B. Raison, R. Caire, O. Devaux, W. Bienia and N. HadjSaid (2008). Radial Network Reconfiguration Using Generic Algorithm Based on the Matroid Theory. *IEEE Transactions on Power System*, Vol. 23, N° 1, pp. 186 – 195.
- [46] J. Z. Zhu, "Optimal Reconfiguration of Electrical Distribution Network using the Refined Genetic Algorithm," *Elect. Power Syst. Res.*, vol. 62, no. 1, pp. 37–42, May 2002.
- [47] D. Shin, J. Kim, T. Kim, J. Choo, and C. Singh, "Optimal Service Restoration and Reconfiguration of Network using Genetic-Tabu Algorithm," *Elect. Power Syst. Res.*, vol. 71, pp. 145–152, 2004.
- [48] Z. Chunjie, X. Chunjie, C. Hui and F. Huajing, "Genetic Algorithm-Based Dynamic Reconfiguration for Networked Control System," *Neural Computing & Applications*, Springer, Mar. 2007
- [49] V. Calderaro, A. Piccolo, and P. Siano, "Maximizing DG Penetration in Distribution Networks by means of GA based Reconfiguration," in *2005 International Conference on Future Power Systems*, Amsterdam, Netherlands, 2005.

- 
- [50] G. Granelli, M. Montagna, F. Zanellini, P. Bresesti, R. Vailati, and M. Innorta, "Optimal Network Reconfiguration for Congestion Management by Deterministic and Genetic Algorithms," *Elect. Power Syst. Res.*, vol. 76, pp. 549–556, Apr. 2006.
- [51] Y.-Y. Hong and S.-Y. Ho, "Determination of Network Configuration Considering Multiobjective in Distribution Systems using Genetic Algorithms," *IEEE Trans. Power Syst.*, vol. 20, no. 2, pp. 1062–1069, May 2005.
- [52] R.M.V Vitorino, H.M.M Jorge, L.M.P Neves, L.M.P, "Network Reconfiguration using a Genetic Approach for Loss and Reliability Optimization in Distribution Systems," in *Power Engineering, Energy and Electrical Drives*, May 2009
- [53] A. Ahuja, S. Das, and A. Pahwa, "An AIS-ACO Hybrid Approach for Multi-objective Distribution System Reconfiguration," *IEEE Transactions on Power Systems*, vol. 22, pp. 1101-1111, August 2007.
- [54] D. Das, "A Fuzzy Multiobjective Approach for Network Reconfiguration of Distribution Systems," *IEEE Trans. Power Deliver*, vol. 21, pp. 202–209, Jan. 2006.
- [55] S. Haffner, L. F. A. Pereira, L. A. Pereira, and L. S. Barreto, "Multistage Model for Distribution Expansion Planning with Distributed Generation—Part I: Problem Formulation," *IEEE Trans. Power Del.*, vol. 23, no. 2, pp. 915–923, Apr. 2008.
- [56] C. Wang and M. H. Nehrir, "Analytical Approaches for Optimal Placement of Distributed Generation Sources in Power System," *IEEE Transactions in Power Systems*, vol.19, pp. 2068–76, Nov. 2004.
- [57] J.E Ramirez-Marquez, D. Coit, "A Heuristic for Solving the Redundancy Allocation Problem for Multistate Series-parallel Systems," *Reliability Engineering & System Safety*, Vol. 83, n. 3, pp 341–9, 2004.
- [58] E. Míguez, J. Cidrás, E. Díaz-Dorado, and J. L. García-Dornelas, "An Improved Branch-exchange Algorithm for Large-scale Distribution Network Planning," *IEEE Trans. Power Syst.*, vol. 17, no. 4, pp. 931–936, Nov. 2002.
- [59] I. J. Ramírez-Rosado and J. L. Bernal-Augustín, "Reliability and Costs Optimization for Distribution Networks Expansion using an Evolutionary Algorithm," *IEEE Trans. Power Syst.*, vol. 16, no. 1, pp. 111–118, Feb. 2001.
- [60] W. El-Khattam, Y. G. Hegazy, and M. M. A. Salama, "An Integrated Distributed Generation Optimization Model for Distribution System Planning," *IEEE Trans. Power Syst.*, vol. 20, no. 2, pp. 1158–1165, May 2005.
- [61] M. Sedighizadeh, and A. Rezazadeh, "Using Genetic Algorithm for Distributed Generation Allocation to Reduce Losses and Improve Voltage Profile", *World Academy of Science, Engineering and Technology*, vol. 27 pp. 251-256, Feb. 2008.

- 
- [62] I. Pisciă, C. Bulac, M. Eremia, "Optimal Distributed Generation Location and Sizing using Genetic Algorithms," in the 15th International Conference on Intelligent System Applications to Power Systems, Curitiba, Brazil, 2009
- [63] Celli G., Ghiani E., Mocci S., Pilo F., "A MultiObjective Formulation for Optimal Sizing and Siting of Embedded Generation in Distribution Networks," in Proc. of Powertech 2003 conference, Bologna (Italy), Jun. 2003.
- [64] J. F. Gómez, H. M. Khodr, P. M. de Oliveira, L. Ocque, J. M. Yusta, R. Villasana, and A. J. Urdaneta, "Ant Colony System Algorithm for the Planning of Primary Distribution Circuits," *IEEE Trans. Power Syst.*, vol. 19, no. 2, pp. 996–1004, May 2004.
- [65] V. Parada, J. A. Ferland, M. Arias, and K. Daniels, "Optimization of Electrical Distribution Feeders using Simulated Annealing," *IEEE Trans. Power Del.*, vol. 19, no. 3, pp. 1135–1141, Jul. 2004.
- [66] A. Augugliaro, L. Dusonchet, and E. R. Sanseverino, "An Evolutionary Parallel Tabu Search Approach for Distribution Systems Reinforcement Planning," *Adv. Eng. Inform.*, no. 16, pp. 205–215, 2002.
- [67] M. Gauthier, C. Abbey, F. Katiraei, J.-L. Pepin, M. Plamondon, and G. Simard, "Planned Islanding as a Distribution System Operation Tool for Reliability Enhancement," *Integration of Decentralized Energy Resources: Publications*, Natural Resources, Canada, 2009.
- [68] J. Driesen and F. Katiraei, "Design for Distributed Energy Resources," *IEEE Power and Energy Magazine*, vol. 6, pp. 34–41, 2008.
- [69] R. Carnieletto, S. Suryanarayanan, M. G. Simoes, and F. A. Farret, "A Multifunctional Single-phase Voltage Source Inverter in Perspective of the Smart Grid Initiative," accepted in Proc. 2009 IEEE Industry Applications Society Annual Conference, Oct 2009, pp. 1–8.
- [70] *IEEE Standard for Interconnecting Distributed Resources with Electric Power Systems*, IEEE1547, 2003.
- [71] R. Lasseter, A. Akhil, C. Marnay, J. Stephens, J. Dagle, R. Guttromson, A. Meliopoulos, R. Yinger, and J. Eto, "The CERTS Microgrid Concept," White paper for Transmission Reliability Program, Office of Power Technologies, U.S. Department of Energy, April 2002
- [72] S. B. Patra, J. Mitra, S. J. Ranade, "Microgrid Architecture: A Reliability Constrained Approach," in Proc. IEEE Power Engineering Soc. General Meeting 2005, San Francisco, CA, Jun. 2005
- [73] J. Mitra, S. B. Patra, S. J. Ranade, "A Dynamic Programming Based Method for Developing Optimal Microgrid Architectures," in Proc. 15th Power Systems Computational Conf., Liege (Belgium), Aug. 2005.

- 
- [74] J. Mitra, S. B. Patra and S. J. Ranade, "Reliability Stipulated Microgrid Architecture using Particle Swarm Optimization," in Proc. 9th Intl. Conf. on Probabilistic Methods Applied to Power Systems, Stockholm (Sweden), Jun. 2006.
- [75] A. P. Agalgaonkar, C. V. Dobariya, M. G. Kanabar, S. A. Khaparde and S. V. Kulkarni, "Optimal Sizing of Distributed Generators in Microgrid", in Proc. IEEE Power India Conf., 10-12 April 2006.
- [76] M. Vallem, J. Mitra, "A Particle Swarm-based Method for Reliability-driven DG Deployment and Feeder Augmentation in Microgrids," in National Power Systems Conference (NPSC), Bombay (India), Dec. 2008.
- [77] "Plug-in Electric Hybrid Vehicles Position Statement Adopted by IEEE-USA Board of Directors," *IEEE USA* 2007.
- [78] L. Dickerman and J. Harrison, "A New Car, a New Grid," *IEEE Power and Energy Magazine*, vol. 8, pp. 55–61, Mar. 2010
- [79] S. Letendre, P. Denholm, P. Lilienthal, "New Load, or New Resource?," *Public Utility Fortnightly*, pp. 28-37, Dec. 2006.
- [80] T. Markel, A. Brooker, T. Hendricks, V. Johnson, K. Kelly, B. Kramer, M. O'Keefe, S. Sprik, K. Wipke, "ADVISOR: A Systems Analysis Tool for Advanced Vehicle Modeling" *Journal of Power Sources*, vol. 110, n. 2 22, pp. 255-266, Aug 2002.
- [81] "Power Train System Analysis Toolkit (PSAT)," Argonne National Laboratory, [Online]. Available: [http://www.transportation.anl.gov/modeling\\_simulation](http://www.transportation.anl.gov/modeling_simulation)
- [82] A. Rousseau, P. Sharer and S. Halbach, "Using Modeling and Simulation to Support Future Medium and Heavy Duty Regulations," in Electric Vehicle Symposium & Exhibition (EVS-25), Shenzhen (China), Nov 2010.
- [83] "Autonomie," Argonne National Laboratory, [Online]. Available: <http://www.autonomie.net>(Accessed on January 2011).
- [84] J. Gonder, T. Markel, M. Thornton, and A. Simpson, "Using Global Positioning System Travel Data to Assess Real-world Energy Use of Plug-in Hybrid Electric Vehicles," Transportation Research Record (TRR), Journal of the Transportation Research Board (TRB), No. 2017, Dec. 2007.
- [85] A. Pesaran T. and Markel, "Battery Requirements for Plug-In Hybrid Electric Vehicles: Analysis and Rationale." Proceedings of 23rd International Electric Vehicles Symposium (EVS 23), Anaheim, CA, Dec. 2007.
- [86] C. Frey, H. Choi, E. Pritchard, J. Lawrence, "In-Use Measurement of the Activity, Energy Use, and Emissions of a Plug-In Hybrid Electric Vehicle," in 102nd Annual Conference and Exhibition; Air & Waste Management Association: Detroit, MI, 2009.

- 
- [87] T. Markel, and A. Simpson, "Cost-Benefit Analysis of Plug-in Hybrid Electric Vehicle Technology," 22nd International Electric Vehicle Symposium, Yokohama (Japan), Oct. 2006.
- [88] K. Parks, P. Denholm, and T. Markel, "Costs and Emissions Associated with Plug-in Hybrid Electric Vehicle Charging in the Xcel Energy Colorado Service Territory," Technical report, National Renewable Energy Laboratory (NREL), 2007.
- [89] S.W. Hadley, A. Tsvetkova, Potential Impacts of Plug-in Hybrid Electric Vehicles on Regional Power Generation, ORNL/TM-2007/150, Oak Ridge National Laboratory, 2008.
- [90] S. Meliopoulos, J. Meisel and T. Overbye, "Power System Level Impacts of Plug-In Hybrid Vehicles (Final Project Report)," PSERC Document 09-12, Oct. 2009.
- [91] L. Pieltain, T. Gómez, C. Mateo, R. Cossent und P. Frías, "Assessment of the Impact of Plug-in Electric Vehicles on Distribution Networks," *IEEE Transactions on Power Systems*, submitted for publication, Dec. 2009.
- [92] Kintner-Meyer, M., K. Schneider, and R. Pratt, "Impact assessments of Plug-in Hybrid Vehicles on Electric Utilities and Regional U.S. Power Grids Part 1: Technical Analysis," Pacific Northwest National Laboratory, 2007
- [93] S.W. Hadley, A.A. Tsvetkova, "Potential Impacts of Plug-in Hybrid Electric Vehicles on Regional Power Generation," *The Electricity Journal*, Vol. 22, n. 10, pp 56-68, Dec 2009.
- [94] A. Brooks, "Vehicle-to-grid Demonstration Project: Grid Regulation Ancillary Service with a Battery Electric Vehicle," AC Propulsion, San Dimas, CA, Rep. 01-313, Dec. 2002.
- [95] W. Kempton and J. Tomic, "Vehicle to grid Implementation: From Stabilizing the Grid to Supporting Large-scale Renewable Energy," *Journal of Power Sources*, vol. 144, no. 1, pp. 280-294, Jun. 2005.
- [96] H. Lund, W. Kempton, "Integration of Renewable Energy into the Transport and Electricity Sectors Through V2G," *Energy Policy*, vol. 36, n. 9, pp. 3578-87, 2008
- [97] W. Kempton and A. Dhanju, "Using Electric Vehicles as Storage for Large Offshore Wind Power," in *Copenhagen Offshore Wind*, Aug. 2005
- [98] A. Srivastava, B. Annabathina, S. Kamalasadana, "The Challenges and Policy Options for Integrating Plug-in Hybrid Electric Vehicle into the Electric Grid," *The Electricity Journal*, vol. 23, n. 3, pp. 83-91, Apr. 2010.

- 
- [99] C. Quinn, D. Zimmerle, and T. Bradley, "The Effect of Communication Architecture on the Availability, Reliability, and Economics of Plug-in Hybrid Electric Vehicle-to-grid Ancillary Services," *Journal of Power Sources*, vol. 195, pp. 1500-1509, Sep. 2009
- [100] C. Guille and G. Gross, "Design of a Conceptual Framework for the V2G Implementation", in *Energy 2030 Conference IEEE*, pp.1-3, 17-18, Nov. 2008.
- [101] M. D. Galus and G. Andersson, "Demand Management for Grid Connected Plug-in Hybrid Electric Vehicles (PHEVs)," in *IEEE Energy 2030*, pages 1–8, Atlanta, GA, USA, 2008.
- [102] C. Roe, J. Meisel, F. Evangelos, T. Overbye, and A. P. Meliopoulos, "Power System Level Impacts of PHEVs," in *42nd Hawaii International Conference on System Sciences, HICSS '09*, pp 1–10, 2009.
- [103] C. Farmer, P. Hines, J. Dowds, S. Blumsack, "Modeling the Impact of Increasing PHEV Loads on the Distribution Infrastructure," in *System Sciences (HICSS), 43rd Hawaii International Conference*, Jan. 2010.
- [104] Shengnan Shao; Pipattanasomporn, M.; Rahman, S.; , "Challenges of PHEV penetration to the residential distribution network," *Power & Energy Society General Meeting 2009*, Jul. 2009
- [105] K. Clement, E. Haesen, L. Driesen, "The Impact of Uncontrolled and Controlled charging of Plug-in Hybrid Electric Vehicles on the Distribution Grid," in *European Ele-Drive Transportation Conference*, Geneva (Switzerland), Mar 2008.
- [106] S. Acha, T. Green and N. Shah, "Effects of Optimized Plug-in Hybrid Vehicle charging Strategies on Electric Distribution Network Losses," in *IEEE PES Conference and exposition on transmission and distribution*, Prague, pp. 1–6, 2010
- [107] K. Clement, E. Haesen and J. Driesen, "The Impact of Charging Plug-in Hybrid Electric Vehicles on the Distribution Grid," in *Proceedings 2008-4th IEEE BeNeLux young researchers symposium in electrical power engineering*, Eindhoven (Netherlands), 2008
- [108] K. Clement, E. Haesen and Driesen J, "Stochastic Analysis of the Impact of Plug-in Hybrid Electric Vehicles on the Distribution Grid," in *CIREN'09 20th International conference on electricity distribution*, Prague (Czech Republic), 2009
- [109] M. Gen, R. Cheng, and L. Lin, *Network Models and Optimization: Multiobjective Genetic Algorithm Approach*, Springer, 2008.
- [110] *Matlab - The Language of Technical Computing*. [Online.]Available: <http://www.mathworks.com/products/global-opt>



- 
- [111] J. D. Glover, M. S. Sarma, and T. J. Overbye, *Power System Analysis and Design*, 4th ed. Toronto, Canada: Thomson Learning, 2008.
- [112] "PowerWorld Simulator," *PowerWorld Corporation*, Champaign, IL, 2009. [Online] Available: <http://powerworld.com/> [Accessed 15 Jan 2011].
- [113] "PowerWorld Simulator - Automation Server (SimAuto)," *PowerWorld Corporation*, Champaign, IL, 2009.
- [114] S. Chakraborty and M. G. Simões, "PV-Microgrid Operational Cost Minimization by Neural Forecasting and Heuristic Optimization," in *Industry Applications Society Annual Meeting* pp. 1-8, Edmonton, Alberta, Canada 2008.
- [115] A. Newman, "EBGN: 555: Linear Programming", Colorado School of Mines, 2010.
- [116] M. Á. Carreira-Perpiñán, "Simplex Method," *MathWorld – A Wolfram Web Resource*, 2010. [Online]. Available: <http://mathworld.wolfram.com/SimplexMethod.html>
- [117] R. Baldick, *Applied Optimization: Formulation and Algorithms for Engineering Systems* New York, Cambridge University Press, 2006.
- [118] A.M. Leite da Silva, W.S. Sales, L.C. Resende, L.A.F. Manso, C.E. Sacramento, and L.S. Rezende, "Evolution Strategies to Transmission Expansion Planning considering Unreliability Costs," In Proc. of the 9<sup>th</sup> PMAPS, Stockholm, Sweden, 11-15/June 2006. [Online] Available: <http://citeseerx.ist.psu.edu/viewdoc/download?doi=10.1.1.92.3907&rep=rep1&type=pdf>
- [119] J. Zhu and M. Chow, "A Review of Emerging Techniques on Generation Expansion Planning", *IEEE Trans. Power Syst.*, vol. 12, no. 4, pp. 1722-1728, Nov. 1997.
- [120] J. F. Manwell, J. G. McGowan, and A. L. Rogers, *Wind Energy Explained: Theory, Design and Application*. Hoboken, NJ: John Wiley & Sons, 2002.
- [109] H.E Brown and S. Suryanarayanan, "Results of the survey on smart distribution systems: An addendum," in *PSERC T-41 Project Wiki*. [Online]. Available: <http://psercsmartdsys.pbworks.com/f/SummaryOfSurveyResults2009>.
- [122] R. C. Dugan, M. F. McGranaghan, S. Santoso, and H. W. Beaty, *Electrical Power Systems Quality*, 2nd ed. New York: McGraw-Hill, 2003.
- [123] R. Billinton and R. N. Allan, *Reliability Evaluation of Engineering Systems*, 2<sup>nd</sup> ed. New York: Plenum Press, 1992.
- [124] C. A. C. Coello, G. B. Lamont, and D. A. VanVeldhuizen, *Evolutionary Algorithms for Solving Multiobjective Problems*, 2<sup>nd</sup> ed. New York: Springer, 2007.
- [125] V. Miranda, D. Srinivasan, L.M. Proenca, "Evolutionary Computation in Power Systems," *Electrical Power & Energy Systems*, vol. 20, n.2, pp. 89–98, Feb. 1998.

- 
- [126] S. Jalilzadeh, H. Shayeghi, M. Mahdavi, and H. Hadadian, "A GA Based Transmission Network Expansion Planning Considering Voltage Level, Network Losses and Number of Bundle Lines," *American Journal of Applied Sciences*, Vol.6, No.5, pp987-994, May2009.[Online]Available:<http://www.scipub.org/fulltext/ajas/ajas65987-994.pdf>
- [127] J.I.R. Rodriguez, D.M. Falcão, G.N. Taranto, and H.L.S. Almeida, "Short-Term Transmission Expansion Planning by a Combined Genetic Algorithm and Hill-Climbing Technique," presented at the International Conference on Intelligent System Applications to Power Systems, Curitiba, Brazil, 2009. [Online] Available: [http://www.isappower.org/PDFs/Paper\\_203.pdf](http://www.isappower.org/PDFs/Paper_203.pdf)
- [128] M. Gholami, H. Yazdanpanahi and G.B. Gharehpetian, "An Approach to Find Most Flexible Plan among Solutions of Transmission Expansion Planning (TEP) Problem," presented at the Hispano-Lusa Conference on Electrical Engineering, Zaragoza, Spain, 2009. [Online] Available: <http://www.aedie.org/11chlie-papers/136-Gholami.pdf>
- [129] J.-B. Park, Y.-M. Park, J.-R. Won, and K.Y. Lee: "An improved Genetic Algorithm for Generation Expansion Planning", *IEEE Trans. On Power Systems*, Vol. 15, No. 3, August 2000, pp. 916-922.
- [130] C.R Houck, J.A Joines and M.G Kay, "A Genetic Algorithm for Function Optimization: A Matlab Implementation," NSCU-IE Technical Report 95-09, North Claroline State Univerisity, 1995.
- [131] M. Srinivas and Lalit M. Patnaik, "Genetic algorithms: A survey," *IEEE Computer*, 27(6):17-26, June 1994.
- [132] R. Billinton, S. Kumar, *et al.*, "A Reliability Test System for Educational Purposes - Basic Data," *IEEE Transactions on Power Systems*, vol. 4, pp. 1238-1244, August 1989.
- [133] R. Billinton and S. Jonnavithula, "A Test System for Teaching Overall Power System Reliability assessment," *IEEE Transactions on Power Systems*, vol. 11, pp. 1670-1676, November 1996.
- [134] *IEEE Standard for Interconnecting Distributed Resources with Electric Power Systems*, IEEE1547, 2003.
- [135] "Energy Analysis", US DOE. [Online]. Available:[http://www.nrel.gov/analysis/tech\\_costs.html](http://www.nrel.gov/analysis/tech_costs.html)
- [136] W. Kersting, *Distribution System Modeling and Analysis*, New York, NY: CRC Press, 2006.
- [137] M. Srinivas and Lalit M. Patnaik, "Genetic Algorithms: A survey," *IEEE Computer*, 27(6):17-26, June 1994.

- 
- [138] Vassilopoulos, P., "Models for the Identification of Market Power in Wholesale Electricity Markets", Industrial Organization, D.E.A 129, September 2003 pp 46 - 47.
- [139] K. Sikes, T. Gross, L. Zhenhong, J. Sullivan, John, T. Cleary and J. Ward, "Plug-In Hybrid Electric Vehicle Market Introduction Study: Final Report," *Oak Ridge National Laboratory (ORNL) Technical Report*, Jan. 2010.
- [140] "One Million Electric Vehicles By 2015," US Department of Energy, February 2011 Status Report. [Online] Available: <http://www1.eere.energy.gov/vehiclesandfuels/pdfs>
- [141] Electric Power Research Institute, Comparing the Benefits and Impacts of Hybrid Electric Vehicle Options, Corporate document 1000349, EPRI, Palo Alto, CA, 2001.
- [142] Electric Power Research Institute, Advanced Batteries for Electric Drive Vehicles: A Technology and Cost Effectiveness Assessment for Battery Electric, Power Assist Hybrid Electric, and Plug-in Hybrid Electric Vehicles, Document 1001577, EPRI, Palo Alto, CA, 2003.
- [143] F. R. Kalhammer, H. Kamath, M. Duvall, M. Alexander, "Plug-in Hybrid Electric Vehicles: Promises, Issues, and Prospects," in Electric Vehicle Symposium (EVS 24), Stavanger (Norway), May 2009.
- [144] "Smart Grid System Report", U.S Department of Energy, Jul. 2009.
- [145] Reliability Test System Task Force of the Application of Probability Methods Subcommittee, "IEEE reliability test system," *IEEE Transactions on Power Apparatus and Systems*, vol. PAS-98, no. 6, pp. 2047-54, November 1979.
- [146] L. Sanna, "Driving the Solution the Plug-in Hybrid Electric Vehicle", *EPRI Journal*, pp. 8-17, 2005.
- [147] "Fuel Economy Test, Detailed Test Information" U.S. Department of Energy (DOE), [Online]. Available : [http://www.fueleconomy.gov/feg/fe\\_test\\_schedules.shtml](http://www.fueleconomy.gov/feg/fe_test_schedules.shtml)
- [148] Serrao, L., Chehab, Z., Guezennec, Y., Rizzoni, G., "An Aging Model of Ni-MH Batteries for Hybrid Electric Vehicles", 2005 IEEE Conference on Vehicle Power and Propulsion
- [149] "Regulated Price Plan (RPP) Time-of-Use (TOU) Prices," Ontario Energy Board (OEB), [Online]. Available: <http://www.oeb.gov.on.ca/OEB/Consumers/Electricity/Electricity+Prices#tou>
- [150] "Residential Service rates," Xcel Energy, [Online]. Available: <http://www.xcelenergy.com/docs/WIResratesbrochure.pdf>

- 
- [151] R. Fourer, D. Gay and B.W. Kernighan, "AMPL: A Mathematical Programming Language," *Computing Science Technical Report No. 133, AT&T Bell Laboratories*, Murray Hill N J, Jan. 1987.
- [152] "Cross-country," Colorado School of Mines, 2010.
- [153] J. Giráldez, A. Jaiantilal, J. Walz, S. Suryanarayanan, S. Sankaranarayanan, H. E. Brown, and E. Chang, "An Evolutionary Algorithm and Acceleration Approach for Topological Design of Distributed Resource Islands," accepted at IEEE PES PowerTech 2011, Trondheim (Norway), Jun. 2011.



## APPENDIX

This appendix contains additional information on the sizing of the components of the 3FDR and RBTS test systems. After that, the programming information for all presented case studies in the first and second parts of this thesis is described. First, the programming information of the MOGA is described for the 3FDR test system example and for both RBTS case studies. Secondly, the codes for the evaluation of the impact of PHEVs are described including the probabilistic simulation methodology and the LP algorithms. The programs in their entirety are found in the electronic appendix.

### A.1 Components of the 3FDR and RBTS system

Tables a.1 and a.2 contain the impedance characteristics of the existing lines in the 3FDR system and of the possible connections to be added in the 3FDR system respectively.

Table A1.1 Line data of the existing connections in the 3FDR test system, reproduced from [20].

Connection	Length [mi.]	R (pu)	X (pu)
Line 2-3	0.2841	0.0066	0.0175
Line 4-5	0.3314	0.0002	0.0006
Line 8-9	0.4213	0.0059	0.0153
Transformer 1-2	N/A	0.0100	0.0600
Transformer 5-6	N/A	0.0100	0.0600
Transformer 7-8	N/A	0.0100	0.0600

### Calculation of the distance between buses in the absence of topographical information

Reference [20] proposed the calculation repeated below to estimate the distance between buses for the possible connections in the absence of topographical information of a test system. A fixed distance is assumed between feeders and the length of a possible connection is given by,

$$\varepsilon = \begin{cases} \sqrt{d^2 + (\xi - \lambda)^2}, & \xi \neq \lambda \\ d, & \xi = \lambda \end{cases} \quad (\text{A.1-1})$$

where  $d$ , the distance between feeders;  $\xi$  the distance of the 'to' bus to the slack bus on the 'to' feeder; and  $\lambda$  the distance of the 'from' bus to the slack bus on the 'from' feeder. Equation (a.1) is directly taken from [20].

Table A1.2 Line data of the possible connections to be added in the 3FDR system reproduced from [20].

Connection <i>i</i>	R (pu)	X (pu)
Line 1-4	0.0001	0.0093
Line 1-5	0.002	0.0186
Line 1-6	0.0159	0.0420
Line 1-7	0.0042	0.0558
Line 1-8	0.0055	0.0144
Line 1-9	0.0079	0.0209
Line 2-4	0.0060	0.0257
Line 2-5	0.0040	0.0105
Line 2-6	0.0046	0.0121
Line 2-7	0.0046	0.0120
Line 2-8	0.0050	0.0131
Line 2-9	0.0083	0.0219
Line 3-4	0.0126	0.0332
Line 3-5	0.0106	0.0280
Line 3-6	0.0050	0.0156
Line 3-7	0.0146	0.0386
Line 3-8	0.0140	0.0369
Line 3-9	0.0200	0.0529
Line 4-7	0.0001	0.0003
Line 4-8	0.0024	0.0063
Line 4-9	0.0064	0.0168
Line 5-7	0.0002	0.0007
Line 5-8	0.0055	0.0145
Line 5-9	0.0081	0.0213
Line 6-7	0.0080	0.0210
Line 6-8	0.0058	0.0153
Line 6-9	0.0054	0.0142

## A.2 Electronic appendix

The electronic appendix included in this thesis is organized in two main folders. The first one named ‘MOGA’, contains the programming codes and the data related to the extended MOGA methodology proposed in Chapter 2 to be applied to the two test systems presented in Chapter 3. In this section, the “Readme\_MOGA.txt” is presented. The second main folder ‘PHEVs’ contains the programming codes for the probabilistic simulation methodology and the LP algorithms described in Chapter 4 and implemented in the RBTS test system. The “Readme\_PHEVs.txt” file is also included in this section.

## Contents of “MOGA”

This folder contains two main functions RunMOGA and RunMOGADGs codes for running optimizations on the RBTS Bus 3 distribution system and on the 3FDR test system respectively. It contains all the sub-functions called by those codes. This folder also contains the PowerWorld files used in the simulations of the test systems. Finally, it contains 6 subfolders named after the objective functions used, with the outputs of the MOGA. The extended MOGA proposed in this thesis is based on the methodology proposed in [], and thus this folder contains functions directly taken from [], functions that are modifications to the code proposed in [], and functions programmed by the author of this thesis particular to the problem addresses.

- Preparation files for the RBTS

PrepFile.m ... used for component sizing and creating the .aux file of possible connections between buses.

PrepFile\_LessConnections.m ...used for component sizing and creating the .aux file of possible connections between buses no longer than 3km

- Optimization files

RBTS: RunMOGA.m ... used to specify the settings and the objective function for the multi-objective optimization of cost and reliability using a genetic algorithm function from Matlab, gamultiobj(). Then, the output of the algorithm is printed to the command line.

3FDR:RunMOGADGs.m ... used to specify the settings and the objective function for the multi-objective optimization of cost and reliability using a genetic algorithm function from Matlab, gamultiobj(). Then, the output of the algorithm is printed to the command line.

- Subfunctions

objeval\_DGs() ... a function is to evaluate the cost and reliability for the multi-objective GA process with annual average loads in the 3FDR test system.

I: x (an individual from the GA)



O: f (the objective function values [cost; rel])

ASU() ... a function to extract information programmed at Arizona State University for the RBTS Bus 3 Distribution System

I: prnt

O: L\_line, LP, Peak\_Avg, fdr\_lens

CreateAux()... a function to create the .aux file of the possible connections between feeders in the RBTS Bus 3 distribution system

I: writefile, feeders, fdr\_lens, d, bus\_names, lims, r\_per\_km, x\_per\_km, cost\_inc

O: cost, (writefile.aux in current directory)

CreateAux\_LessConnections ()... a function to create the .aux file of the possible connections between feeders no longer than 3km in the RBTS Bus 3 distribution system

I: writefile, feeders, fdr\_lens, d, bus\_names, lims, r\_per\_km, x\_per\_km, cost\_inc

O: cost, (writefile.aux in current directory)

Exfunc () ... a function to switch data types before writing information to the .aux file

LP\_line () ... a function that links the load points to the line that serves them. Output in format [load point; line serving]

I: none

O: L\_line

RBTS\_lines() ... a function establishing the physical connection between buses in the system

I: N\_B, N\_LINES

O: LINE, y

RBTSobjeval\_AV() ... a function is to evaluate the cost and reliability for the multi-objective GA process with annual average loads in the RBTS test system.

I: x (an individual from the GA)

O: f (the objective function values [cost; rel])

RBTSobjeval\_AV\_LessConnections() ... a function is to evaluate the cost and reliability for the multi-objective GA process with annual average loads, and connections no longer than 3km in the RBTS test system.

I: x (an individual from the GA)

O: f (the objective function values [cost; rel])

RBTSobjeval\_LD() ... a function is to evaluate the cost and reliability for the multi-objective GA process with step-load duration curve representation in the RBTS test system.

I: x (an individual from the GA)

O: f (the objective function values [cost; rel])

RBTSobjeval\_LD\_LessConnections() ... a function is to evaluate the cost and reliability for the multi-objective GA process with step-load duration curve representation and connections no longer than 3km in the RBTS test system.

I: x (an individual from the GA)

O: f (the objective function values [cost; rel])

DevListDispReduced() ... a function to extract bus and branch info

I: A, prnt (T/F value to print results)

O: basic bus & branch info

branchEXreduced() ... a function to extract the branch information

I: A, output\_branch, branchflds

O: chng\_branch

BranchFormat() ... a function to arrange the branch information into a the format recognized by SimAuto

I: chng\_branch

O: valuelist, num\_elems

EENSreducedDGs\_LD() ... a function to determine the power not supplied

I: A, T, genflds, output\_gen, slack\_buses

O: PNS

DG\_sizing() ... a function to extract the annual avrage load information to size DG

I: A,output\_gen, genfields,slack\_buses)

O: L\_average, tot\_load

genEXreducedDG1() ... a function to extract the information about system generators and slack buses

I: A, output\_gen, genflds, slack\_buses

O: slackgen, regen, reqdinf\_re, reqdinf

GenFormat() ... a function to arrange the information into a format recognized by Simauto functions

I: reqdinf\_re

O: valuegenlist, num\_genelems

Load\_BusDG() ... a function to obtain a vector of connected loads in the buses of the system

I: loads,regen

O: L

LoadFormat() ... a function to arrange the information into a format recognized by Simauto functions

I: loads\_Beta

O: valueloadlist, num\_loadelems

flatstart() ... a function to reset the system generators to the flat start condition of 1 pu at an angle of 0 deg.

I: A

O: none

runmode() ... a function to enter SimAuto "Run" mode

I: A

O: none

editmode() ... a function to enter SimAuto "Edit" mode

I: A

O: none

resetslack()... a function to reset buses that are no longer slack to zero output

I: A, reqd\_gen, slack\_buses, reqdGENfields

O: none

loading() ... a function to extract the branch loading information

I: A, output\_branch, branchflds

O: maxpercent

v\_level() ... a function to extract the bus voltage information

I: A, output\_bus, busflds

O: puvolt

penalty() ... a function to create the penalty scaling variable for line and voltage constraint violations

I: maxpercent, puvolt

O: p\_scale

- PowerWorld files

RBTS\_Bus3Dist.pwb (.pwb) - power world simulator file and display file of the base system. This has no DGs.

RBTS\_Bus3DistFull.pwb - power world simulator file of the base system, plus the possible connection lines as open lines. This has no DG.

RBTS\_Bus3Dist\_ALLDGs.pwb - power world simulator file of the base system. This has DGs in all the buses with zero power output and average annual loads in the load points.

RBTS\_Bus3Dist\_FullALLDGs.pwb - power world simulator file of the base system, plus the possible connection lines as open lines. This has DGs in all the buses with zero power output and average annual loads in the load points.

RBTS\_Bus3Dist\_ALLDGs\_PeakLoad.pwb - power world simulator file of the base system. This has DGs in all the buses with zero power output and annual peak loads in the load points.

RBTS\_Bus3Dist\_FullALLDGs\_PeakLoad.pwb - power world simulator file of the base system, plus the possible connection lines as open lines. This has DGs in all the buses with zero power output and peak annual loads in the load points.

RBTS\_Bus3Dist\_ALLDGs\_PeakLoadPS.pwb - power world simulator file of the base system. This has DGs in all the buses with zero power output and annual peak loads with PHEVs for Peak-shaving in the load points.

RBTS\_Bus3Dist\_FullALLDGs\_PeakLoadPS.pwb - power world simulator file of the base system, plus the possible connection lines as open lines. This has DGs in all the buses with zero power output and peak annual loads with PHEVs for Peak-shaving in the load points.

RBTS\_Bus3Dist\_ALLDGs\_PeakLoadTOU.pwb - power world simulator file of the base system. This has DGs in all the buses with zero power output and annual peak loads with PHEVs with TOU pricing in the load points.

RBTS\_Bus3Dist\_FullALLDGs\_PeakLoadTOU.pwb - power world simulator file of the base system, plus the possible connection lines as open lines. This has DGs in all the buses with zero power output and peak annual loads with PHEVs with TOU pricing in the load points.

RBTS\_Bus3Dist\_ALLDGs\_PHEV.pwb - power world simulator file of the base system. This has DGs in all the buses with zero power output annual average loads with PHEVs in the load points.

RBTS\_Bus3Dist\_FullALLDGs\_PHEV.pwb - power world simulator file of the base system, plus the possible connection lines as open lines. This has DGs in all the buses with zero power output and average annual loads with PHEVs in the load points.

RBTS\_Bus3Dist\_ALLDGs\_NewAv.pwb - power world simulator file of the base system. This has DGs in all the buses with zero power output and annual average loads using synthetic data presented in Chapter 4 in the load points.

RBTS\_Bus3Dist\_FullALLDGs\_NewAv.pwb - power world simulator file of the base system, plus the possible connection lines as open lines. This has DGs in all the buses with zero power output and annual average loads using synthetic data presented in Chapter 4 in the load points.

- Subfolders:

The following subfolders contain the output to the MOGA and are named after the objective function used.

@objeval\_DGs(3FDR) , @RBTSobjeval\_AV,  
@RBTSobjeval\_AVLessConections, @RBTSobjeval\_LD,

@RBTSobejval\_LDLessConnections

and

@RBTSObjeval\_AVLessConections\_PHEV

## **Contents of “PHEVs”**

This folder is organized in 3 subfolders: ‘ProbSimMethod’, ‘LPs’, and ‘RBTSChapter4’. Each of these subfolders contains a Readme\_’subfolder name’.txt file in which the contents of the subfolder is explained and repeated below.

### *Readme\_ProbSimMethod.txt*

‘ProbSimMethod’ contains the main function PHEVSim() to generate the required PHEV data for the LPs and the subfunctions of PHEVSim(), which are listed below.

- Main function:

PHEVSim () ... a function generating the design and behavioural characteristics of a PHEV fleet for the RBTS test system and required by the LPs.

I: none

O: B, DE\_res, DE\_com, DE\_off, Arr\_res, Arr\_com, Arr\_off, Dep\_res, Dep\_com, Dep\_off

- Subfunctions used:

PHEVsClass () ... use to compute the PHEV population size per class

I: Nt\_res, Pphev, p

O: Nphev

Design\_param() ... use to compute design and performance characteristics per vehicle class

I: BC\_range, kphev\_range, ro, aE, bE

O: B, kphev, E

Daily\_paramRES\_LPformat () ... this function returns the daily energy required and time parameters for each vehicle for a year in a residential load type

I: N\_phev\_tot\_res, u\_m, r\_m, u\_dt, u\_at, r\_dt, r\_at

O: Arr\_res, Dep\_res, DE\_res

Daily\_paramOff\_LPformat () ... this function returns the daily energy required and time parameters for each vehicle for a year in an office building load type

I: N\_phev\_tot\_off, u\_m, r\_m, u\_dt, u\_at, r\_dt, r\_at

O: Arr\_off, Dep\_off, DE\_off

Daily\_paramCom\_LPformat () ... this function returns the daily energy required and time parameters for each vehicle for a year in a commercial load type

I: N\_phev\_tot\_com, u\_m, r\_m, u\_dt, u\_at, r\_dt, r\_at

O: Arr\_com, Dep\_com, DE\_com

SNV() ... used to compute a standard normal value of dimension n

I: n

O: N

### *Readme\_LPs*

'LPs' contains the files necessary to run the LP algorithm with the objective of utility peak-shaving actions and with the objective of minimizing the customer energy bill with TOU pricing rates ('LP\_TOU'). Peak-shaving purpose is numbered objective number 1 and reducing the energy bill is objective number 2. Recall that the LPs are solved separately for residential load types and one vehicle class at a time (there are a total of 4 classes), for office building load type and all vehicle classes, and for commercial demand type and all vehicle classes at a time.

- Files:



phev\_L123\_c'class number'\_o'objective number'.dat ... contains the data for running the LP for 3 residential load types for vehicle class 'class number' and for 'objective number' purposes.

phev\_L123\_c'class number'\_o'objective number'.run ... is the run file for running the LP for 3 residential load types for vehicle class 'class number' and for 'objective number' purposes.

phev\_Lcom\_'objective number'.dat ... contains the data for running the LP for commercial load type for vehicle all vehicle classes and for 'objective number' purposes.

phev\_Loff\_'objective number'.dat ... contains the data for running the LP for office building load type for vehicle all vehicle classes and for 'objective number' purposes.

phev\_Lcom\_'objective number'.run ... is the run file for the LP for commercial load type for vehicle all vehicle classes and for 'objective number' purposes.

phev\_Loff\_'objective number'.run ... is the run file for the LP for office building load type for vehicle all vehicle classes and for 'objective number' purposes.

phev\_o'objective number'\_cmin.mod ... is the model file for running the LP with objective function 'objective number' and for vehicle classes 1 and 2

phev\_o'objective number'\_cmax.mod ... is the model file for running the LP with objective function 'objective number' and for vehicle classes 3 and 4

- Subfolder 'phev\_out' contains the output files of the solving the LPs with Cplex solver

#### *Readme\_RBTSCChapter4*

This folder contains the codes used to compute the demand of the RBTS with uncontrolled charging strategy of the PHEV fleet and delayed charging strategy in a subfolder named 'Uncontrolled+Delayed\_charging'. 'Load duration curves' is a subfolder with the functions used to obtain the load duration curves presented in Chapter 4 for the RBTS test system.

- Subfolder 'Uncontrolled+Delayed\_charging': contains the functions Uncontrolled\_phev() and Delayed\_phev() and the data necessary to compute the 8736 hourly load of the RBTS system
- Subfolder 'Load duration curves' : contains the necessary functions and data to compute the load duration and step-load duration curves of the RBTS system base load and with PHEVs

Load\_totPS() ... plots the load duration and step-load duration curves for the RBTS base load and with PHEVs optimized with LP\_Peakshaving

Load\_totTOU() ... plots the load duration and step-load duration curves for the RBTS base load and with PHEVs optimized with LP\_TOU

Load\_totUNC() ... plots the load duration and step-load duration curves for the RBTS base load and with PHEVs with uncontrolled charging

Load\_totDEL() ... plots the load duration and step-load duration curves for the RBTS base load and with PHEVs optimized with delayed charging

809002